ADDIS ABABA UNIVERSITY
ADDIS ABABA INSTITUTE OF TECHNOLOGY
SCHOOL OF CIVIL AND ENVIRONMENTAL ENGINEERING

Study of Steel I beam with the trapezoidal corrugated versus flat web for LTB with respect to Linear and Non-linear FEM.

A Thesis in structural Engineering

By

Habtamu Getu Mihret

August ,2021

Addis Ababa

A Thesis

Submitted in Partial Fulfillment of the Requirements for the Degree of Master of Science

The undersigned have examined the thesis proposal entitled '**Study of Steel I beam with the trapezoidal corrugated versus flat web for LTB with respect to Linear and Non-linear FEM.'** presented by **HABTAMU GETU MIHRET**, a candidate for the degree of **Master of Science in Structural Engineering** and hereby certify that it is worthy of acceptance.

Advisor	Signature	Date
Internal Examiner	Signature	Date
External Examiner	Signature	Date
Chair person	Signature	Date

UNDERTAKING

I certify that research work titled **"**Study of Steel I beam with the trapezoidal corrugated versus flat web for LTB with respect to Linear and Non-linear FEM**"** is my own work. The work has not been presented elsewhere for assessment. Where material has been used from other sources it has been properly acknowledged / referred.

Signature of Student

Habtamu Getu Mihret

ABSTRACT

Steel beams with corrugated web are widely used because of their high load-carrying capacity and optimized configuration to resist **lateral-torsional buckling (LTB)**. The purpose of this thesis is to provide a comparative study of elastic buckling analysis and linear FE analysis and nonlinear FE analysis as well as hand calculation. The author focuses on LTB of plate girders with **trapezoidal corrugated** and **flat webs**. This comparative study is performed through two groups of plate girders with corrugated and flat webs under consideration four types of steel classes. While in the numerical study, the elastic-plastic material model, residual stress distribution, and geometrical imperfections factors are considered for both flat and corrugated web. Thirty individual data types of different sample dimensions were examined for two types of girders, one girder with flat webs and an identical girder with the corrugated web. The samples are 15 flat web beams with three slenderness categories and 15 corrugated web beams with the same three slenderness categories. For the sake of control, the expected outcome, initial random cross-section dimensions are generated concerning three values of non-dimensional **slenderness ratio ranges:** 0.4, 0.6, and 1.2, corresponding to very stocky, intermediate, and very slender slenderness properties respectively to draw a sample which represents a total population. Besides, the comparison considers one type of plate girder with flat and an identical corrugated web within particular engineering parameters. To carry out a comparative study into the behavior of trapezoidal corrugated steel and flat webs, an advanced finite element analysis has been employed to understand buckling problems and to investigate the behavior of beams. FE-simulations are performed to represent the conditions of reality as good as possible and empirical hand calculations are made to verify the results. The corrugated web has an increased load capacity and stiffness by (32-67%), (12-31.3%) and (0.058%-0.418%) for very slender, intermediate, and very stocky respectively than flat web beams. A comparison study between flat web with web stiffeners and corrugated web I beam is suggested as a topic for future research.

Keywords: Corrugated web, Flat web, Lateral torsional buckling (LTB), slenderness ratio.

ACKNOWLEDGMENTS

Before everything else, I would like to thank the Glory God who had shaped the universe and all life in it using only in his words.

I would like to extend my deepest gratitude to my supervisor Professor Girma Zerayohannes for his help throughout this work. All Electronic and published books and papers are duly acknowledged.

Finally, I would like to dedicate this master's thesis to the memory of my childhood friend Mr. Daniel Yazie who was supposed to get old together with me.

TABLE OF CONTENTS

TABLE OF CONTENTS

LIST OF TABLES

LIST OF FIGURES

Acronyms

CAE- Computer Aided Engineering

LTB-lateral torsional buckling

FEM -Finite element Method

NCCI- National Correct Coding Initiative

Notations

E Modulus of elasticity

G Shear modulus

L Longitudinal length

M_{cr} The critical buckling moment for a laterally unrestrained beam

M_y Bending Moment in the major direction

α Imperfection factor for lateral torsional buckling

e_o Initial bow imperfection

Iz Moment of inertia around the weak axis (xy plane)

Iy Moment of inertia around strong axis (xz plane)

It Torsion constant

Iw Warping constant for corrugated webs

Wy Section modulus

Wpl Section modulus in class 1 or 2,

Wel Cross-sections in class 3

Weff Sections in class 4.

λ Eigenvalue regarding buckling or non-dimensional slenderness

χ Reduction factor for out of plane buckling

α Corrugation angle

ε Engineering strain

tf Flange thickness

tw Web thickness

v Poison's ratio

$b1$ Width of the flange in compression

$b2$ Width of the flange in tension

fy Yield stress limit

A Length of longitudinal panel

b Projected length of inclined panel

c Length of inclined panel

d Maximum eccentricity of web

cw Torsion constant increasing factor for corrugated web

Ux Critical lateral-torsional buckling moment due corrugated web

CHAPTER 1 INTRODUCTION

1.1 Background

The use of steel structures has been increasing in the world as it is more efficient and effective with high stiffness and strength. Currently many developed as well as developing countries are widely used steel frame structures in various architectural forms. With this rapid growth of technology and innovation, a lot of countries have been working their research on optimization of many structures' forms, as well as tried to understand the nonlinear response with their own country codes context (Al-Emrani, 2018).

According to (Sokolowski & Kaminski, 2015) the positive effect of the corrugated web has continued to increase in steel structure construction industry since its appearance in the 1990s, mainly due to its high transverse rigidity, which is essentially higher than for plate girders with a flat web because of larger torsional stiffness capacity. Corrugated webs targeted to replace classical traditional I beam-columns with respected flat webs. In addition, corrugated webs are broadly used for both as homogenous long span steel bridge girders and composite bridge girders as heterogenous properties. The importance of corrugated web has been introduced and adapted by its technological advancement and leads to save material usage up to 30% in terms of steel and 10-30% of overall production cost in company level. (Ameer AL-Kanon & suhiel, 2019) studied experimentally also on the corrugated web lateral torsional buckling resistance for plate girder and experimentally proved that lateral tortional buckling capacity of flat web less than 15-37% than capacity of corrugated web. Also (kumar, et al., 2018) also confirmed on their study that corrugated web steel beams are 1.5-2 times more resistance that flat web I beam.

Corrugated web beams are built-up girders with a thin-walled, corrugated web and wide plate flanges as you can see it Figure 1.1. Corrugated web beams may be used as beams (roof or slab beams as building structural beams and main girder beam) components which subject to normal forces virtually without structural limitations. Corrugated web instead of flat web type of beam basically avoids failure of the beam due to loss of stability before the plastic limit-loading for the web is reached. In addition to benefits for production technology capacity perspective, the sinusoidal type of corrugation web has the advantage

over trapezoidal profiling of highly reducing local buckling of the flat plate strips (Al-Emrani, 2018).

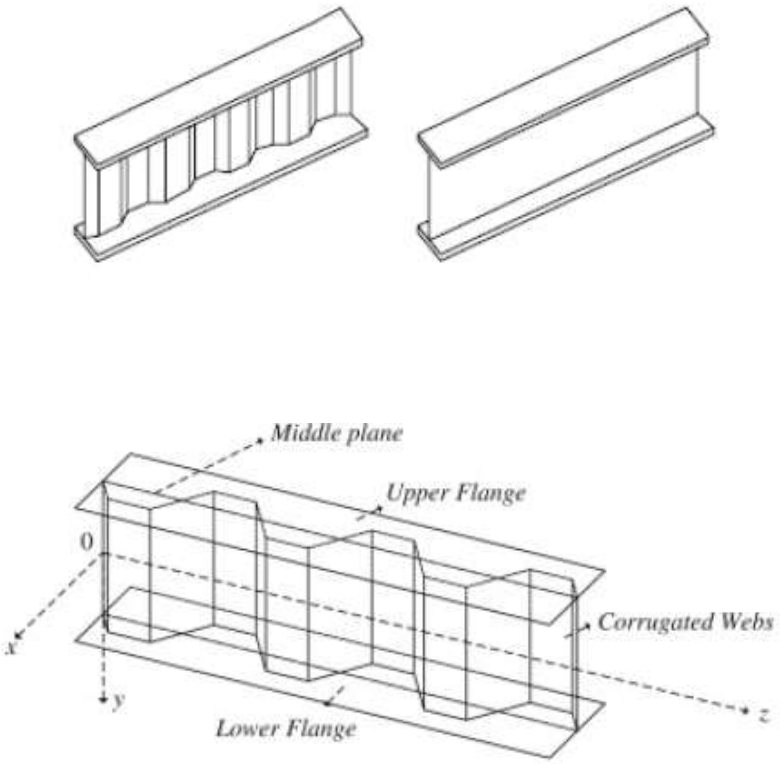

Figure 1-1 Beams with corrugated vs Flat web

1.2 Objectives

The aim of this research was to study the lateral-torsional buckling behavior of beams for both flat and trapezoidal corrugated webs and to provide a comparative study of elastic buckling analysis and linear FE analysis and nonlinear FE analysis along with hand calculation verification. The paper mainly focuses on a parametric study on LTB of a simply supported beam with trapezoidal corrugated and flat webs with variable sizes. This comparative study is performed through two groups of plate girders with corrugated and flat webs under consideration of four types of steel classes as well as three values of non-dimensional slenderness ratio ranges**:** 0.4, 0.6, and 1.2 corresponding to very stocky, intermediate, and very slender slenderness properties respectively. While in the numerical study, the elastic-plastic material model, residual stress distribution, and initial geometrical imperfections are considered for both flat and corrugated web to represent the conditions of reality as good as possible.

This Master thesis has intended to answer the following questions

1. How far it is possible to utilize possible additional contribution to the LTB resistance provided by the corrugated web under consideration of non-dimensional slenderness and different steel class?
2. Are there any published results available regarding the contribution due to corrugated web? What calculation model should be applied for corrugated I beam?
3. There is an expected hypothesis that a corrugated web would be able to provide some additional restraint to the flange regarding LTB, thus, how is it practical in the parametric study?
4. How large a contribution the corrugated web gives compared to a flat web? The comparison will be carried out in three different methods, such as
    - Static analysis
    - Elastic Linear buckling
    - Nonlinear FE analysis (2^{nd} order buckling)

1.3 Computational model description.

Finite element modeling was employed to be carried out for modeling of steel beams of the European double symmetrical welded profile. FE-simulation for I sections beams is considered as simply supported with fork end boundary conditions and load as a bending moment M on both ends which are represented as a case of pure bending. Computational and implementation of this strategy is performed in three methods Static analysis (linear material), Linear buckling (linear material), and non-linear analysis (elastic-plastic material). FE simulation in the non-linear analysis is performed by employing the static risk algorithm, load-deflection, and moment-rotation response. Python scripting has been employed to provide a consistent design procedure with the demand of the Eurocodes for both elastic linear buckling and non-linear analysis.

1.4 Scope and limitations.

Thirty individual data types of different sample dimensions were examined for two types of girders, one girder with flat webs and an identical girder with the corrugated web. The

samples are 15 flat web beams with three slenderness categories and 15 corrugated web beams with the same three slenderness categories.

One of the limitations of this study is that the output of the study applies only for welded I sections, in other words, it excludes rolled I section beams. Similarly, the study also considered the same material properties for flange and webs. In Addition, boundary conditions are simplified and limited to simply support types of models. However, this does not always represent real beams adequately but it is sufficient for this study since it is possible to fulfill the main objective.

1.5 Outline of the thesis.

There are five chapters in this thesis. Chapter one is introduction which includes background, objectives, research questions, and limitations of the study. Chapter two is literature study which provides the theoretical understanding of the main concepts of the thesis. Chapter three explains the methodologies and material that are used for conducting this study. Chapter four presents the results and discussion with the help of theories from the literature study. And finally, chapter five is concluding the findings of the study and provides recommendations for future research.

CHAPTER 2 LITERATURE REVIEW

To understand the calculation methods which has been used for buckling analysis more thoroughly, this chapter provides the reader with a brief summary regarding the general behavior on a particular focus on buckling of steel members. First, an overview of the research on the girders with corrugated webs types as well as their advantage. Then, classical Euler's buckling theory is presented according to factors that affect the real behavior of elements with reference to global instability and second order effects. Finally, the last part provides knowledge to the reader regarding the method about the elastic critical moment which prepared by (SN003a-EN-EU, August 2007): elastic critical moment for lateral torsional buckling. Meanwhile, in this chapter, a brief review of the recently conducted research is also presented.

2.1 Overview of research on girders with corrugated webs

The use of steel structures has been common in the construction industry since it is more efficient and effective under considerations of stiffness and strength. In order to accomplish more strength and stiffness, steel beams with corrugated web are widely used because of their light weight, high resistance of LTB and high load carrying capacity (kumar, et al., 2018).

There are several types of steel beams that are available for construction projects. Steel beams corrugated web are widely used at the current construction time while constructing long span bridges, steel buildings and structures of different types. The webs for I beams must be thin to use the optimized strength of material. Yet, optimization process for reducing thickness is not easy process as it is expected. Thus, to overcome this corrugated web beams are introduced a long-lasting solution. Corrugated web beams are made-up from the steel factories by using two steel plates which act as flanges and corrugated steel sheet as web are welded to form a corrugated web I-beam. Corrugated web steel beam is a structural type of element that differs from the classical and traditional flat web I beam in many ways. The main benefit of corrugated web beams is that the increased stability against lateral torsional buckling and it helps to invent a good economic design either by reducing web stiffeners but without additional stiffeners or by increasing the web thickness (kumar, et al., 2018) (Balzannikov, et al., 2015) also studied that the about advantages of

corrugated web beam are their optimized metal intensity which is a result of reducing its web thickness at the design and construction process. Besides, strengthening weak axis and strong axis moment of inertia which used to resisting such webs buckling problems are used in these beams. In addition to the economic benefits of either minimizing or replacing stiffeners for the capability to use very thin webs. In another point of view, there is also benefits regarding the increased stiffness resistance of the corrugated profile which promote a series of other valuable merits are: increased robustness during transportation and assembly. For example, regarding regular flat webs, usually requires double sided welds between web and flanges. However, corrugated profiles are applicable to use single-sided welds. To summarized, the structural stability and strength to weight ratio of corrugated steel webs has merits respectively not only in structural-strength, rather it is more helpful and mandatory during transportation and erection.

Based on (Sokolowski & Kaminski, 2015) outstanding shape of the corrugated web certifies to changes of the stress re-distribution as plate on the applied loads leads to expected normal stress, bending moments have completely transferred the flanges. Besides, the corrugated web delivers exclusively for transfer of the shear and torsion and work out as same as a stiffener of the flanges which resist by transferring loads to diagonals and verticals of a lattice girder. Thus, the corrugated web has positive effect resist of bending resistance around the weak axis, which leads to a better resistance regarding for both torsion and remarkably high lateral buckling resistance.

As mentioned earlier, the number of published results regarding corrugated webs is relatively limited so far. Nevertheless, as the concept of corrugated webs is not completely new, the collected data from experiments performed over the past half century gives rather good conclusions concerning the lateral buckling resistance. However, in addition to lateral torsional buckling resistance some other disadvantage of corrugated web conceptual theoretical studies also carried-out. For example, according to (Sokolowski & Kaminski, 2015) most of the structures designed with corrugated but sinusoidal type waviness of the web's girder types are exposed to corrosion which leads to second order problems failures, However, it is more dangerous for elements with small thickness. Finally, (Sokolowski & Kaminski, 2015) emphasized that since many mathematical computational problems are connected with corrugated web beams are unresolved so far. As a result of that, most of

the design codes of standards take relatively large margin safety for the sake of unknown problems.

More than a few publications and experiment as well as theoretical study on girders with corrugated webs have been carried out in developing countries with in number of researchers and educational institutes. Although lateral-torsional buckling behavior is an important issue, studies regarding this problem for I-beams with corrugated webs are still insufficient as it has been expected (Tohamy, et al., 2013). To summarized this paper targeted to contribute somehow since further investigation need to be carried out. Thus, afterwards this paper will inspect and investigate the behavior of beams with corrugated webs versus flat webs in terms of lateral torsional buckling based main literature point view.

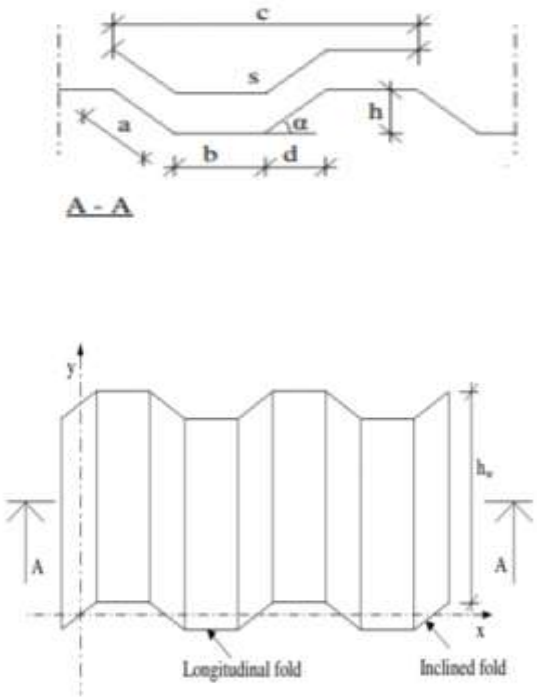

Figure 2-1: Schematic illustration of a trapezoidal corrugated web and its geometrical pattern

2.2 Types of corrugated web Profile.

Steel I beam with the corrugated webs are used as structural elements of the building as well as bridge structures. Corrugated webs beams are comparable with traditional steel

girders mainly by reason of their lower weight for economy, increased web stiffness and also further aesthetic look (Gorecki, et al., 2017). The corrugated steel plate has been used in many fields of application for long time because of its favorable properties for three best design criteria's: strength, economy and aesthetic. This innovative process has helped engineers to design more optimal structures (Tohamy, et al., 2013). However, based on many experiential and theoretical studies, the most commonly used corrugated web plates types of corrugation profile is the trapezoidal profile. Besides, there are many types like sinusoidal, triangular and others types profile of corrugated web. See Figure 2-2 (Balzannikov, et al., 2015). Therefore, this paper mainly aimed to compete for the best of corrugated profile which is trapezoidal corrugated web type with the classical flat web.

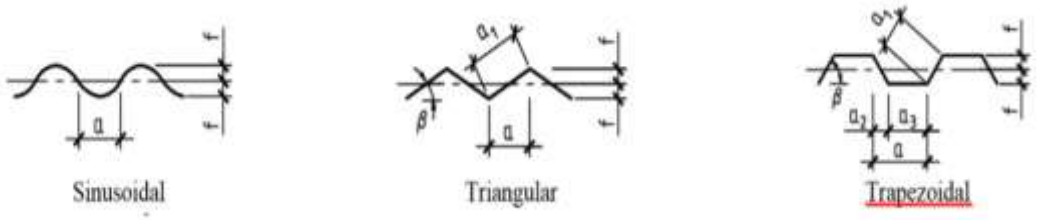

Figure 2-2: Profile of corrugated web

2.3 Advantage of corrugated webs.

There are a lot of research has been conducted regarding corrugated webs. Thus, some of summarized the main advantages are listed below:

Based on the (Sokolowski & Kaminski, 2015) experimented that the spread of the corrugated web has been forced by its technological advancement and which allowing that superior material usage of saving up to 30% in terms of steel and 10-30% of the overall production cost. In addition, this is also achieved by an extensive reduction in web thickness and the contribution is 30-40% of the overall weight of the I beam. (Ameer AL-Kanon & suhiel, 2019) also defined corrugated web as new systems which is invented for, I beam that strength transverse stiffener which includes from vertical, horizontal and inclined plates and helps to reduce web thickness accordingly.

(Gorecki, et al., 2017) similarly studied that in bridge construction which most likely longer span has used larger steel profiles. Hence, with sinusoidally corrugated webs as a bridge beams, a study with beams with web thickness of 7 mm was better resistant than a

traditional flat webs which have a thickness of not less than 10mm, In addition, summarized as even trapezoidal web is better performance than sinusoidal corrugated web, (Sokolowski & Kaminski, 2015) likewise it was mentioned that sinusoidal waviness types of webs are exposed to corrosion than trapezoidal web which especially dangerous for elements with small thickness. Furthermore, most the (Sokolowski & Kaminski, 2015) give emphasis that still problems which are connected with corrugated web beams are unsolved. So, it was pointed out corrugated web as an identified as a future research area.

2.4 The load-carrying capacity of slender plates loaded in compression

(EN-1993-1-5, 2006) proposed a plate which has the capacity for a post-critical reserve strength and enables for an additional loading capacity after that buckling has occurred. This post-critical reserve strength is shown below in the load/displacement diagram in Figure 2-3, this schematic load-displacement diagram is for a plate with no initial imperfections.

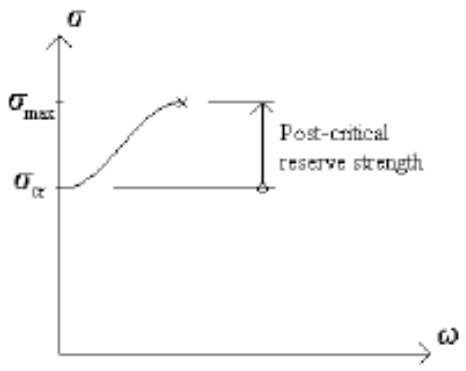

Figure 2-3: Load vs lateral displacement for a prefect plate load in compression

Von Karman realized that buckling of the plate will result in a redistribution of stresses from the middle part of the plate. The plate is able to carry additional load after buckling has occurred, and this is due to the formation of a membrane that stabilizes the buckle through a transverse tension band. When the central part of the plate buckles, it loses the major part of its stiffness, and then the load is forced to be linked around this weakened zone into the stiffer parts on each side, this means, along the supports parallel to the direction of load. Due to this redistribution, a transverse membrane in tension is formed

and anchored. Study the plate below in the post-critical range, Refer, Figure2-4, which explains the post-critical zone, with respective of strut-and-tie analogy.

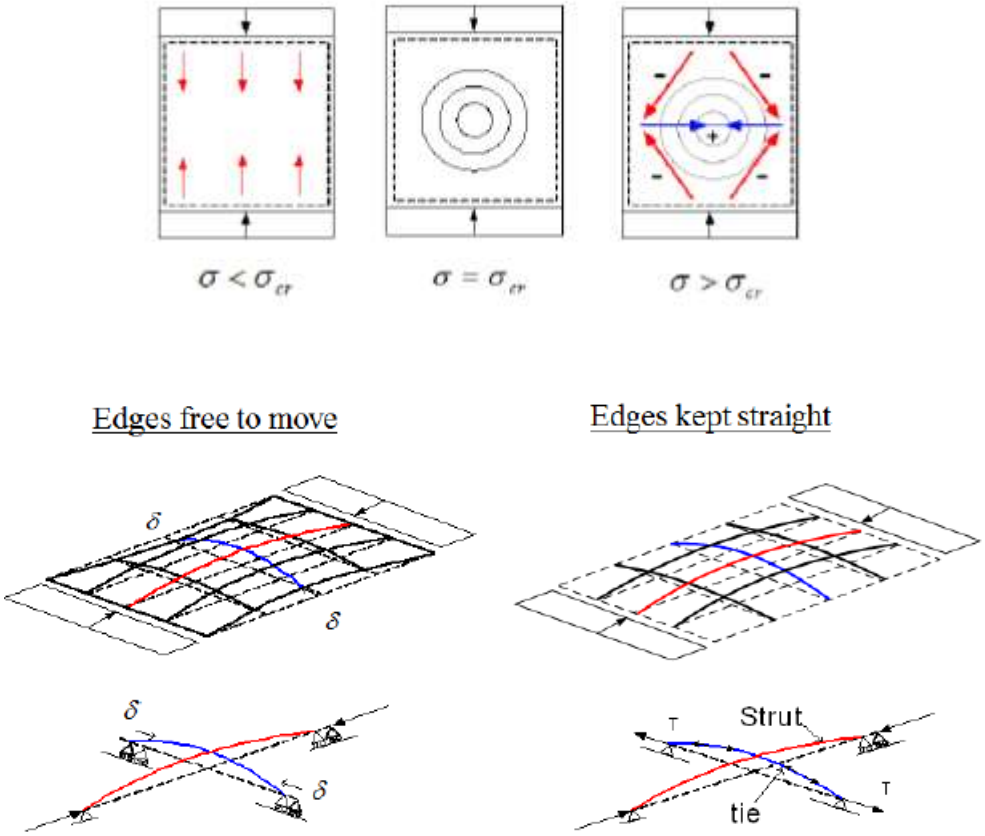

Figure 2-4: A strut and tie model showing the transversal tension field formed after buckling.

2.5 cross-section class

(EN-1993-1-1, 2005) describes four cross-section classes with reference to the local buckling problems. Those mentioned class that determines which particular class a cross-section belongs to is the slenderness ratio of each type of plates. What follows, depending on the slenderness ratio of level which determines the plastic rotational ability of bending moment i.e., its ability (or inability) to grow on the tensile side and compress (possibly risk buckling) in the opposite direction. These four classes of Eurocodes (Class 1-4) are in place of receiving bending moments defined in Figure 2-5.

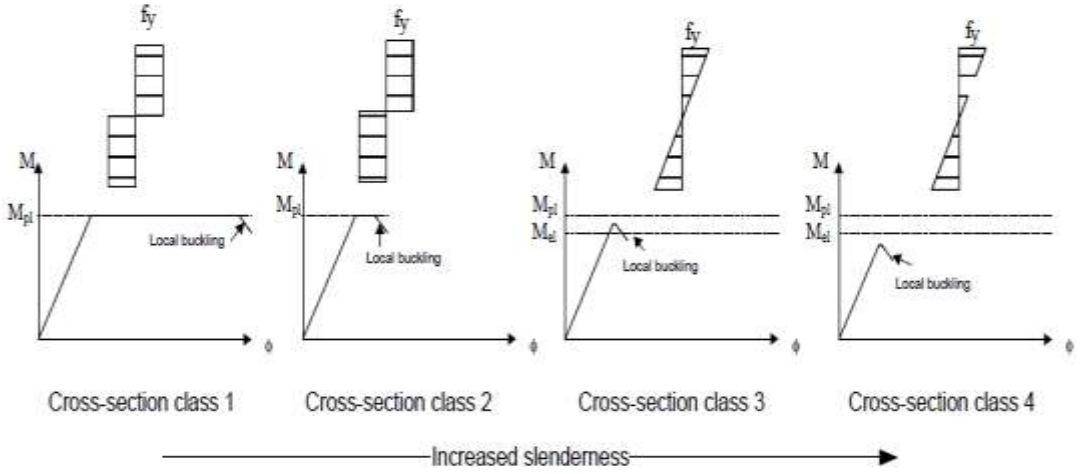

Figure 2-5: The effect of plate slenderness

2.6 Classical linear elastic buckling theory

In 1757, Euler derived an equation for the maximum axial load on a straight, prismatic, simply supported, slender and elastic column. The elastic buckling theory has been considered.

According to (Al-emrani & Åkesson, 2013) the classical buckling theory so called Euler buckling. This is a classical elastic buckling problem, also known as the bifurcation problem. The following assumptions are considered for ideal design conditions.

1. The column is initially 'perfect', this means with no geometrical imperfections in the respective of of straightness.
2. An elastic material behavior is assumed.
3. No residual stresses or other inner stresses.
4. Loading is applied centrically to the column.

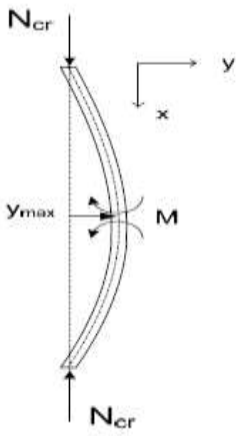

$$P_{cr} = \frac{\pi^2 EI}{{L_{cr}}^2} \ldots\ldots f(I, E, L_{cr}) \ldots\ldots\ldots\ldots\ldots (2.1)$$

Figure 2-6: Euler Buckling

$$\sigma_{cr} = \frac{P_{cr}}{A} = \frac{\pi^2 EI}{A{L_{cr}}^2} \ldots\ldots\ldots\ldots\ldots\ldots\ldots\ldots\ldots\ldots\ldots\ldots\ldots\ldots\ldots\ldots\ldots\ldots\ldots\ldots\ldots\ldots (2.2)$$

$$i = \sqrt{\frac{I}{A}} \ldots\ldots\ldots\ldots\ldots\ldots\ldots\ldots\ldots\ldots\ldots\ldots\ldots\ldots\ldots\ldots\ldots\ldots\ldots\ldots\ldots\ldots\ldots\ldots\ldots\ldots (2.3)$$

$$\sigma_{cr} = \frac{\pi^2 E}{\left(\frac{L_{cr}}{i}\right)^2} \ldots\ldots\ldots\ldots\ldots\ldots\ldots\ldots\ldots\ldots\ldots\ldots\ldots\ldots\ldots\ldots\ldots\ldots\ldots\ldots\ldots\ldots\ldots\ldots\ldots\ldots (2.4)$$

$$\sigma_{cr} = \frac{\pi^2 E}{\lambda^2} \ldots\ldots\ldots\ldots\ldots\ldots\ldots\ldots\ldots\ldots\ldots\ldots\ldots\ldots\ldots\ldots\ldots\ldots\ldots\ldots\ldots\ldots\ldots\ldots\ldots\ldots (2.5)$$

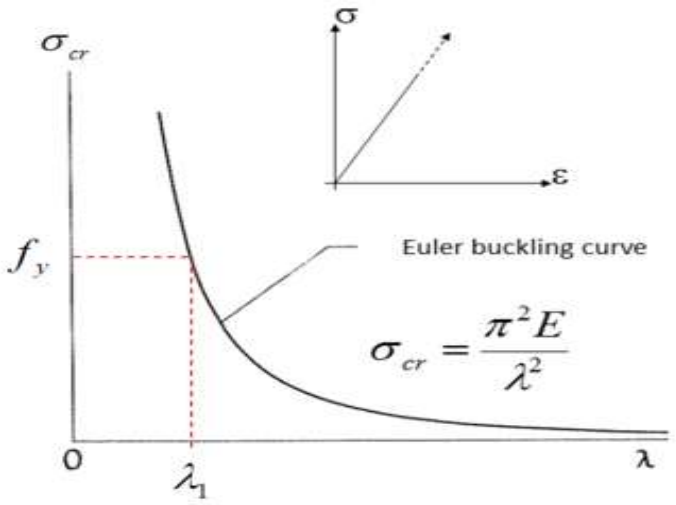

$$\sigma_{cr} = \frac{\pi^2 E}{{\lambda_1}^2} = f_y \text{.....(2.6)}$$

$$\lambda_1 = \pi\sqrt{\frac{E}{f_y}} \text{.....(2.7)}$$

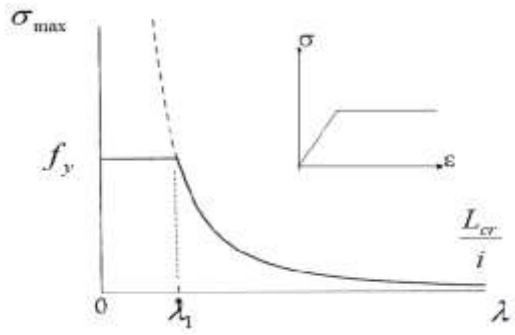

Figure 2-7: The relation between slenderness and the critical buckling stress according to the classical buckling theory.

$$\sigma_{cr} = \frac{\pi^2 E}{\lambda^2} \quad \lambda = \pi\sqrt{\frac{E}{\sigma_{cr}}} \text{.....(2.8)}$$

$$\lambda_1 = \pi\sqrt{\frac{E}{f_y}} \text{.....(2.9)}$$

$$\frac{\lambda}{\lambda_1} = \sqrt{\frac{f_y}{\sigma_{cr}}} = \sqrt{\frac{N_y}{N_{cr}}} \text{.....(2.10)}$$

$$\bar{\lambda} = \sqrt{\frac{N_y}{N_{cr}}} \text{.....(2.11)}$$

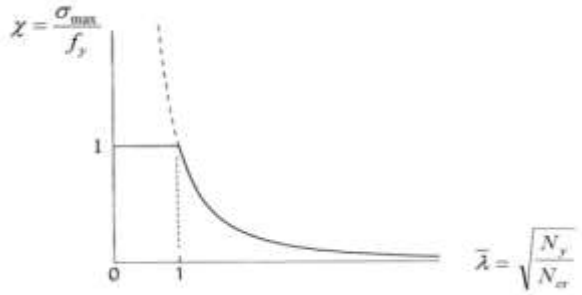

Figure 2-8: a buckling curve desribes the relation bewteen the relaative slenderess ratio vs buckling reducation factor

2.7 Behavior of real columns/Beams

2.7.1 2nd order analysis of columns

In general, real beam-column is not straight. The buckling curves which are presented in (EN-1993-1-1,2005) are already taking an assumption regarding the effect of initial imperfection within some specified tolerance. When an axial force is applied to an initially defective column, a bending moment is created in all sections along its very length, resulting in bending deformation.

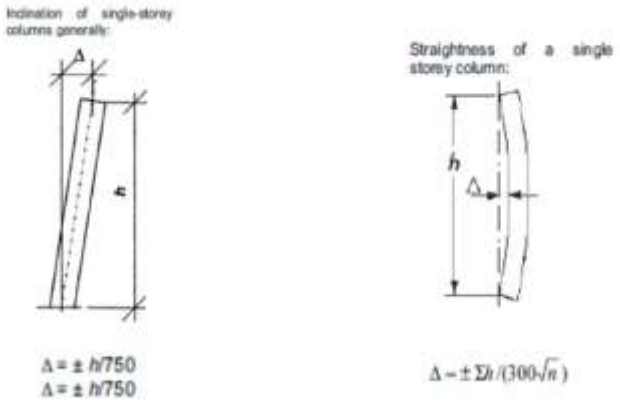

Figure 2-9: Eurocode's classification and treatment of initial imperfection

The Figure 2-6, the expression below shows that the lateral deflections increase non-linearly from zero to infinity when the load while increases from zero to Ncr.

$$M = N(e_0 + e_1) \quad \text{.....(2.12)}$$

$$-EI \cdot e_1'' = N(e_0 + e_1) = N(e_0 \cdot sin\frac{\pi x}{l} + e_1) \quad \text{.....(2.13)}$$

$$e_1 = \frac{e_0}{1-\frac{N}{N_{cr}}} sin\frac{\pi x}{l} \quad \text{.....(2.14)}$$

$$e_{max} = \frac{e_0}{1-\frac{N}{N_{cr}}} \quad \text{.....(2.15)}$$

$$M_{II} = \frac{e_0}{1-\frac{N}{N_{cr}}} \cdot N \quad \text{.....(2.16)}$$

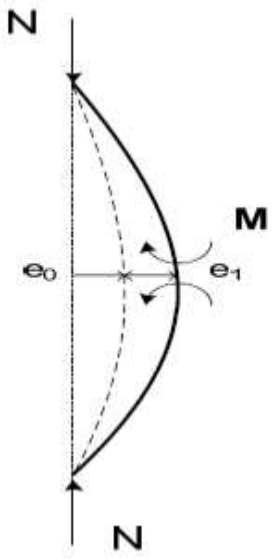

Figure 2-10: Column with initial bow imperfection

$$\sigma_{max} = \frac{N}{A} + \frac{M_{II}}{W} = f_y \text{.....(2.17)}$$

$$M_{II} = \frac{e_0}{1-\frac{N}{N_{cr}}} \cdot N \text{.....(2.18)}$$

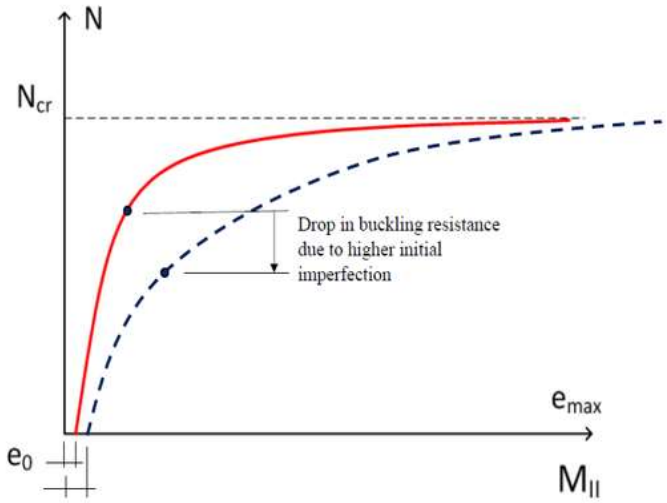

Figure 2-11: Column which having different initial imperfection magnitudes.

2.7.2 Initial imperfection.

Comparing the design buckling curve (EN-1993-1-1 (2005)) with the theoretical Euler buckling curve as shown in Figure 2-11, it can be explained that the load-carrying capacity may be different due to its relatively non dimensional slenderness ratio. However, the difference is big for intermediate slenderness zone, which means a non-dimensional slenderness ratio range of 0.4 up to 1.2. The main reason for this effect is material and geometrical imperfection. Members with very stocky zone of beam-column are less affected by this because their load capacity is governed by yielding rather than buckling. The load-bearing capacity of very slender members is dominated by elastic buckling, where the stress is much lower than the yield stress. The load-bearing capacity of very thin members is dominated by elastic buckling, where the stress is much lower than the yield stress.

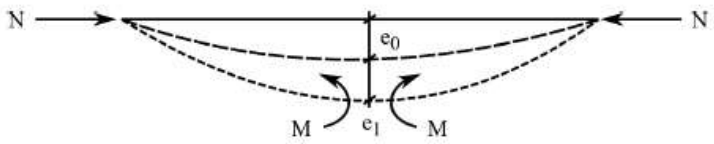

Figure 2-12: A member with an initial bow imperfection

$$\bar{\lambda} = \frac{\lambda}{\lambda_1} \quad \text{.....(2.19)}$$

$$\lambda = \frac{L_{cr}}{i} \quad \text{.....(2.20)}$$

$$\lambda_1 = \pi\sqrt{\frac{E}{f_y}} \quad \text{.....(2.21)}$$

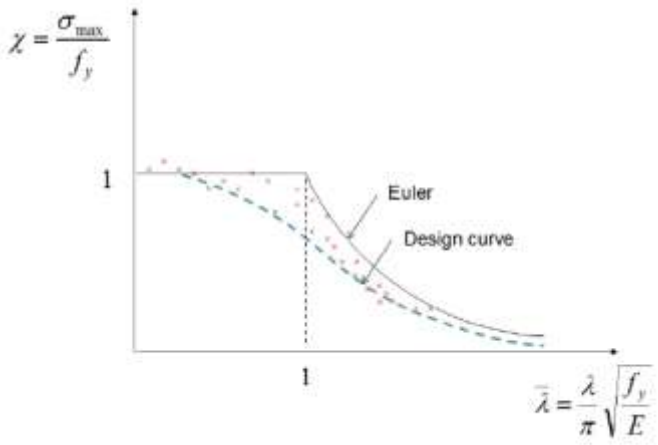

Figure 2-13: Test result of steel columns in relation to the buckling curve derived according to classical buckling theory.

Accoding to (Al-emrani & Åkesson, 2013) the Euler buckling curve in relation to test results on columns with different slenderness and three obesrrvation can be put forward (a schematic illustartion as it explained at Figure 2-15.

1. **Very low slenderness**: very Stocky column is actually higher than the value corresonding to yielding. In the other word, a short column for which the load carrying is not governed by instability ,but rather by yielding.
    - The load carrying capaicty of stocky columns is rather insenstive to the magnitude of intial imprefaction.
2. **Intermediate slenderness**: show a load carrying capacity which is well below what is predicated by Euler buckling
    - Initial imperfection have a substantial effect on the load carrying capacity of columns with intermediate slenderness due to more pronunced (Second) 2^{nd} order effects in these columns.
3. **Very slender columns**: have a load carrying that is equivalent to what is predicated by the linear elastic buckling theory,(Eular buckling).
    - The magnitude of intial imprefections will only have a marginal effect of load carrying capacity of such columns.

2.7.3 Effect of residual stresses.

Residual stresses, which also is referred to as material imperfections. In steel manufacturing process high temperature are used to shape steel members. Residual stress is a consequence of differential heating and cooling in the rolling and forming process (Wang & Yang, 2016). According to (Al-emrani & Åkesson, 2013) also clarified that welded and hot rolled steel sections contain in general a state of inner stress caused by the heating and the subsequent cooling process, so called residual stress. In another word, residual stress are self-balancing stresses with parts of the cross-section in tension and others experiencing compression. The magnitude and distribution of residual stress depend on several parameters such as the manufacturing method (welding and rolling), the shape of the cross section and its dimensions (such as flange thickness). Welding of material is often associated with the stress that is built in welded detail, see Figure 2-14.

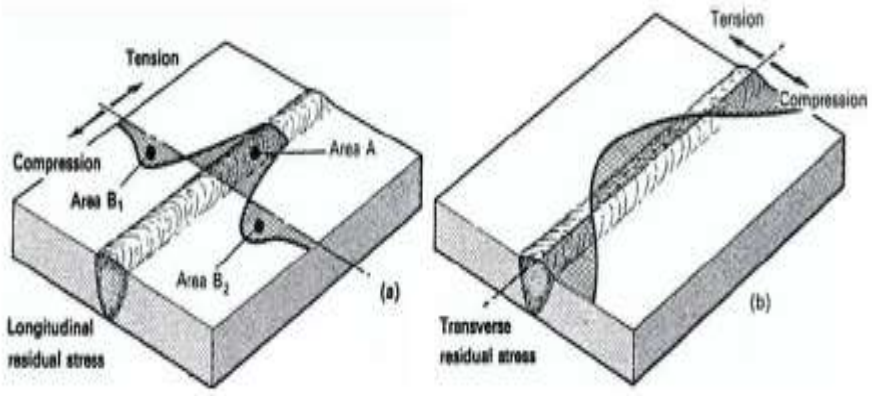

Figure 2-14: Residual stress distribution as a result of welding.

In summarized, both initial imperfections and residual stresses play a major role in reducing the load capacity of columns with intermediate slenderness. Very stocky and very slender columns are affected to much lesser degree.

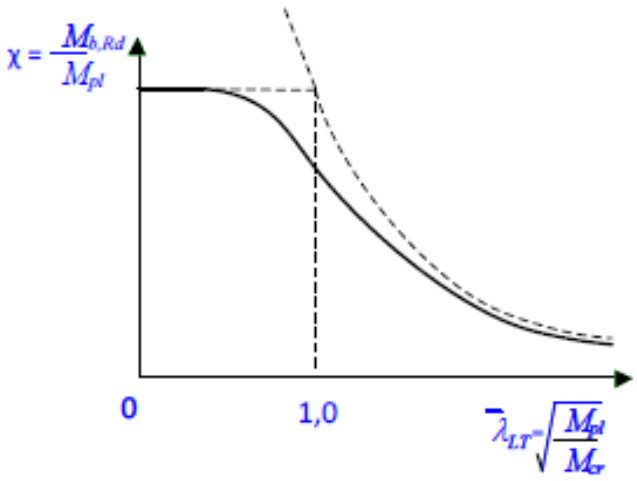

Figure 2-15: Initial imperfection and residual stress influence vs Euler buckling curve.

2.7.4 Effect of material.

Strain hardening effects tend to be ignored by Structural Engineers in most of the country, which in fact provides a margin of safety. The onset of first yield will not be affected, but the buckling load may be increased. For this, For the elastic-plastic material model we use the approximation adopted in EN 1993-1-5, where the stress-strain relationship is assumed to follow an elastic-plastic material with strain hardening, see Figure 2-16.

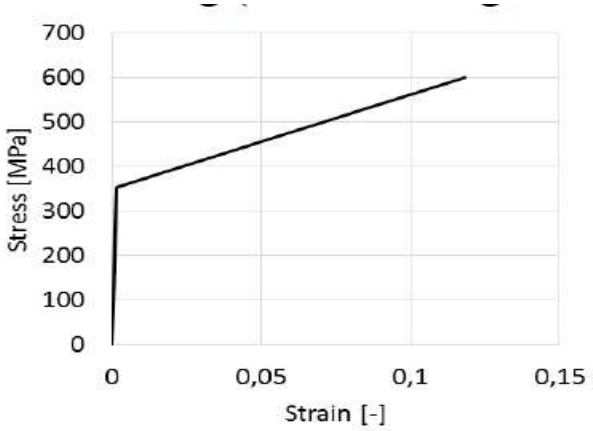

Figure 2-16: Stress-strain relationship

2.8 Design Methodology in EN 1993-1-1:2005

According to EN1993-1-1 there are two principal methods can be applied for the design of beam-columns: Buckling curve and second order analysis.

2.8.1 Buckling curve

The simplest and most convenient design principle for beam-columns is designed depending on the use of buckling curves for regarding imperfection class. The imperfection factor and the buckling curve are chosen based on dependent multiple parameters with respect to Figure 2-17, which affects the buckling resistance of all columns.

In (EN-1993-1-1, 2005), one of the design methods used to determine the buckling resistance of a column is based on the five buckling curves in Figure 2-17.

Table 2-1: Imperfection factors for buckling curves

Buckling curve	a_0	a	b	c	d
Imperfection factor, α	0.13	0.21	0.34	0.49	0.76

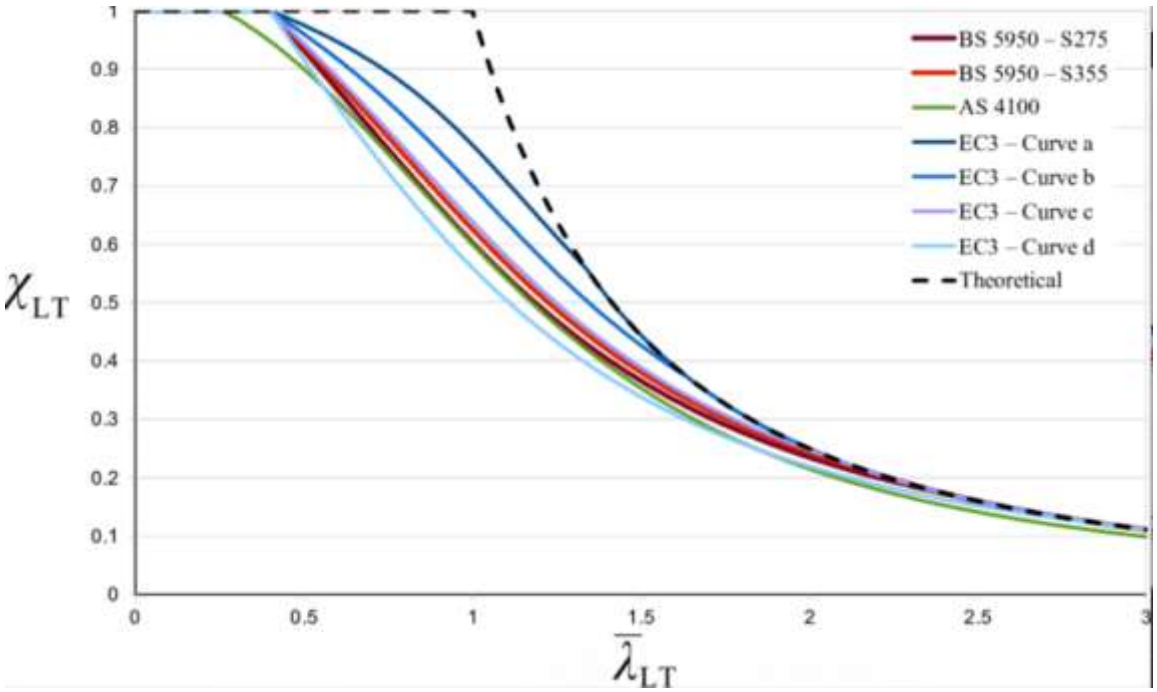

Figure 2-17: Five types buckling curves in EN 1993-1-1

The reduction factor can be calculated analytically, but also directly from the buckling curves, see Figure 2-16. The correct buckling curve is selected by following Figure 2-16, which is a simplified version of the one in (EN-1993-1-1, 2005).

Note: Imperfections factors include the effect of initial out of straightness and residual stress.

Cross section		Limits		Buckling about axis	Buckling curve: S 235 S 275 S 355 S 420	Buckling curve: S 460
Rolled sections	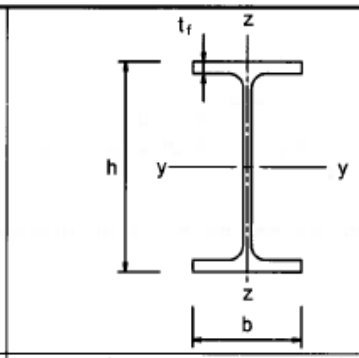	$h/b > 1,2$	$t_f \le 40$ mm	y – y z – z	a b	a_0 a_0
			40 mm < $t_f \le 100$	y – y z – z	b c	a a
		$h/b \le 1,2$	$t_f \le 100$ mm	y – y z – z	b c	a a
			$t_f > 100$ mm	y – y z – z	d d	c c
Welded I-sections	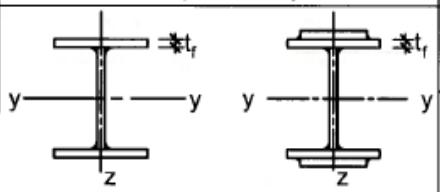	$t_f \le 40$ mm		y – y z – z	b c	b c
		$t_f > 40$ mm		y – y z – z	c d	c d
Hollow sections	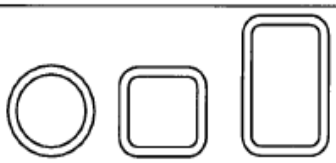	hot finished		any	a	a_0
		cold formed		any	c	c
Welded box sections	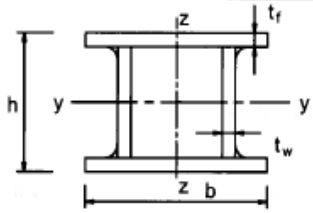	generally (except as below)		any	b	b
		thick welds: $a > 0,5t_f$ $b/t_f < 30$ $h/t_w < 30$		any	c	c
U-, T- and solid sections	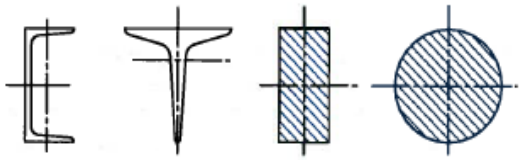			any	c	c
L-sections				any	b	b

Table 2-2: Selection of buckling curve for the cross section at EN-1993-1-1

2.8.2 Second order analysis.

The effect of initial imperfection and residual stresses is indirectly explained by the in the buckling curve method, based on the imperfection factor. The method is easy and does not require length calculation. However, this method is only be applied to uniform prismatic members. Rather, non-prismatic members are need more advance Finite element software's. For example, the tapered column should consider other approaches like FEM. This method is applicable to the single structural elements as well as multiple structures. In general, computer analysis is required to perform a reliability analysis that takes into account secondary effects, but in the case of a simple basic case, it can also be calculated by hand (for simple basic cases). (Al-emrani & Åkesson, 2013) as it is referred on Appendix.

Table 2-3: Design values of intial local bow imprefection.

Buckling curve acc. to Table 6.1	elastic analysis e_0 / L	plastic analysis e_0 / L
a_0	1 / 350	1 / 300
a	1 / 300	1 / 250
b	1 / 250	1 / 200
c	1 / 200	1 / 150
d	1 / 150	1 / 100

The geometrical imperfections and residual stresses are considered by defining a maximum deformation to the first buckling mode and using it as the initial geometry of the beam in the non-linear analysis. The maximum deformation is calculated as the initial bow imperfection in (EN-1993-1-1, 2005), in Table 5.1. Its value depends on the length of the beam and the buckling curve of the cross-section (Al-Emrani, 2018).

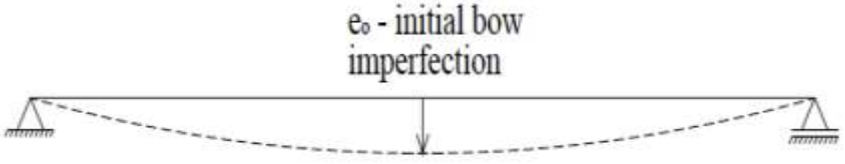

$$M_{II} = N \cdot \left(\frac{N_{cr}}{N_{cr}-N} \cdot (e_{0,d} + v_1)\right) \text{.....(2.22)}$$

$$M_{II} = M_I + M_{II} \text{.....(2.23)}$$

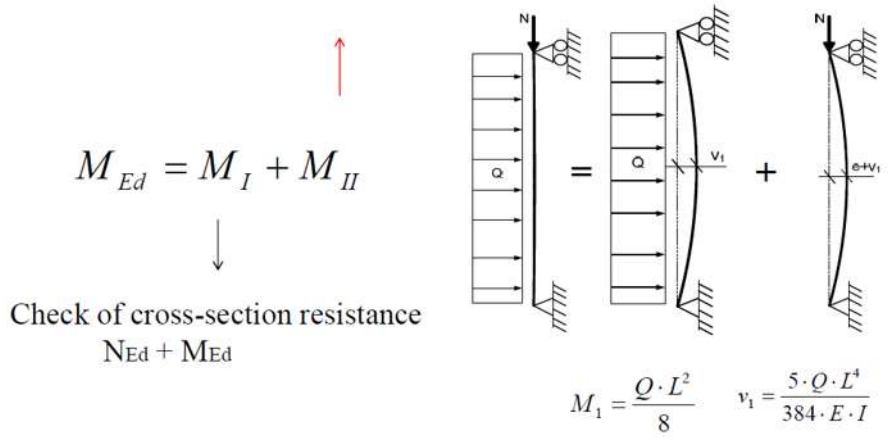

Figure 2-18: Initial bow imperfection.

2.9 Lateral Torsional Buckling.

When a beam is bent about the axis of greatest flexural rigidity it may twist before it reaches its strength limit state. This stability limit state is most commonly referred to as lateral torsional buckling of a beam, see Figure 2-18. (P. A. G., et al., 2000).

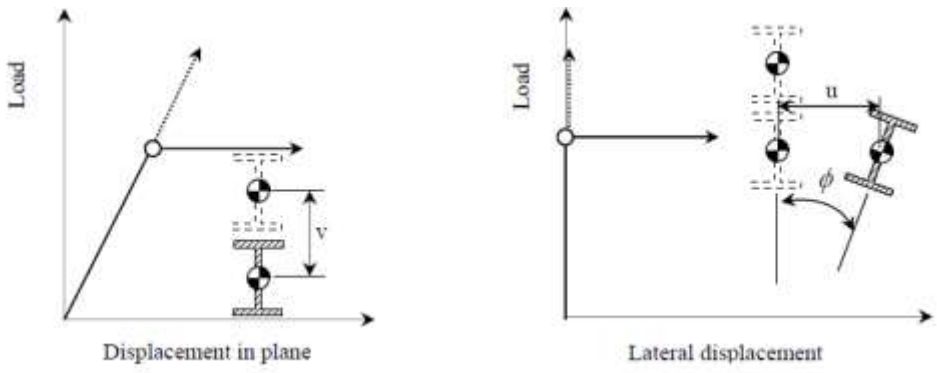

Figure 2-19: Lateral Torsional buckling concept

The lateral torsional buckling of beams (Figure 2-19) includes both lateral displacements out of the plane of bending and twist rotations. In this case, the twist rotations create the applied moments which act like out of original plane of bending. In addition, the lateral

rotations make the applied moments to cause torque around the axis of twist on the shear center.

2.10 Simple approach to LT-buckling

Based on (Al-emrani & Åkesson, 2013) rather simplified manner by considering the basic situation of a simply supported, double symmetric I beam with fork supports, loaded with equal and opposite moment. In this thesis, the simplified approach which consider that the bending moment acting on the beam is resisted by a couple of forces in the upper (compression) and lower (tension) flanges. The forces, F, in each flange is constant along the flange length (the beam is subjected to a constant moment) and can easily be calculated as N=M/h, with h being the distance between the center of the gravity of the two flanges, see Figure 2-20.

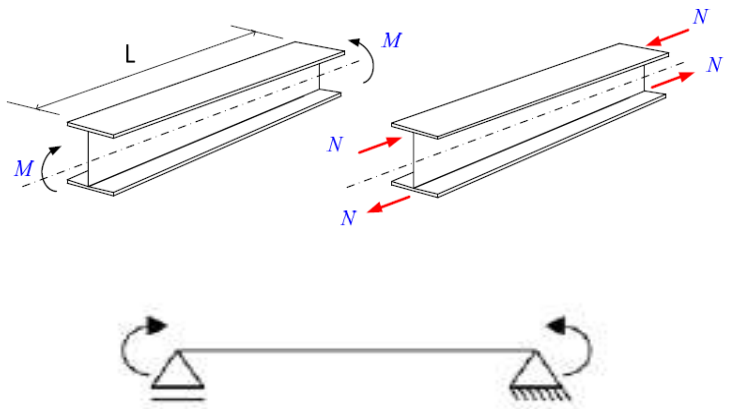

Figure 2-20: Column analogy for the compression flange in I beam along with fork support

2.11 Critical buckling moment in NCCI-SN003a-EN-EU.

Based on (SN003a-EN-EU, August 2007), the critical buckling moment for a laterally unrestrained beam.

$$M_{cr,0} = \frac{I^2 \cdot EI_2}{L^2}\sqrt{\frac{I_w}{I_s} + \frac{L^2 \cdot GI_t}{\pi^2 \cdot EI_2}} \quad \text{.....(2.24)}$$

According to (Al-emrani & Åkesson, 2013) the three relevant cross-section constants which mentioned on the top are all found on the critical buckling moment. A more general expression which can be applied in more general support and loading conditions is the so-called the three-factors formula given in Equation 2.25 below. The new factors in this formula also reveal the influence of other factors affecting the lateral-torsional behavior of beams in bending.

The elastic critical moment is derived and formulated from the buckling theory-corrugated I beam: The extra capacity in terms of critical buckling lateral torsional buckling moment obtained for girders with corrugated webs is attributed to an increased torsional constant by introducing equation (2.30).

$$M_{cr} = \frac{\pi^2 \cdot EI_z}{L^2}\sqrt{\frac{I_w}{I_z} + \frac{L^2}{\pi^2 EI_z}(GI_t + C_w)} \quad \text{.....(2.25)}$$

The second moment of area about the weak axis:

$$I_z := \frac{t_f \cdot {b_f}^3}{6} \quad \text{.....(2.26)}$$

The torsion constant:

$$I_t := \frac{1}{3} \cdot \left(2 \cdot b_f \cdot {t_f}^3 + h_w \cdot {t_w}^3\right) \quad \text{.....(2.27)}$$

The warping constant:

$$I_w := \frac{I_Z \cdot (h_{beam} + t_f)^2}{4} \quad \text{.....(2.28)}$$

$$u_x := \frac{h_w}{2 \cdot G_a \cdot t_w} + \frac{{h_w}^2 \cdot (a+b)^3}{25 \cdot a^2 \cdot E \cdot b_f \cdot {t_f}^3} \quad \text{.....(2.29)}$$

$$C_w := \frac{(2 \cdot d)^2 \cdot {h_w}^2}{8 \cdot u_x \cdot (a+b)} \quad \text{.....(2.30)}$$

According to (SN003a-EN-EU, August 2007), Elastic critical moment for lateral torsional buckling provides the following table document stated that the C1 and C2 factors depend on various parameters: section properties, support conditions, and moment diagram.

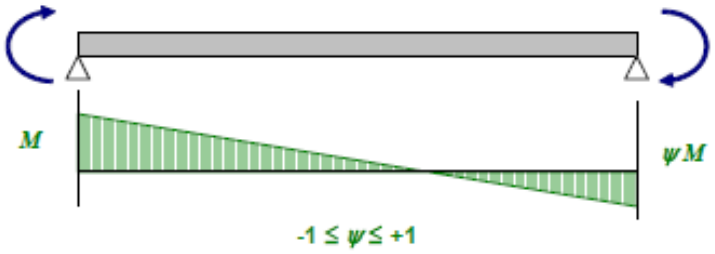

Figure 2-21: Moment distribution factor C1 for moment with end moment only.

Loading and support conditions	Bending moment diagram	C_1	C_2
		1,127	0,454
		2,578	1,554
		1,348	0,630
		1,683	1,645

Note : the critical moment M_{cr} is calculated for the section with the maximal moment along the member

Figure 2-22: Moment distribution factor C1 for various loading and support conditions.

CHAPTER 3 METHODS AND MATERIAL

In this chapter, is divided into two main sections, methodology and FE-Modeling along with hand calculation verification procedures. First section, the research methods and sampling techniques are presented. Besides, the main reason why specific methods were chosen also explained. The main research strategy chosen were quantitative and systematic sampling. Second, FE-modeling procedures and output-data verifications for conducting this paper are presented. Each verifications parts regards both hand and FE-analysis procedures.

3.1 Research method

3.1.1 Research strategy.

Research can be classified as qualitative research and quantitative research when the issue at hand is the approaches to be employed in conducting research. Regardless for this paper the author was chosen quantitative research which will focuses on the quantifying the collected FE-simulations data as well as hand verification. In addition, a deductive approach also used since the research gave emphasis to compare the provisional hypothesis. Then, it was planned to test the hypothesis is lead to either confirmation or rejection.

3.1.2 Sampling data

Since it is difficult to focuses on the whole population of data, here it is trying to draw a sample to represent a total population. Sampling is the process of selecting a number of representatives from its defined population. Thus, systematic random sampling technique were used for the sake of time and fund saving.

The theoretical concept and the formulated hypothesis are stated qualitatively on the previous section. Here, the statement tries to present the experiment quantitatively. The analysis process is intended to gather the information resulted by simulating the sampled beams using computer software. The simulation is carried out by using ABAQUS software finite element analysis method.

Three categories of data are considered with three different customs. Which take account of very low slender, intermediate and very slender samples, totally, the samples are 15 flat web beams with three slenderness category and 15 corrugated web beams with the same three slenderness category (0.3,0.6,1.2 range). Besides, both sampling categories consider comparison and controlling parameters which means one girder with flat web and an identical girder with corrugated web with in particular engineering parameters like cross section data and material property.

Table 3-1: Sample recorded

			Flat Web				Corrugated			
	Trial	h_w (mm)	t_w (mm)	Ls(m)	b_f	t_f	a	b	d	angle(α)
	1	150	3	1.5	75	5	70	29	25	60
	2	200	4	2.4	100	7	70	31	33	65
I	3	250	5	3.5	125	8	70	31	42	70
	4	300	6	4.8	150	10	70	47	50	65
	5	350	7	6.3	175	12	70	42	58	70
	6	450	8	8	225	14	70	67	58	60
	7	500	9	8.8	250	16	70	54	58	65
II	8	550	10	10.1	275	18	70	42	58	70
	9	650	12	12.7	260	22	70	67	58	60
	10	750	12	12.7	300	22	70	54	58	65
	11	1000	14	1.5	400	22	70	45	39	60
	12	1050	14	1.0	420	14	70	47	50	65
III	13	1100	12	1.5	440	12	70	42	58	70
	14	1200	10	1.5	480	10	70	31	42	70
	15	1500	16	2	600	16	70	54	58	65

Note: Values are in millimteres except for the span lenngth.

h_w, t_w – web height and thickness

b_f, t_f – flange width and thickness

Ls – sample length

a-Length of longitudinal panel

b-Projected length of inclined panel

c-Length of inclined panel

d-Maximum eccentricity of web

α-Angle of inclined panel

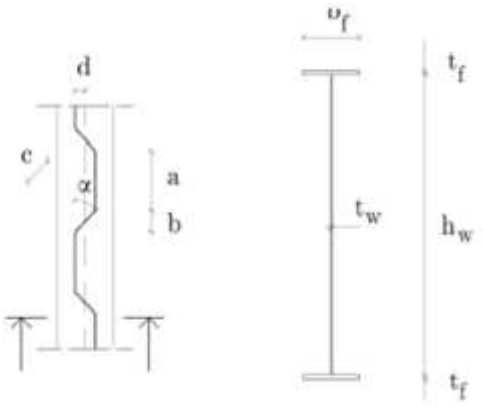

Figure 3-1: Notations of the geometry of the cross section and corrugation profile.

The data collecting contains categorizing the flat and corrugated web beam in equal amount sampling. As presented on table top 15 samples were taken from each category. Totally, the encountered samples are 30. All samples modeled separately and analyzed accordingly. Both the flat and corrugated web beams are taken as universal beam based on their shape. Finally, as it can be seen below on Table 3-1. Sample recorded data has been chosen to have a better understanding about the real-life scenario. Here is down below, the cross-section dimensions which were generated systemically for the consideration of non-dimensional slenderness value with in datum line: 0.3,0.6,1.2. For the encountered samples, all parameters were included as consequative trials.

3.2 Finite element model (FEM)

The finite element model is used for the structural model which helps to illustrate and understand the real physical structure. To execute a finite element model material property as well as the geometry and boundary conditions have been determined. Besides, to generate the detail understanding of the structure, the simulation was carried out by using advance finite element analysis software, ABAQUS CAE 2017.

3.2.1 Design Assumptions and Procedure

3.2.1.1 Structural Model

The main objective of this thesis, as mentioned in previous sections, is to determine and investigate the behavior of beams with corrugated webs in terms of lateral torsional

buckling as well as the model is to represent the conditions of reality as good as possible, the model illustrates a physical model of I-beam section where the structural behavior is shown with structural elements and boundary, see Figure 3-2. In order to achieve this, certain material assumptions will use the approximation adopted in (EN-1993-1-1, 2005), where the stress-strain relationship is assumed to follow an elastic-plastic material with strain hardening.

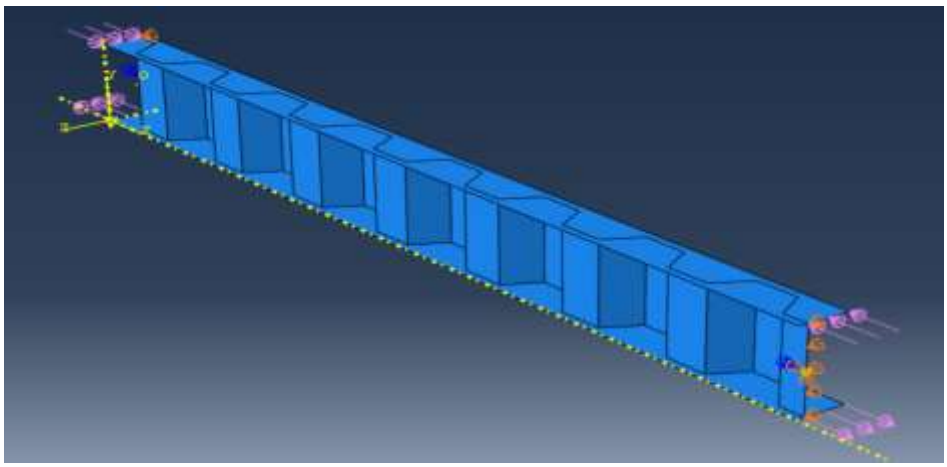

Figure 3-2: Corrugated I beam load

3.2.1.2 Boundary conditions.

The boundary conditions are equivalent to fork supports at the ends and are simulated as follows; The support system can be seen Figure 3-3 and 3-4, these boundary conditions have been applied according to the coordinate system in the figure below.

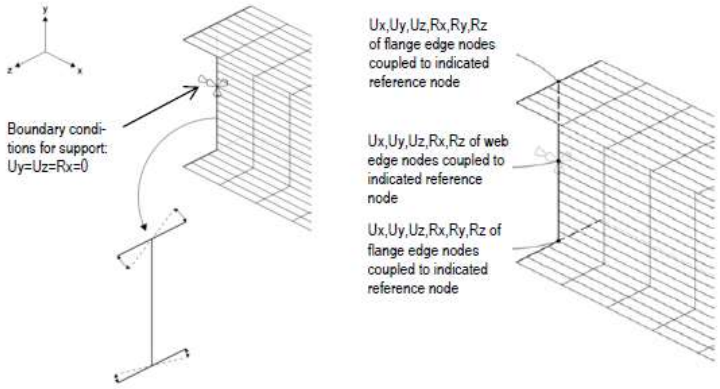

Figure 3-3: Boundary conditions for support on the left, kinematic coupling constraints for the cross-section on the right

- First point a: is restrained in all coordinate directions at x, y and z. And it is also free to rotate about the longitudinal axis (x). However, no lateral and torsional displacement on the supported section.
- Second Point b: is also restrained from translating in vertical (z) and lateral (y) direction. However, it is restrained to rotate on longitudinal axis (x).
- Line A and line B are restrained to displace in the lateral (y) direction, see figure below.

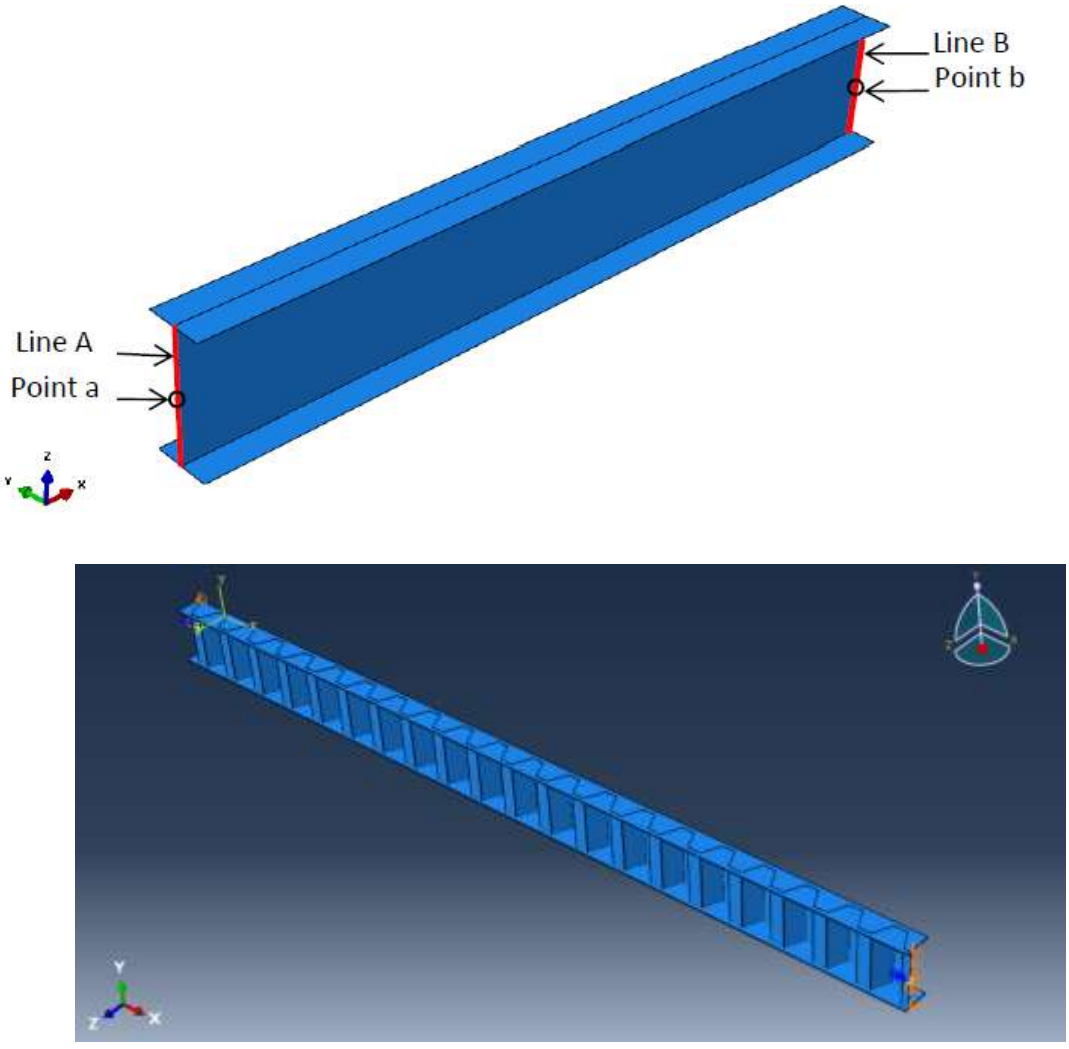

Figure 3-4: boundary conditions.

3.2.1.3 Load distribution.

In order to simulate a constant moment, an evenly distributed load should be applied on the flanges of the beam. Beams have been modelled as a simply supported with fork-end

boundary conditions and load as pure bending. In order to simulate a constant moment, an evenly distributed load have been applied on the flanges of the beam.

Since ABAQUS do not use pure bending simulation, it was chosen to use "Shell edge loading" type of loading to be able to compare the results with empirical hand calculation. Thus, for all types of beams the load has been considered to apply a constant moment of 100kNm in both directions, see Figure 3-5.

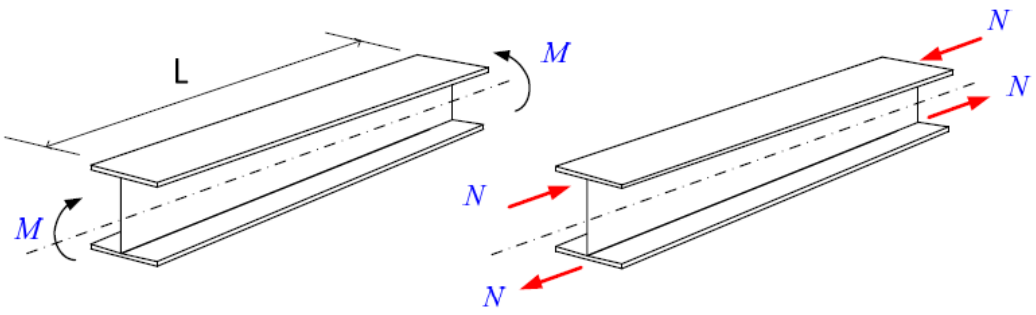

Figure 3-5: Simplified approach for pure bending

The calculation of shell edge loading has been carried out as follow as it can be seen, Figure 3-6 in order to get a moment of 100kNm.

$$M = F_{\text{shell edge}} * b_f * h \quad \text{.....(3.1)}$$

where $h = t_w + h_w$

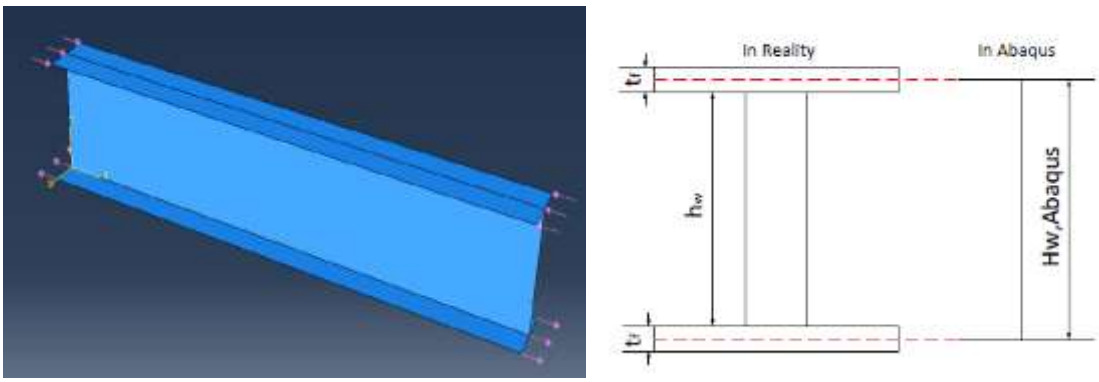

Figure 3-6: Abaqus Shell edge loading.

3.2.1.4 Material Properties.

The value of the steel material such as yield stress, elastic modulus as well as ultimate stress and a plastic strain was obtained from Eurocode 3 and presented in Table 3-2, and

Figure 3-7, a table that summarizes the material properties that is being used for the elastic-plastic material.

Steel class	S355
Yield stress, f_y [MPa]	355
Ultimate stress, f_{uy} [MPa]	600
Elasticity modulus E,[GPa]	210
plastic strain, ε	0.1167
Poisson's ratio, v	0.3

Table 3-2: Material properties of steel

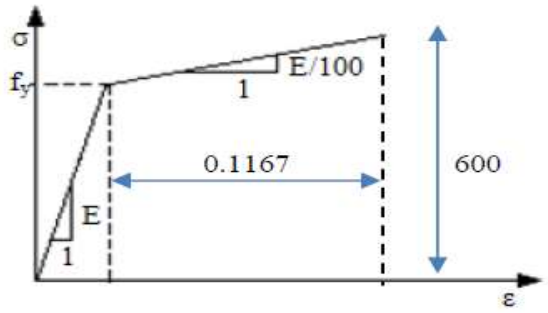

Figure 3-7: The elastic-plastic material

3.2.1.5 Mesh convergence study

The mesh convergence study was made to find out for an appropriate mesh size to be chosen. The results from the analysis are highly dependent on the mesh size, ratio of the sides and internal angles of the mesh. These parameters decide the accuracy of the results. Therefore, mainly depending on the size of span of beam, either four or five mesh sizes were decided to be studied. For instance, for Model-2 on as it can be seen below, mesh size 30,25,20,15, and 10. Thus, based on the results of the mesh convergence study, the mesh size for flat web and corrugated that is going to be used for analysis was chosen to be 25 and 10 respectively since the curve down below converge as an inflection point which leads to an acceptable size of the mesh, see Figure 3-8.

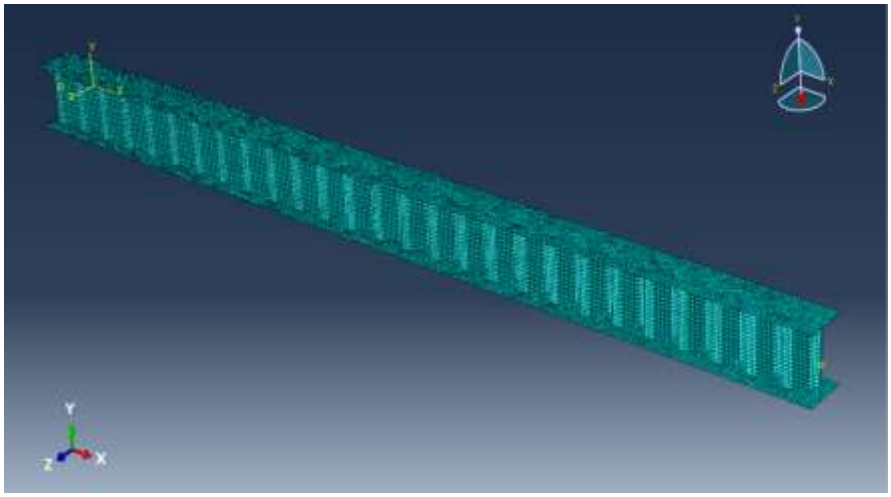

Figure 3-8: Mesh the geometry

Flat web

	Linear Buckling		
Flat	Mesh	Eigen value	
1st	30	0.55422	Mode 1
2nd	25	0.55388	Mode 1
3rd	20	0.56872	Mode 1
4th	15	0.56825	Mode 2
5th	10	0.57543	Mode 1

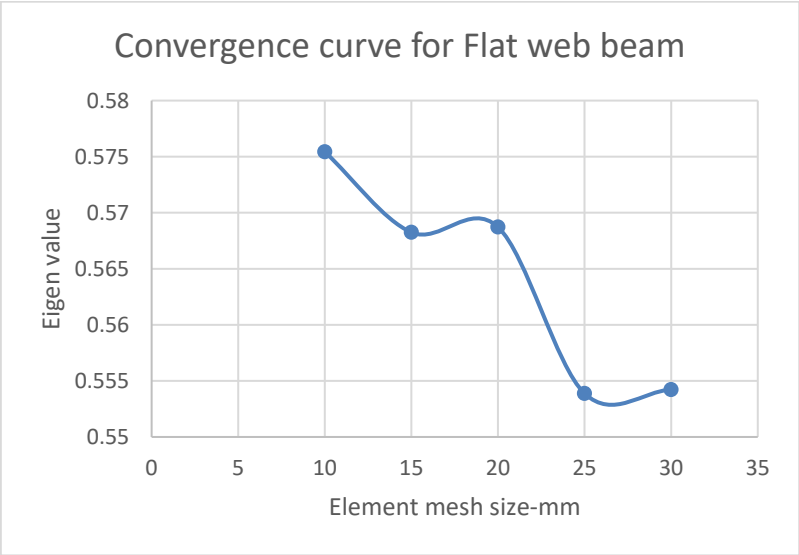

Corrugated web

	Linear Buckling		
corrugated	Mesh	Eigen value	
1st	25	0.70364	Mode 1
2nd	20	0.70775	Mode 1
3rd	15	0.70683	Mode 1
4th	10	0.71323	Mode 1

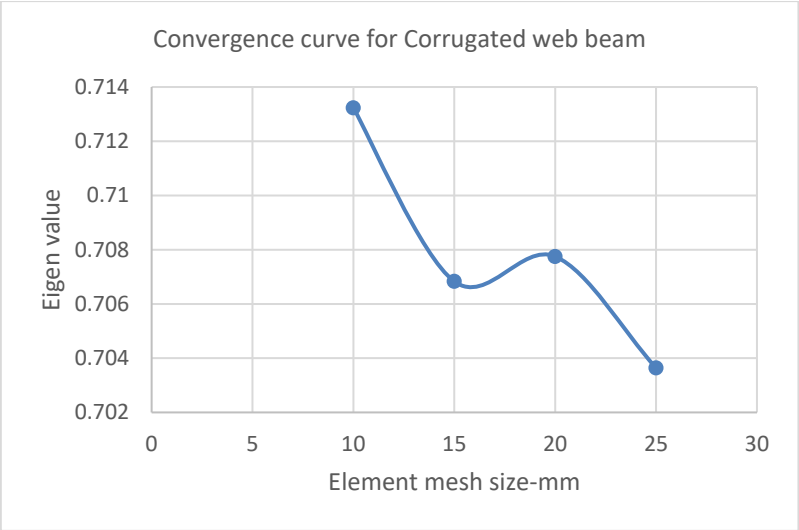

Figure 3-9: Convergence curve for corrugated web vs Flat web

3.3 Verification

To verify the FE-Model a selected part of the structure has been analyzed according to (EN-1993-1-1, 2005) and (SN003a-EN-EU, August 2007): Elastic critical moment for lateral torsional buckling codes of standard for both corrugated and flat webs. To verify the FE-model some checks have been made. One of the checks that is included in the verification of the FE models are categorized into three methods. Which is Static analysis (linear material), Linear buckling (linear material) and non-linear analysis (elastic-plastic material). To study the mesh convergence as well as the credibility of the empirical calculation in three methods is also verified using FE-model, with Abaqus software. Besides, a comparison of empirical calculation with FE model is also executed.

3.3.1 Hand calculation verification

3.3.1.1 Static analysis (linear material)

Deflection and stresses have been calculated here in this hand calculations to verify the model and mesh density. However, for corrugated, the contribution of web to bending is very small so only consider the flanges in the section modulus.

3.3.1.2 Linear buckling (linear material)

Elastic critical moment for lateral torsional buckling gives the formula of the, Mcr elastic critical moment for doubly symmetric cross-sections. This helps to calculate the elastic critical moment from the following formula that derived from buckling theory (SN003a-EN-EU, August 2007).

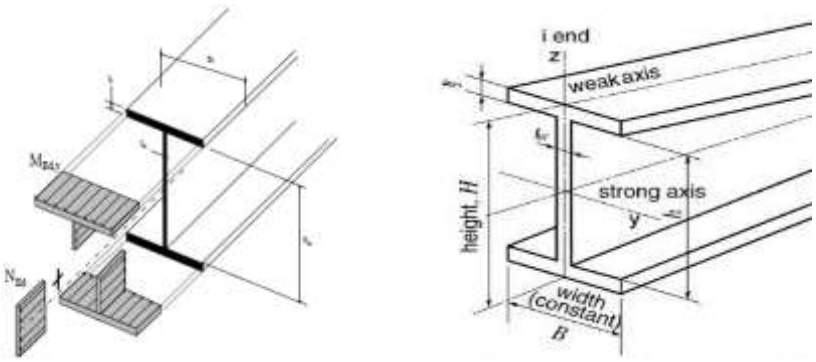

Figure 3-10: Moment of inertia -weak and strong axis

The moment of inertia about the weak axis, the warping constant and the torsion constant It have been calculated using the same expressions for girders with flat webs. However, the contribution of the corrugated web to the moment of inertia around the weak axis is negligible since corrugated the webs contribution to bending is very small., so it was only considered the flanges in the section modulus. Besides, the above calculation is also dependent on class of web and flange. For instance, refer, Model 14, Appendix section. when both flange and web were class IV, and where hand verification was so complicated since there was asymmetry, I beam section due to reduction factor, refer Figure 3-11.

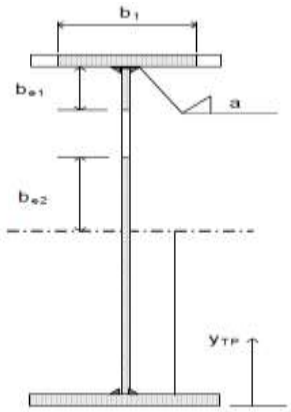

Figure 3-11: Asymmetry I beam section.

3.3.1.3 Non-linear analysis (elastic-plastic material)

Here in this step a non-linear material property has been considered including with geometrical and material non-linearity. In addition to that, the linear buckling analysis has been used it in the non-linear analysis, by assuming a geometrical imperfection shape as the LT-shape. The geometrical imperfections and residual stresses are taken into account by defining a maximum deformation to the first buckling mode and using it as the initial geometry of the beam in the non-linear analysis. The maximum deformation is defined as the initial bow imperfection in (EN-1993-1-1, 2005), in Table 5.1. Its value depends on the length of the beam and the buckling curve of the cross-section as is shown below.

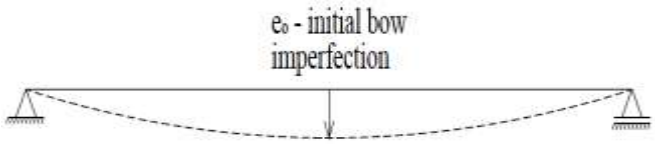

Figure 3-12: initial bow imperfection.

The lateral-torsional buckling of a beam in bending has been considered based on (EN-1993-1-1, 2005) (section 5.3.4) by a factor *k* which multiplying the initial bow imperfection. Thus, no additional torsional imperfection needed as long as the procedures follow the following formula. The value of *k* is equal to 0.5.

$$e_{max} = k * e_0 \quad \text{..... (3.2)}$$

3.3.2 FE-analysis validation

As it has been discussed FE-analysis of the paper is divided into three types which is dependent on the output data and level of simulation which are: a static analysis, a buckling analysis and a second order buckling analysis. To perform geometrically and materially nonlinear analysis including imperfections for steel I -beam lateral torsional buckling, the size and shape of the geometric imperfection can be obtained from EN 1993-1-1. The shape is prescribed as an initial bow along the weak axis of the section, excluding torsion of the cross-section, refer Appendix Model 1. The shape of the imperfection be able to alternatively be taken equal to the lateral torsional buckling mode, including torsion. Several tables and formulas referred to determine the size of the imperfection. Further advance type of design rules (Non-linear) is considered for the case that a plastic cross-section to be used in non-linear Finite Element Analyses (FEA) for lateral torsional buckling of beams.

Within each model has been executed with a sequence of one or more analysis steps. Each step sequences provides same type of loading and boundary conditions for regarding model. In addition, steps are executed with FEM the analysis procedure, the data output, and various controls with by using advance finite element analysis software, ABAQUS CAE 2017.

3.3.2.1 A static analysis-FEM procedure

The first analysis type is a “Static, General”, which was used for the static analysis and it helps to obtain for stable problems which include only linear elastic material behavior. The procedure type is General and Static is used to obtain the stresses, deformations and reaction forces. Particularly, for this paper, the maximum number of increments was chosen to the fixed value of 100 with increment size 1. The equation solver method was direct with full Newton as solution technique. see Figure 3-13.

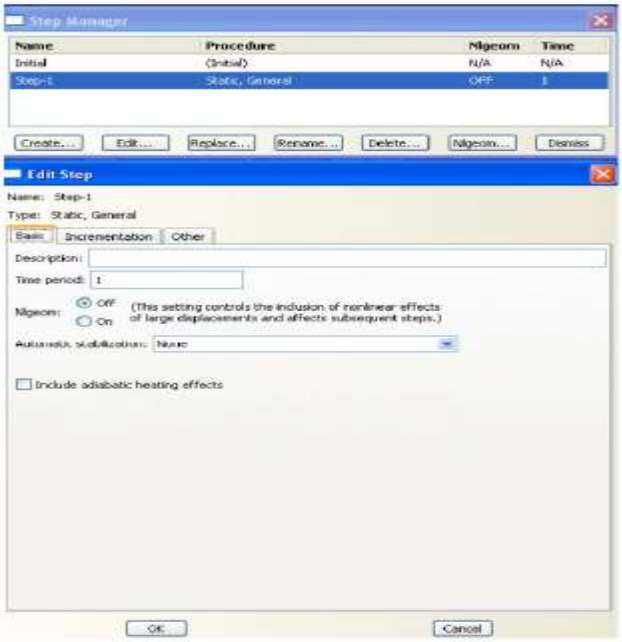

Figure 3-13: Analysis -Step manager- static analysis

3.3.2.2 A buckling analysis--FEM procedure

This type of procedure so called "Linear perturbation, buckle" which helps to execute the buckling analysis. As it is explained on Abaqus manual, at linear buckling analysis the linear buckling load capacity estimated with the formula of 3.3. This method executed an iteration based an assumption of small deformation before the collapse. The algorithm solves carried out its iteration on the linearized eigenvalue problem in EQ1 with consideration of preloading the structure as a shell load reference load, P_{ref}. Thus, the procedural eigen pair (eigenvalue and eigenmode) are formulated as follow.

$(K-\lambda K)\Phi=0$…..Eq(1) $P=\lambda P_{ref}$.....Eq(2)……(3.3)

The python scripting has been used in this method since the first buckling curve mode was of major interest as follow. This procedure analysis is also used as a startup for non-linear buckling analysis iteration which would give a complete information regarding the collapse of the structure.

" *NODE FILE, GLOBAL=YES, LAST MODE=1"
" U "

At last, the eigenvalue which obtained in this method from Abaqus was compared to the reduction factor χ for comparison of the FE-results and hand-calculations on the next chapter.

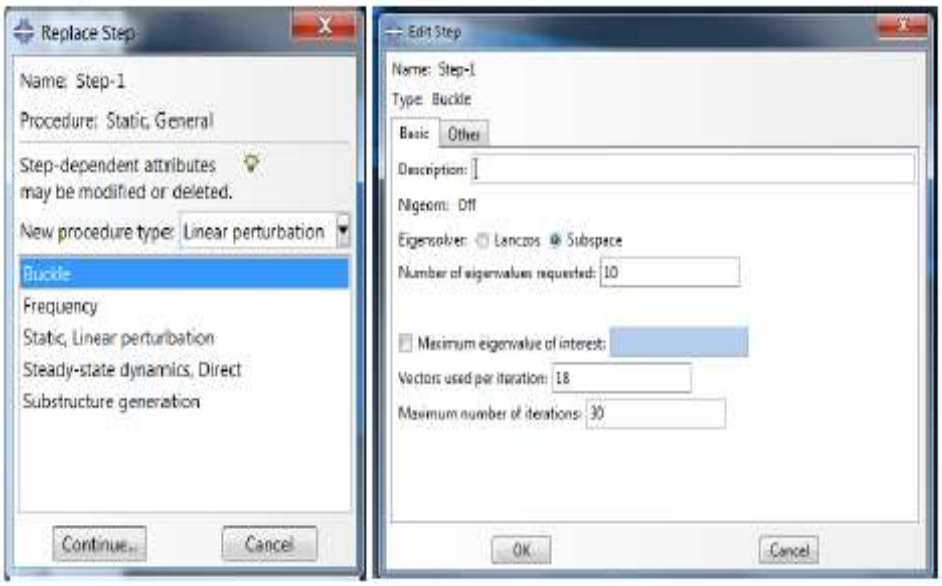

Figure 3-14: Analysis -Step manager- buckling analysis

3.3.2.3 A second order buckling (Non-linear analysis)- -FEM procedure

Regarding FEM procedure for the second order buckling analysis (non-linear analysis), which names a “Static, Risks” are applied. This analysis type is executed by targeting the limit load for structures which leads to unstable collapse. Besides, it is possible to include geometrical both initial geometrical and material imperfection as well as residual stress according to (EN-1993-1-1, 2005), in Table 5.1.

To summarize, this method has a FEM-algorithm that helps to computes the non-linear buckling load capacity for a more realistic structural behavior, which means. with geometrical imperfections, residual stresses and non-linear material behavior.

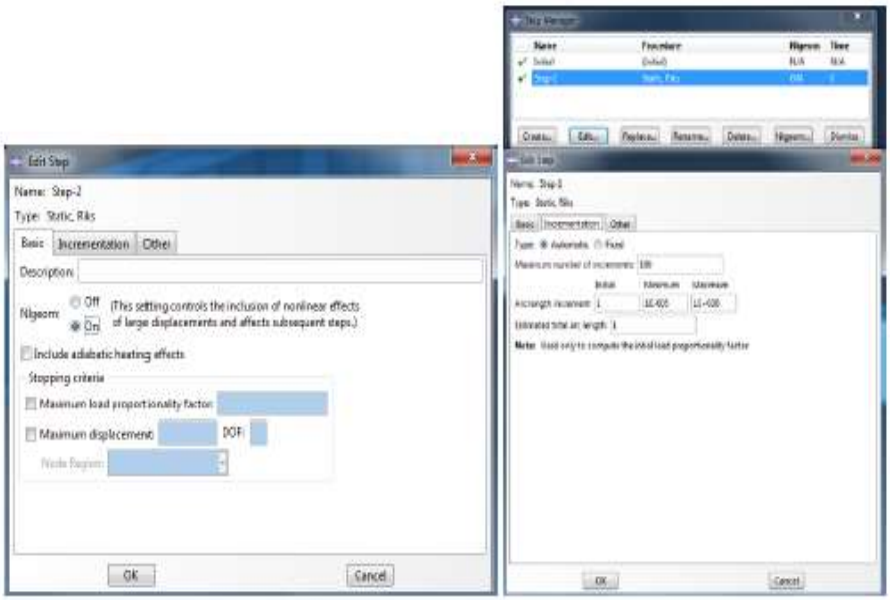

Figure 3-15: Analysis -Step manager- nonlinear analysis

Based ABQUS manual. FEM-algorithm has been carried out with procedural iteration with automatic load stepping process. In the non-linear buckling analysis, the load was applied in 100 increments regarding this research paper. The mentioned geometrical imperfection was calculated with hand based (EN-1993-1-1, 2005) and included at python script of the non-linear model by adding following line of code.

" *IMPERFECTION, FILE=**.fil*, STEP=1"
" 1, *(e*0*_L)"*

```
*IMPERFECTION, FILE=Job-6, STEP=2
1, 42.3333
** STEP: Step-1
**
*Step, name=Step-1, nlgeom=YES
*Static, riks
0.1, 1., 1e-05, , ,
```

Figure 3-16: nonlinear python script

CHAPTER 4 RESULT AND DISCUSSION

This chapter provides the results which are obtained from the conducted research. The results are presented with associated reflections and summary based on the scientific theory which has been collected on a literature review to easier follow the reasoning.

4.1 Introduction based on theory.

This section intentions to give a remark and reflect about the significant choices and observations that has been made throughout the comparison study regarding both corrugated and flat web I beam section.

Thus, the results are presented to the reader into separate three parts as it mentioned on the top. Each part including both an empirical calculation which based on formulas presented in EN-1993-1-1 (2005) as well as NCCI: Elastic critical moment for lateral torsional buckling (SN003A-EN-EU) and Abaqus (FE-model) results. For each model, resulted hand empirical calculation and Abaqus values are presented below in comparison manner. The deviation between the analytical and Abaqus software result is computed in percentage. The difference occurred is due to the consideration of residual stress and geometrical imperfection. In other words, with help of FE software (Abaqus), the result obtained is more realistic and accurate. For instance, imperfection, residual stress and plastic type material properties are added by using Python scripting which leads to execute both a buckling analysis and a second order buckling analysis (non-linear). Abaqus software computes Eigen value buckling analysis whereas by using the analytical method only M_y and M_{cr} are computed. The difference encountered labeled as percentage as follow.

4.2 Very slender principal behavior

Most of the current research papers elaborated that a slender beam which subjected to moment around its stiff axis may fail due to instability. Those instability behaviors undergo to lateral and torsional deformation which is called lateral torsional buckling. Regarding resistance of lateral torsional buckling, RHS/SHS-rectangular/square hollow sections have even effective flanges and also less slender than I beam. The main reason which resistance of LTB-Lateral torsional buckling is affected by the stiffness of the cross section around

the strong axis. However, the I beam with the wider flange is the stiffer when it comes to torsion since the web contribution is almost negligible. Thus, this research paper gives a remark regarding utilizing possible additional contribution to the lateral torsional resistance using corrugated web instead of flat web I beam section. For the sake of controlling parameters same flange dimensions and cross section height has been used for the comparison.

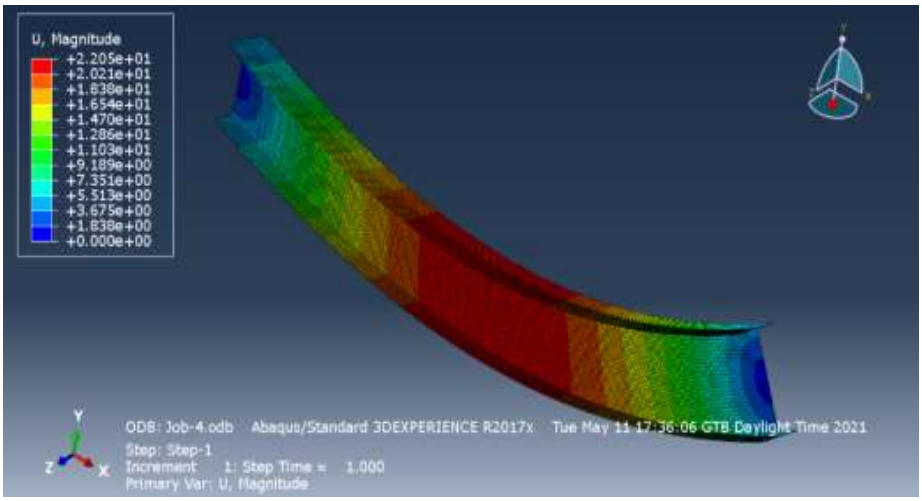

Figure 4-1: 3D illustration of the obtained deformation for Flat web

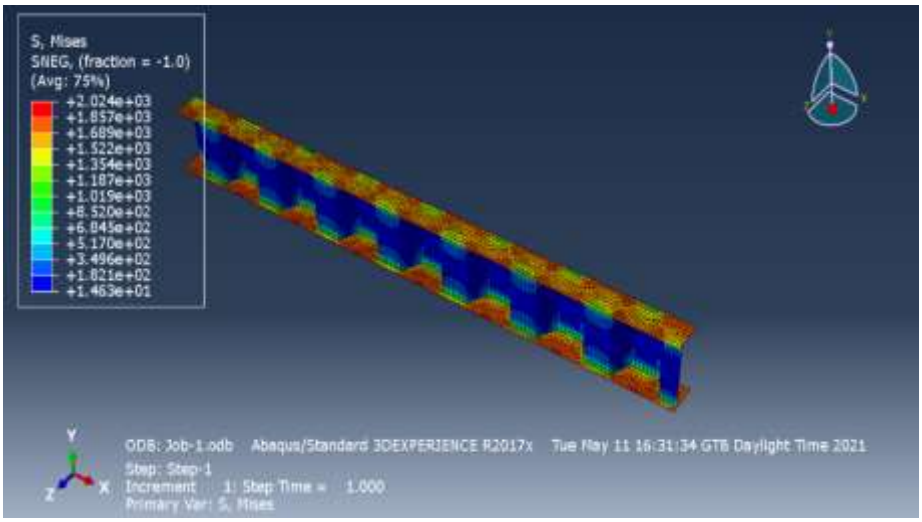

Figure 4-2: 3D illustration of the obtained stress for corrugated web

Table 4-1-Result Model 7

Model-7 Slenderness

h_w *(mm)*	t_w (mm)	Ls (m)	b_f (mm)	t_f (mm)	Corrugation profile					Flat Web	Corrugated Web
					a	b	d	α		λ=(My/Mcr)^0.5	λ=(My/Mcr)^0.5
500	9	8.8	250	16	70	54	58	65		1.54	1.14
										very slender	Intermediate

Flat web							
	Static analysis						
	Analytical	Abaqus	Difference (%)				
δ [mm]	7.39	8.012	-8.88%				
σ [mPa]	42.46	45.23	-6.12%				
	Linear buckling						
	Analytical		Abaqus			Difference (%)	
δ [mm]	My	Mcr	Mref	Eigenvalue	McrAbaqus		
σ [mPa]	932.41	394.191	100	4.0945	409.45	-3.87%	
	Ultimate strength						
	Analytical Eurocode			Abaqus			
δ [mm]	Mult	λ=(My/Mcr)^0.5	χ	MultAba	λ=(My/McrAbaqus)^0.5	χ=Mult/My	Diff Mult
σ [mPa]	304.81	1.54	0.33	321.23	1.51	0.34	-5.39%

Corrugated web							
	Static analysis						
	Analytical	Abaqus	Difference (%)				
δ [mm]	8.65	9.51	-9.90%				
σ [mPa]	49.94	51.63	-3.39%				
	Linear buckling						
	Analytical		Abaqus			Difference (%)	
δ [mm]	My	Mcr	Mref	Eigenvalue	McrAbaqus		
σ [mPa]	732.72	565.367	100	5.8145	581.45	2.77%	
	Ultimate strength						
	Analytical Eurocode			Abaqus			
δ [mm]	Mult	λ=(My/Mcr)^0.5	χ	MultAba	λ=(My/McrAbaqus)^0.5	χ=Mult/My	Diff Mult
σ [mPa]	355.385	1.14	0.49	371.85	1.12	0.55	4.43%

Table 4-2-Result Model 8

Model-8 Slenderness

h_w *(mm)*	t_w (mm)	Ls (m)	b_f (mm)	t_f (mm)	Corrugation profile					Flat Web	Corrugated Web
					a	b	d	α		λ=(My/Mcr)^0.5	λ=(My/Mcr)^0.5
550	10	10.1	275	18	70	42	58	70		1.58	1.12
										very slender	Intermediate

Flat web							
	Static analysis						
	Analytical	Abaqus	Difference (%)				
δ [mm]	6.48	7.23	11.62%				
σ [mPa]	31.26	32.56	-4.0%				
	Linear buckling						
	Analytical		Abaqus			Difference (%)	
δ [mm]	My	Mcr	Mref	Eigenvalue	McrAbaqus		
σ [mPa]	1266.59	508.07	100	5.2123	521.23	-2.59%	
	Ultimate strength						
	Analytical Eurocode			Abaqus			
δ [mm]	Mult	λ=(My/Mcr)^0.5	χ	MultAba	λ=(My/McrAbaqus)^0.5	χ=Mult/My	Diff Mult
σ [mPa]	398.65	1.58	0.31	422.74	1.56	0.33	-6.04%

Corrugated web							
	Static analysis						
	Analytical	Abaqus	Difference (%)				
δ [mm]	7.6	8.01	-5.37%				
σ [mPa]	36.68	38.56	5.12%				
	Linear buckling						
	Analytical		Abaqus			Difference (%)	
δ [mm]	My	Mcr	Mref	Eigenvalue	McrAbaqus		
σ [mPa]	998.12	798.556	100	8.2345	823.45	3.02%	
	Ultimate strength						
	Analytical			Abaqus			
δ [mm]	Mult	λ=(My/Mcr)^0.5	χ	MultAba	λ=(My/McrAbaqus)^0.5	χ=Mult/My	Diff Mult
σ [mPa]	494.427	1.12	0.5	510.42	1.10	0.51	3.13%

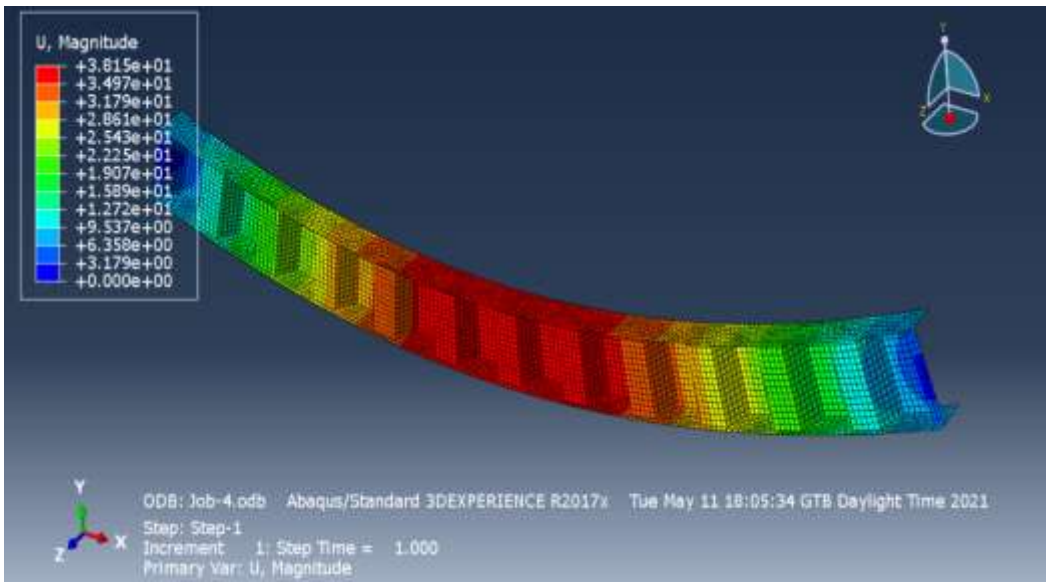

Figure 4-3: 3D illustration of the obtained deformation at corrugated web

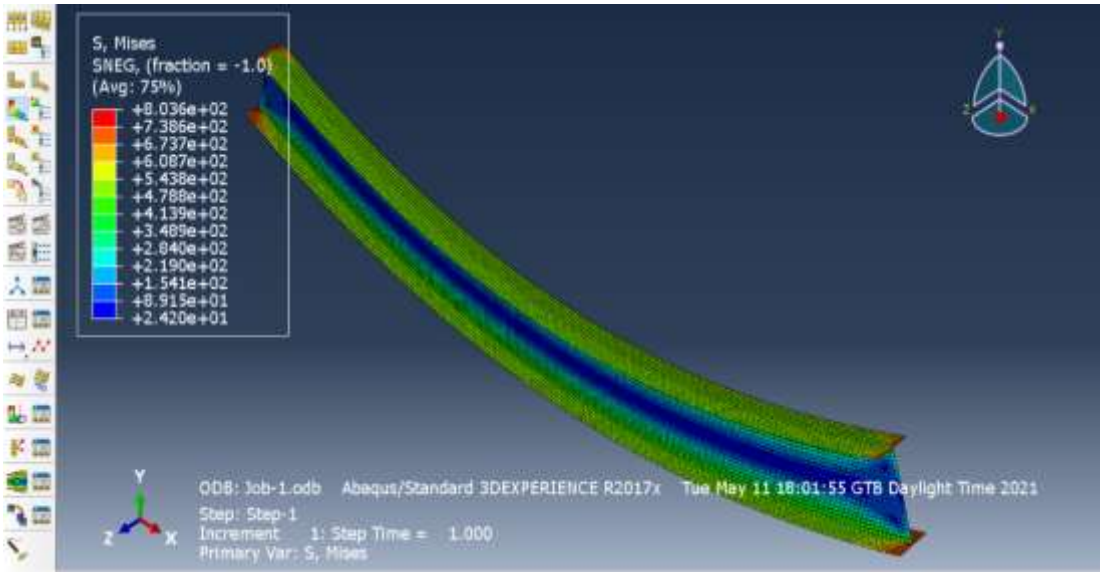

Figure 4-4: 3D illustration of the obtained stress at Flat web

Table 4-3-Result Model 3

Model-3										Slenderness	
h_w *(mm)*	t_w (mm)	Ls (m)	b_f (mm)	t_f (mm)	Corrugation profile					Flat Web	Corrugated Web
					a	b	d	α		λ=(My/Mcr)^0.5	λ=(My/Mcr)^0.5
250	5	3.5	125	8	70	31	42	70		1.29	0.94
										very slender	Intermediate

Flat web							
	Static analysis						
	Analytical	Abaqus	Difference (%)				
δ [mm]	18.32	16.29	11.08%				
σ [mPa]	334.14	352.1	-5.10%				
	Linear buckling						
	Analytical		Abaqus			Difference (%)	
δ [mm]	My	Mcr	Mref	Eigenvalue	McrAbaqus		
σ [mPa]	119.32	71.61056606	100	0.76871	76.871	-7.35%	
	Ultimate strength						
	Analytical Eurocode			Abaqus			
δ [mm]	Mult	λ=(My/Mcr)^0.5	χ	MultAba	λ=(My/McrAbaqus)^0.5	χ=Mult/My	Diff Mult
σ [mPa]	49.56	1.29	0.42	51.23	1.25	0.43	-3.37%

Corrugated web							
	Static analysis						
	Analytical	Abaqus	Difference (%)				
δ [mm]	21.90	18.81	14.12%				
σ [mPa]	399.49	385.65	-3.46%				
	Linear buckling						
	Analytical		Abaqus			Difference (%)	
δ [mm]	My	Mcr	Mref	Eigenvalue	McrAbaqus		
σ [mPa]	91.59	103.1840943	100	1.1018	110.18	6.35%	
	Ultimate strength						
	Analytical Eurocode			Abaqus			
δ [mm]	Mult	λ=(My/Mcr)^0.5	χ	MultAba	λ=(My/McrAbaqus)^0.5	χ=Mult/My	Diff Mult
σ [mPa]	54.45462402	0.94	0.59	57.46	0.91	0.63	5.23%

Table 4-4-Result Model 4

	Model-4									Slenderness	
h_w (mm)	t_w (mm)	Ls (m)	b_f (mm)	t_f (mm)	Corrugation profile					Flat Web	Corrugated Web
					a	b	d	α		λ=(My/Mcr)^0.5	λ=(My/Mcr)^0.5
300	6	4.8	150	10	70	47	50	65		1.42	1.05
										very slender	Intermediate

Flat web							
	Static analysis						
	Analytical	Abaqus	Difference (%)				
δ [mm]	16.02	14.1398	11.74%				
σ [mPa]	186.92	175.176	6.70%				
	Linear buckling						
	Analytical		Abaqus			Difference (%)	
δ [mm]	My	Mcr	Mref	Eigenvalue	McrAbaqus		
σ [mPa]	213.00	105.5364362	100	1.1641	116.41	-10.30%	
	Ultimate strength						
	Analytical			Abaqus			
δ [mm]	Mult	λ=(My/Mcr)^0.5	χ	MultAba	λ=(My/McrAbaqus)^0.5	χ=Mult/My	Diff Mult
σ [mPa]	77.85	1.42	0.37	83.47	1.35	0.39	-7.22%

Corrugated web							
	Static analysis						
	Analytical	Abaqus	Difference (%)				
δ [mm]	19.02	18.56	2.42%				
σ [mPa]	221.91	231.4	4.27%				
	Linear buckling						
	Analytical		Abaqus			Difference (%)	
δ [mm]	My	Mcr	Mref	Eigenvalue	McrAbaqus		
σ [mPa]	165.08	150.9090277	100	1.5321	153.21	1.50%	
	Ultimate strength						
	Analytical Eurocode			Abaqus			
δ [mm]	Mult	λ=(My/Mcr)^0.5	χ	MultAba	λ=(My/McrAbaqus)^0.5	χ=Mult/My	Diff Mult
σ [mPa]	88.11813186	1.05	0.53	90.23	1.04	0.55	2.34%

Table 4-5-Result Model 5

Model-5										Slenderness	
h_w *(mm)*	t_w (mm)	Ls (m)	b_f (mm)	t_f (mm)	Corrugation profile					Flat Web	Corrugated Web
					a	b	d	α		λ=(My/Mcr)^0.5	λ=(My/Mcr)^0.5
350	7	6.3	175	12	70	42	58	70		1.54	1.05
										very slender	Intermediate

Flat web							
	Static analysis						
	Analytical	Abaqus	Difference (%)				
δ *[mm]*	14.52	14.3	1.55%				
σ *[mPa]*	114.97	115.62	-0.57%				
	Linear buckling						
	Analytical		Abaqus			Difference (%)	
δ *[mm]*	My	Mcr	Mref	Eigenvalue	McrAbaqus		
σ *[mPa]*	345.97	145.6602377	100	1.476	147.6	-1.33%	
	Ultimate strength						
	Analytical Eurocode			Abaqus			
δ *[mm]*	Mult	λ=(My/Mcr)^0.5	χ	MultAba	λ=(My/McrAbaqus)^0.5	χ=Mult/My	Diff Mult
[mPa]	112.77	1.54	0.33	121.13	1.53	0.35	-7.42%

Corrugated web							
	Static analysis						
	Analytical	Abaqus	Difference (%)				
δ *[mm]*	17.16	16.67	2.88%				
σ *[mPa]*	135.86	137.13	0.94%				
	Linear buckling						
	Analytical		Abaqus			Difference (%)	
δ *[mm]*	My	Mcr	Mref	Eigenvalue	McrAbaqus		
σ *[mPa]*	269.87	244.9264453	100	2.4692	246.92	0.81%	
	Ultimate strength						
	Analytical Eurocode			Abaqus			
δ *[mm]*	Mult	λ=(My/Mcr)^0.5	χ	MultAba	λ=(My/McrAbaqus)^0.5	χ=Mult/My	Diff Mult
σ *[mPa]*	143.490544	1.05	0.53	152.13	1.05	0.56	5.68%

The flat web beam has λ_LT value greater than 1.2, which means moment resistance approaches theoretical M_cr.. this means the beam is very slender and Moment required to cause buckling will be close to M_cr as it shown below on Figure 4-5.

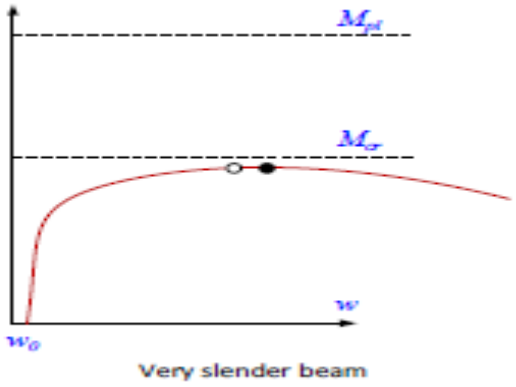

Figure 4-5: a schematic of the behavior of very slender beam.

However, for corrugated web beam, λ_Lt is lower than 1.2, which means moment required to cause buckling will be very low than M_cr. This signifies that corrugated web beam is intermediate slender beam. The difference is largest for beams with intermediate slenderness which is the real LT-behavior of beams differs from that anticipated by Euler buckling theory. Because, Euler classical buckling theory adopts an assumption of a steel with "prefect" section. Which means the sections is assumed no geometrical imperfections and an elastic material with no residual stress is encountered. However, as it is mentioned at the top, the above summery comparison table in contrary with the Euler buckling curve comprises geometrical imperfection and residual stress. In fact, level of accuracy also presented as a deviation between empirical and Abaqus values is computed as a percentage.

The corrugated web section exhibits high resistance to critical moment than the flat web section. This ability is due to the reduction of slenderness even though the sample chosen is equal with the flat section. The critical buckling stress is expressed as a function of section material property and slenderness parameter (λ).

λ computed for both flat corrugated web sections made a different slenderness categorization in the sample result presented above. λ for flat web section is greater than 1.2 whereas for corrugated web section it is much more lesser than 1.2. thus, the

slenderness category for the same material and span length samples the property of corrugations results clear difference.

The corrugated shape increases M_{cr} significantly as it put here on table 4-6 but due to higher unrestrained length, this plays little role in increasing buckling strength,

Model Number	Mcr-Flat [Mpa]	My-flat [Mpa]	Mcr-corrugated [Mpa]	My corrugated [Mpa]	Difference (Mcr) [Mpa]
Model 7	394.191	932.41	565.367	732.72	43.42%
Model 8	508.07	1266.59	798.556	998.12	57.17%
Model 3	71.6106	119.32	103.184	91.59	44.09%
Model 4	105.536	213.00	150.909	165.08	42.99%
Model 5	145.66	345.97	244.93	269.87	68.151%

Table 4-6: comparison Mcr Flat web vs corrugated web with very slenderness

Buckling behaviors is similar for both beams. As top flange is loaded under compression, it will buckle in the middle first and then the web and bottom flange subsequently follow buckling. This can be validated from the images taken at different points of nonlinear analysis, see Figure 4-6.

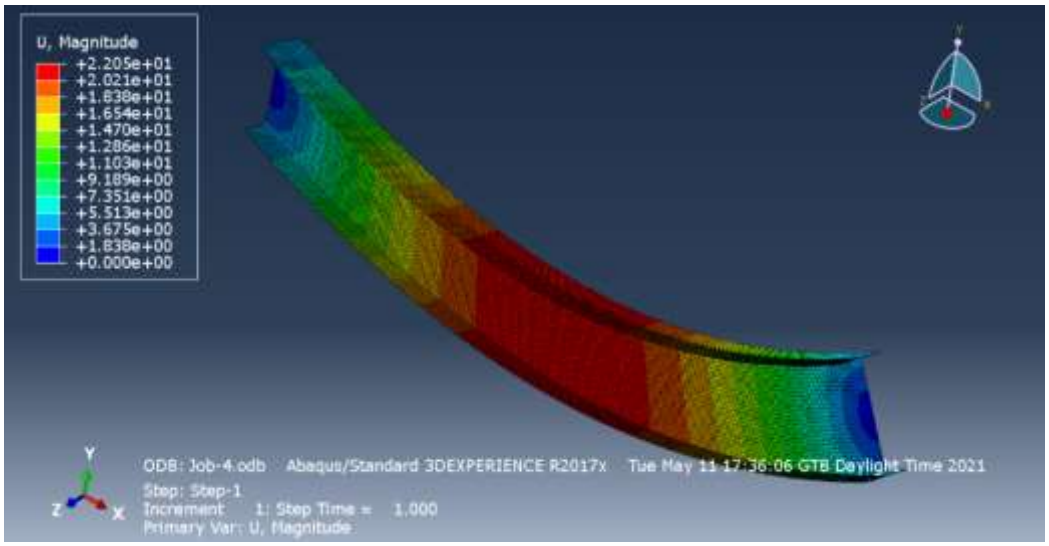

Figure 4-6: very slenderness -Buckling behavior for Flat web.

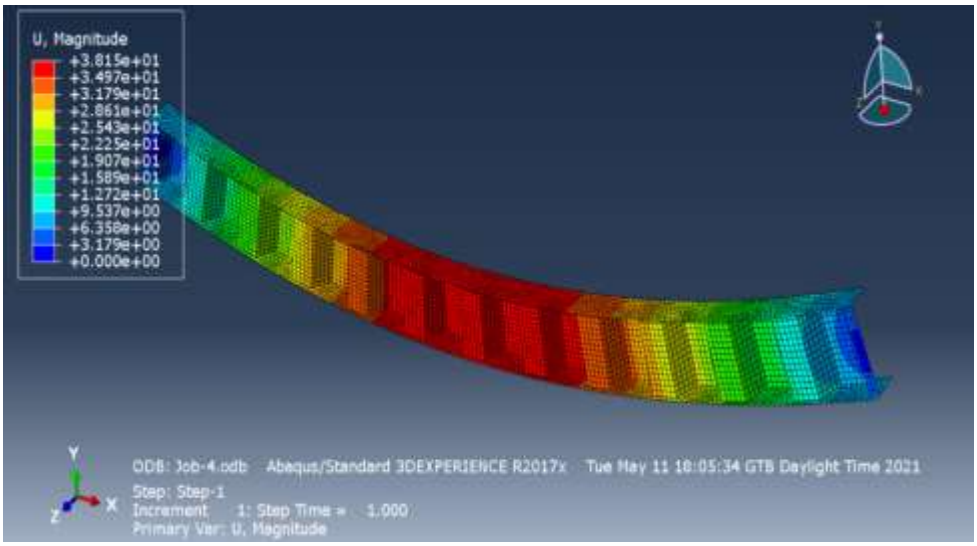

Figure 4-7: very slenderness -buckling behavior for corrugated web

4.3 Intermediate slenderness principal behavior

As it is studied (Al-emrani & Åkesson, 2013) While beams with intermediate slenderness will suffer the most sever reduction of moment capacity due to the interaction of 2nd order effects (due to initial imperfections) and material plasticity. In addition, many research papers like (Gizejowski, et al., 2017) and (Vales & Stan, 2017) and others summarized that both initial imperfection and residual stress play major role in reducing the load capacity of beams with intermediate slenderness. Whereas, very stocky and very slender columns are affected to much lesser degree in a comparison, see Figure 4-8.

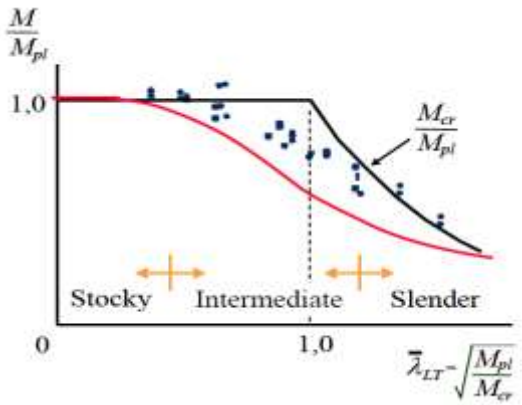

Figure 4-8: initial imperfection and residual stress influence for three types of slenderness.

Table 4-7-Result Model-6

Model-6										Slenderness	
h_w *(mm)*	t_w (mm)	Ls (m)	b_f (mm)	t_f (mm)	Corrugation profile					Flat Web	Corrugated Web
					a	b	d	α		λ=(My/Mcr)^0.5	λ=(My/Mcr)^0.5
450	8	8	225	14	70	67	58	60		1.41	1.13
										Very slender	Intermediate

Flat web							
	Static analysis						
	Analytical	Abaqus	Difference (%)				
δ [mm]	9.53	9.66	1.42%				
σ [mPa]	59.76	60.23	-0.78%				
	Linear buckling						
	Analytical		Abaqus			Difference (%)	
δ [mm]	My	Mcr	Mref	Eigenvalue	McrAbaqus		
σ [mPa]	662.64	271.866	100	2.9256	292.56	-7.61%	
	Ultimate strength						
	Analytical Eurocode			Abaqus			
δ [mm]	Mult	λ=(My/Mcr)^0.5	χ	MultAba	λ=(My/McrAbaqus)^0.5	χ=Mult/My	Diff Mult
σ [mPa]	212.00	1.56	0.32	225.12	1.50	0.34	-6.19%

Corrugated web							
	Static analysis						
	Analytical	Abaqus	Difference (%)				
δ [mm]	11.23	12.06	-7.38%				
σ [mPa]	70.46	70.12	-0.48%				
	Linear buckling						
	Analytical		Abaqus			Difference (%)	
δ [mm]	My	Mcr	Mref	Eigenvalue	McrAbaqus		
σ [mPa]	518.87	361.29	100	3.8145	381.45	5.28%	
	Ultimate strength						
	Analytical Eurocode			Abaqus			
δ [mm]	Mult	λ=(My/Mcr)^0.5	χ	MultAba	λ=(My/McrAbaqus)^0.5	χ=Mult/My	Diff Mult
σ [mPa]	236.639	1.20	0.46	245.12	1.17	0.47	3.46%

Model-9

h_w *(mm)*	t_w (mm)	Ls (m)	b_f (mm)	t_f (mm)	Corrugation profile					Slenderness	
					a	b	d	α		Flat Web	Corrugated Web
										λ=(My/Mcr)^0.5	λ=(My/Mcr)^0.5
650	12	7	260	22	70	67	58	60		1.25	0.96
										Very Slender	Intermediate

Flat web							
	Static analysis						
	Analytical	Abaqus	Difference (%)				
δ [mm]	1.86	1.952	-4.85%				
σ [mPa]	22.15	24.59	-9.92%				
	Linear buckling						
	Analytical			Abaqus		Difference (%)	
δ [mm]	My	Mcr	Mref	Eigenvalue	McrAbaqus		
σ [mPa]	1814.53	1153.62	100	11.9201	1192.01	-3.33%	
	Ultimate strength						
	Analytical Eurocode			Abaqus			
δ [mm]	Mult	λ=(My/Mcr)^0.5	χ	MultAba	λ=(My/McrAbaqus)^0.5	χ=Mult/My	Diff Mult
σ [mPa]	781.97	1.25	0.43	825.63	1.23	0.46	-5.58%

Corrugated web							
	Static analysis						
	Analytical	Abaqus	Difference (%)				
δ [mm]	2.26	2.415	-6.98%				
σ [mPa]	26.86	28.96	7.83%				
	Linear buckling						
	Analytical			Abaqus		Difference (%)	
δ [mm]	My	Mcr	Mref	Eigenvalue	McrAbaqus		
σ [mPa]	1364.56	1426.3	100	14.8562	1485.62	-3.99%	
	Ultimate strength						
	Analytical Eurocode			Abaqus			
δ [mm]	Mult	λ=(My/Mcr)^0.5	χ	MultAba	λ=(My/McrAbaqus)^0.5	χ=Mult/My	Diff Mult
σ [mPa]	781.569	0.98	0.57	830.15	0.96	0.61	5.85%

Table 4-8-Result Model-9

Table 4-9-Result Model-10

Model-10										Slenderness	
h_w *(mm)*	t_w (mm)	Ls (m)	b_f (mm)	t_f (mm)	Corrugation profile					Flat Web	Corrugated Web
					a	b	d	α		λ=(My/Mcr)^0.5	λ=(My/Mcr)^0.5
750	12	7	300	22	70	54	58	65		1.14	0.89
										Intermediate	Intermediate

Flat web							
	Static analysis						
	Analytical	Abaqus	Difference (%)				
δ [mm]	1.22	1.3602	-11.40%				
σ [mPa]	16.62	17.85	6.91%				
	Linear buckling						
	Analytical		Abaqus			Difference (%)	
δ [mm]	My	Mcr	Mref	Eigenvalue	McrAbaqus		
σ [mPa]	2407.86	1867.02	100	19.3212	1932.12	-3.49%	
	Ultimate strength						
	Analytical Eurocode			Abaqus			
δ [mm]	Mult	λ=(My/Mcr)^0.5	χ	MultAba	λ=(My/McrAbaqus)^0.5	χ=Mult/My	Diff Mult
σ [mPa]	1171.22	1.14	0.49	1253.15	1.12	0.52	6.99%

Corrugated web							
	Static analysis						
	Analytical	Abaqus	Difference (%)				
δ [mm]	1.48	1.61	-8.59%				
σ [mPa]	20.18	22.15	9.76%				
	Linear buckling						
	Analytical		Abaqus			Difference (%)	
δ [mm]	My	Mcr	Mref	Eigenvalue	McrAbaqus		
σ [mPa]	1808.8	2280.74	100	23.4562	2345.62	2.77%	
	Ultimate strength						
	Analytical Eurocode			Abaqus			
δ [mm]	Mult	λ=(My/Mcr)^0.5	χ	MultAba	λ=(My/McrAbaqus)^0.5	χ=Mult/My	Diff Mult
σ [mPa]	1134.32	0.89	0.63	1256.23	0.88	0.69	9.70%

Table 4-10-Result Model-1

Model-1										Slenderness	
hw (mm)	tw (mm)	Ls (m)	bf (mm)	tf (mm)	Corrugation profile					Flat Web	Corrugated Web
					a	b	d	α		λ=(My/Mcr) ^0.5	λ=(My/Mcr)^0.5
150	3	1.5	75	5	70	29	25	60		0.96	0.79
										Intermediate	Intermediate

Flat web							
	Static analysis						
	Analytical	Abaqus	Difference (%)				
δ [mm]	25.03337784	22.0431	11.9				
σ [mPa]	1495.327103	1420.93	5.24				
	Linear buckling						
	Analytical		Abaqus			Difference (%)	
δ [mm]	My	Mcr	Mref	Eigenvalue	McrAbaqus		
σ [mPa]	26.625	28.81161252	100	0.29092	29.092	-0.97	
	Ultimate strength						
	Analytical			Abaqus			
δ [mm]	Mult	λ=(My/Mcr)^0.5	χ	MultAba	λ=(My/McrAbaqus)^0.5	χ=Mult/My	Diff Mult
σ [mPa]	15.51	0.961	0.582	19.2141	0.9566	0.721	-23.81

Corrugated web							
	Static analysis						
	Analytical	Abaqus	Difference (%)				
δ [mm]	29.72	28.492	4.13%				
σ [mPa]	1775.31	1757.65	-0.99%				
	Linear buckling						
	Analytical		Abaqus			Difference (%)	
δ [mm]	My	Mcr	Mref	Eigenvalue	McrAbaqus		
σ [mPa]	20.63	32.735	100	0.32497	32.497	-0.73%	
	Ultimate strength						
	Analytical Eurocode			Abaqus			
δ [mm]	Mult	λ=(My/Mcr)^0.5	χ	MultAba	λ=(My/McrAbaqus)^0.5	χ=Mult/My	Diff Mult
σ [mPa]	14.28	0.79	0.69	18.7746	0.80	0.91	23.94%

Flat web			
	Linear Buckling		
Flat	Mesh	Eigen value	
1st	25	0.29118	Mode 1
2nd	20	0.29092	Mode 1
3rd l	15	0.29931	Mode 1
4th	10	0.30201	Mode 2
5thl	5	0.30454	Mode 1

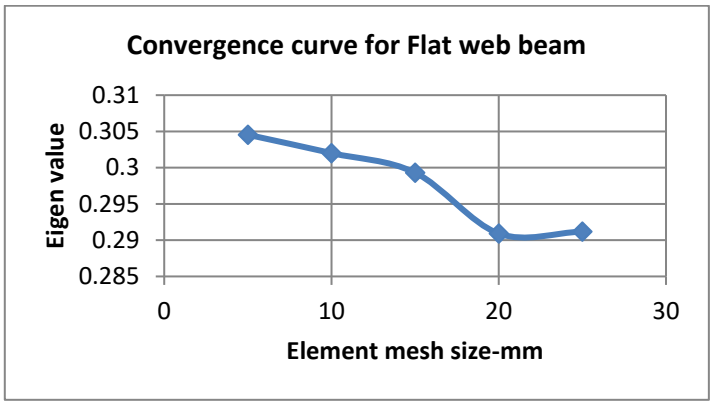

Corrugated web			
	Linear Buckling		
	Mesh	Eigen value	
1st	35	0.32813	Mode 2
2nd	30	0.32087	Mode 1
3rd	25	0.32491	Mode 2
4th	20	0.32842	Mode 1
5th	15	0.33037	Mode 2

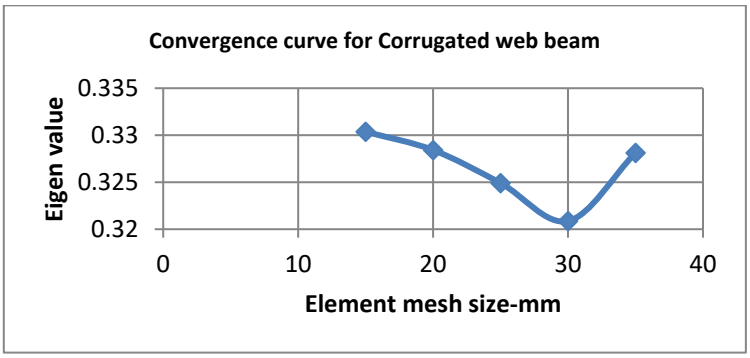

Figure 4-9: Convergence curve for eigen vector

Table 4-11-Result Model-2

Model-2										Slenderness	
h_w *(mm)*	t_w (mm)	Ls (m)	b_f (mm)	t_f (mm)	Corrugation profile					Flat Web	Corrugated Web
					a	b	d	α		λ=(My/Mcr)^0.5	λ=(My/Mcr)^0.5
200	4	1	100	7	70	31	33	65		0.5	0.43
										Intermediate	Intermediate

Flat web							
	Static analysis						
	Analytical	Abaqus	Difference (%)				
δ [mm]	3.37	3.45	-2.41%				
σ [mPa]	605.56	610.53	-0.81%				
	Linear buckling						
	Analytical		Abaqus			Difference (%)	
δ [mm]	My	Mcr	Mref	Eigenvalue	McrAbaqus		
σ [mPa]	65.64	260.87	100	2.6654	266.54	-2.17%	
	Ultimate strength						
	Analytical			Abaqus			
δ [mm]	Mult	λ=(My/Mcr)^0.5	χ	MultAba	λ=(My/McrAbaqus)^0.5	χ=Mult/My	Diff Mult
σ [mPa]	60.14	0.5	0.91	65.23	0.5	0.99	-8.65%

Corrugated web							
	Static analysis						
	Analytical	Abaqus	Difference (%)				
δ [mm]	3.97	3.85	2.96%				
σ [mPa]	713.20	718.23	0.71%				
	Linear buckling						
	Analytical		Abaqus			Difference (%)	
δ [mm]	My	Mcr	Mref	Eigenvalue	McrAbaqus		
σ [mPa]	51.44	279.62	100	2.8652	286.52	2.41%	
	Ultimate strength						
	Analytical			Abaqus			
δ [mm]	Mult	λ=(My/Mcr)^0.5	χ	MultAba	λ=(My/McrAbaqus)^0.5	χ=Mult/My	Diff Mult
σ [mPa]	50.166	0.43	0.98	55.62	0.42	1.08	9.81%

An initial imperfection caused by some geometrical deviations results in higher 2nd order moment when it is in higher amount. Very slender and stocky sections are less likely affected by both initial imperfections and residual stress. Very slender sections have a load carrying capacity that has equivalent to what is predicted by linear elastic buckling theory.

Slenderness categorization is computed by the ratio of M_y and M_{cr} (λ). As shown in the result in this section on the top, the λ for corrugated web sections reduced as compared to the flat web sections. this is due to the corrugated web M_y is not much farther than $M_{cr.}$, see figure xx. This resulted in reduction of slenderness categories.

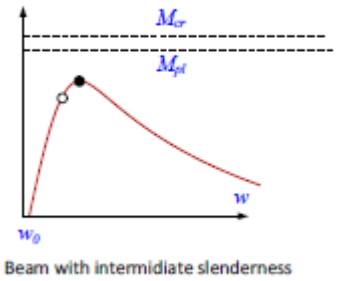

Figure 4-10: a schematic of the behavior of intermediate slenderness beam

Intermediate slenderness sections are more affected by both initial imperfection and residual stress. Residual stress reduces the ultimate capacity of sections with intermediate slenderness. According to (Al-emrani & Åkesson, 2013) this is due to 2nd order effect in sections are definite on intermediate sections. The axial and bending stress from external loading will be added to the compressive residual stress resulting in "early" partial yielding in cross section.

Thus, intermediate slenderness beams which are well below what is predicated by Euler buckling curve regarding load caring capacity due to some geometrical and material deviations existed in intermediate region.

Even if intermediate slenderness sections are more affected by initial imperfection and residual stress. Still, the corrugated shape increases M_cr significantly as it is summarized below on table 4-12. However, the percentages of increment of contribution due to corrugated web is less than when it compares with very slenderness principal behavior.

Table 4-12: comparison Mcr Flat web vs corrugated web with intermediate

Model Number	Mcr-Flat [Mpa]	My-flat [Mpa]	Mcr-corrugated [Mpa]	My corrugated [Mpa]	Difference (Mcr) [Mpa]
Model 6	271.866	662.64	361.29	518.87	32.89%
Model 1	28.8116	26.63	32.7347	20.63	13.6%
Model 2	260.87	65.64	279.62	51.44	7.18%
Model 9	1153.62	1814.53	1426.3	1364.56	23.63%
Model 10	1867.02	2407.86	2280.74	1808.8	22.15%

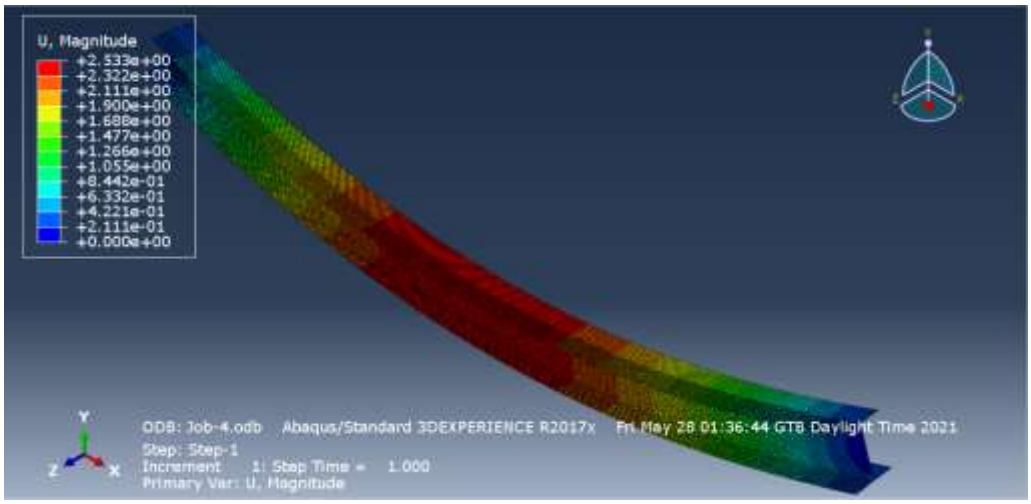

Figure 4-11: intermediate -buckling behavior for Flat web.

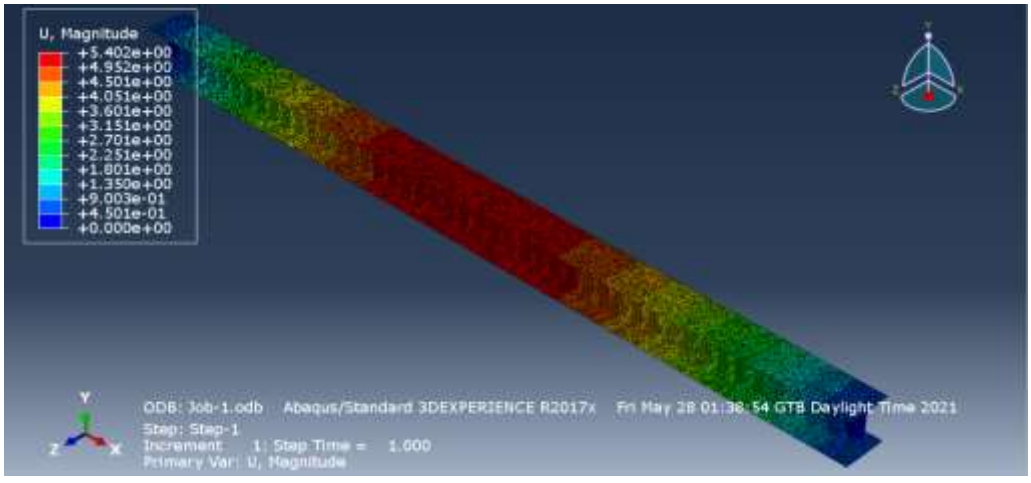

Figure 4-12: intermediate -buckling behavior for corrugated web.

Buckling behaviors is similar for both beams. As top flange is loaded under compression, it will buckle in the middle first and then the web and bottom flange subsequently follow buckling, see Figure 4-11 and Figure 4-12.

4.4 Very stocky/ very low slenderness principal behavior

Stocky sections load caring capacity is not governed by instability rather it by section yielding. According to (Al-emrani & Åkesson, 2013) the load carrying capacity of very low slenderness columns is rather insensitive to the magnitude of initial imperfection, see Figure 4-13.

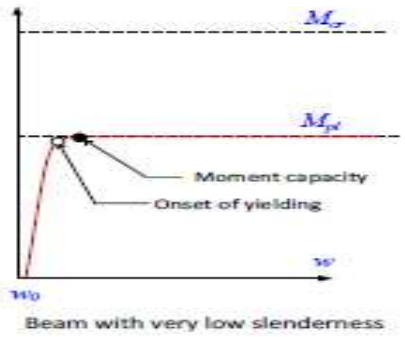

Figure 4-13: a schematic of the behavior of very stocky/ very low slenderness beam

Here below the FEM is presented with the deflection contour diagram.

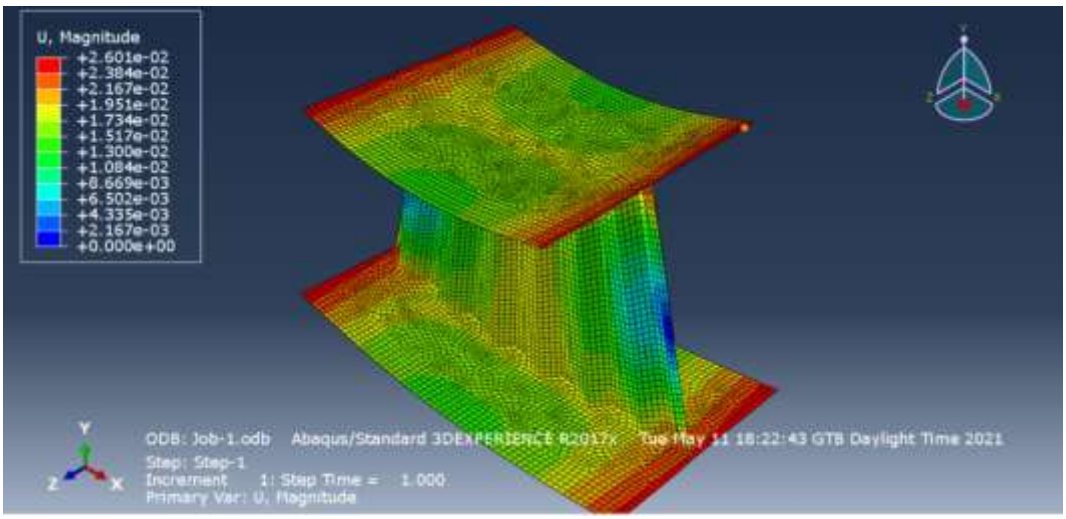

Figure 4-14: Very stocky -buckling behavior for Corrugated web

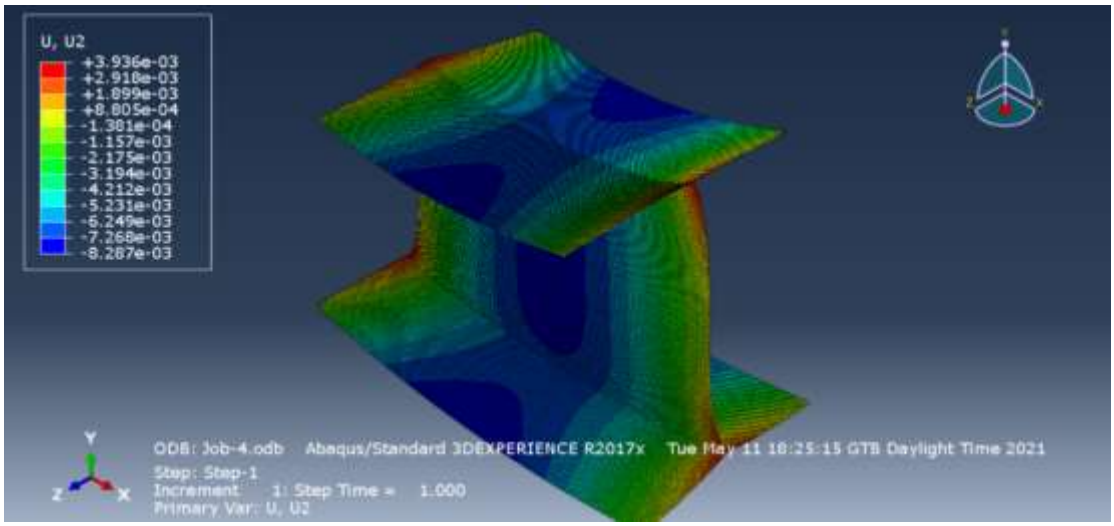

Figure 4-15: Very stocky -buckling behavior for Flat web

Table 4-13-Result Model-11

			Model-11							Slenderness	
h_w *(mm)*	t_w (mm)	Ls (m)	b_f (mm)	t_f (mm)	Corrugation profile					Flat Web	Corrugated Web
					a	b	d	α		λ=(My/Mcr)^0.5	λ=(My/Mcr)^0.5
1000	14	2.2	400	10	70	45	39	60		0.38	0.29
										Intermediate	very low slender

Flat web							
	Static analysis						
	Analytical	Abaqus	Difference (%)				
δ [mm]	0.1029	0.1149	-11.67%				
σ [mPa]	18.2138	19.2341	-5.30%				
	Linear buckling						
	Analytical		Abaqus			Difference (%)	
δ [mm]	My	Mcr	Mref	Eigenvalue	McrAbaqus		
σ [mPa]	2099.85	14531.7	100	150.2389	15023.89	-3.39%	
	Ultimate strength						
	Analytical Eurocode			Abaqus			
δ [mm]	Mult	λ=(My/Mcr)^0.5	χ	MultAba	λ=(My/McrAbaqus)^0.5	χ=Mult/My	Diff Mult
σ [mPa]	2136.1	0.38	1.02	1996.23	0.37	0.95	6.55%

Corrugated web							
	Static analysis						
	Analytical	Abaqus	Difference (%)				
δ [mm]	0.1784	0.1925	-7.89%				
σ [mPa]	31.58	32.5045	-2.91%				
	Linear buckling						
	Analytical		Abaqus			Difference (%)	
δ [mm]	My	Mcr	Mref	Eigenvalue	McrAbaqus		
σ [mPa]	1210.86	14548.92	100	151.2356	15123.56	3.80%	
	Ultimate strength						
	Analytical Eurocode			Abaqus			
δ [mm]	Mult	λ=(My/Mcr)^0.5	χ	MultAba	λ=(My/McrAbaqus)^0.5	χ=Mult/My	Diff Mult
σ [mPa]	1332.07	0.29	1.10	1445.23	0.28	1.19	7.83%

Table 4-14-Result Model-12

Model-12										Slenderness	
h_w *(mm)*	t_w (mm)	Ls (m)	b_f (mm)	t_f (mm)	Corrugation profile					Flat Web	Corrugated Web
					a	b	d	α		λ=(My/Mcr)^0.5	λ=(My/Mcr)^0.5
1050	14	1	420	14	70	47	50	65		0.16	0.13
										very low slender	very low slender

Flat web							
	Static analysis						
	Analytical	Abaqus	Difference (%)				
δ [mm]	0.0167	0.0172	-3.29%				
σ [mPa]	15.0794	16.125	-6.48%				
	Linear buckling						
	Analytical		Abaqus			Difference (%)	
δ [mm]	My	Mcr	Mref	Eigenvalue	McrAbaqus		
σ [mPa]	2755.36	102825.4	100	1041.8541	10418541	-1.32%	
	Ultimate strength						
	Analytical Eurocode			Abaqus			
δ [mm]	Mult	λ=(My/Mcr)^0.5	χ	MultAba	λ=(My/McrAbaqus)^0.5	χ=Mult/My	Diff Mult
σ [mPa]	3377.19	0.16	1.23	3561.23	0.16	1.29	-5.45%

Corrugated web							
	Static analysis						
	Analytical	Abaqus	Difference (%)				
δ [mm]	0.0279	0.0288	-3.22%				
σ [mPa]	25.2658	26.315	-4.15%				
	Linear buckling						
	Analytical		Abaqus			Difference (%)	
δ [mm]	My	Mcr	Mref	Eigenvalue	McrAbaqus		
σ [mPa]	1644.48	102859.49	100	1042.4561	104245.61	1.33%	
	Ultimate strength						
	Analytical Eurocode			Abaqus			
δ [mm]	Mult	λ=(My/Mcr)^0.5	χ	MultAba	λ=(My/McrAbaqus)^0.5	χ=Mult/My	Diff Mult
σ [mPa]	2084.56142	0.13	1.27	2216.45	0.13	1.35	5.95%

Table 4-15-Result Model-13

Model-13										Slenderness	
h_w *(mm)*	t_w (mm)	Ls (m)	b_f (mm)	t_f (mm)	Corrugation profile					Flat Web	Corrugated Web
					a	b	d	α		λ=(My/Mcr)^0.5	λ=(My/Mcr)^0.5
1100	12	1.5	440	12	70	42	58	70		0.24	0.18
										Very low slender	Very low slender

Flat web							
	Static analysis						
	Analytical	Abaqus	Difference (%)				
δ [mm]	0.0396	0.04002	-0.96%				
σ [mPa]	16.634	16.854	-1.31%				
	Linear buckling						
	Analytical		Abaqus			Difference (%)	
δ [mm]	My	Mcr	Mref	Eigenvalue	McrAbaqus		
σ [mPa]	2552.58	45822.9	100	462.4152	46241.52	-0.91%	
	Ultimate strength						
	Analytical Eurocode			Abaqus			
δ [mm]	Mult	λ=(My/Mcr)^0.5	χ	MultAba	λ=(My/McrAbaqus)^0.5	χ=Mult/My	Diff Mult
σ [mPa]	2937.10	0.24	1.15	3121.23	0.23	1.22	-6.27%

Corrugated web							
	Static analysis						
	Analytical	Abaqus	Difference (%)				
δ [mm]	0.0692	0.07002	-1.20%				
σ [mPa]	29.0349	30.1256	-3.76%				
	Linear buckling						
	Analytical		Abaqus			Difference (%)	
δ [mm]	My	Mcr	Mref	Eigenvalue	McrAbaqus		
σ [mPa]	1462.37	45953.482	100	464.1245	46412.45	-0.99%	
	Ultimate strength						
	Analytical Eurocode			Abaqus			
δ [mm]	Mult	λ=(My/Mcr)^0.5	χ	MultAba	λ=(My/McrAbaqus)^0.5	χ=Mult/My	Diff Mult
σ [mPa]	1769.20	0.18	1.21	1875.53	0.18	1.28	5.67%

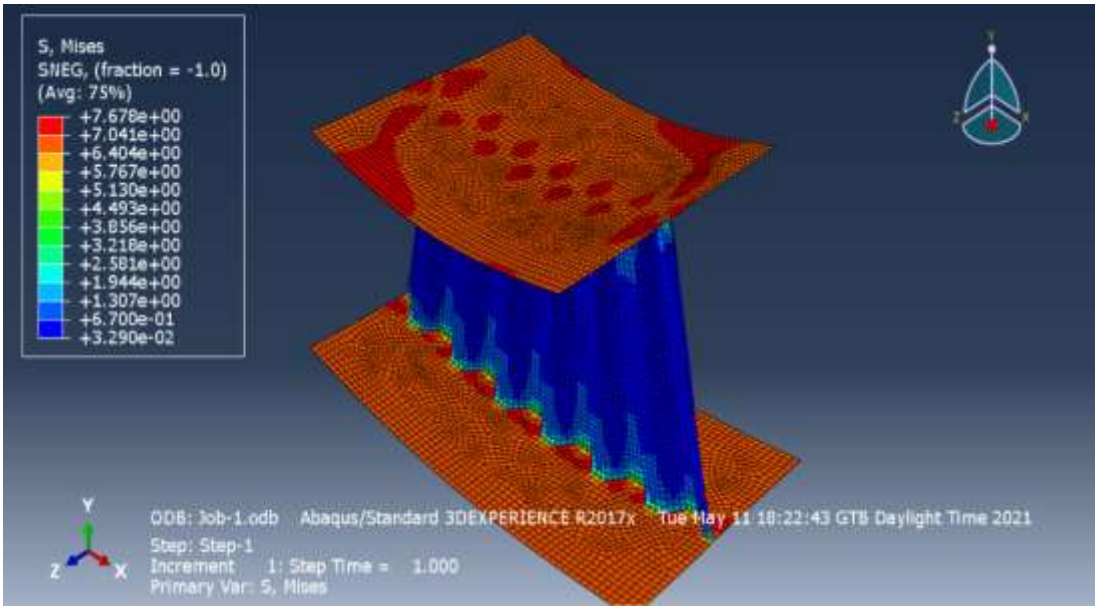

Figure 4-16: 3D illustration of the obtained deformation for Flat web

Table 4-16-Result Model-14

Model-14										Slenderness	
h_w *(mm)*	t_w (mm)	Ls (m)	b_f (mm)	t_f (mm)	Corrugation profile					Flat Web	Corrugated Web
					a	b	d	α		λ=(My/Mcr)^0.5	λ=(My/Mcr)^0.5
1200	10	1.5	480	10	70	31	42	70		0.24	0.18
										Very low slender	Very low slender

Flat web							
	Static analysis						
	Analytical	Abaqus	Difference (%)				
δ [mm]	0.0476	0.0498	-4.68%				
σ [mPa]	21.6683	21.892	-1.02%				
	Linear buckling						
	Analytical			Abaqus		Difference (%)	
δ [mm]	My	Mcr	Mref	Eigenvalue	McrAbaqus		
σ [mPa]	2370.47	41488.9	100	421.5654	42156.54	-1.61%	
	Ultimate strength						
	Analytical Eurocode			Abaqus			
δ [mm]	Mult	λ=(My/Mcr)^0.5	χ	MultAba	λ=(My/McrAbaqus)^0.5	χ=Mult/My	Diff Mult
σ [mPa]	2720.5	0.24	1.15	2954.61	0.24	1.25	-8.61%

Corrugated web							
	Static analysis						
	Analytical	Abaqus	Difference (%)				
δ [mm]	0.0834	0.0912	-9.37%				
σ [mPa]	37.9797	38.564	1.54%				
	Linear buckling						
	Analytical			Abaqus		Difference (%)	
δ [mm]	My	Mcr	Mref	Eigenvalue	McrAbaqus		
σ [mPa]	1352.4	41571.383	100	423.1544	42315.44	1.76%	
	Ultimate strength						
	Analytical Eurocode			Abaqus			
δ [mm]	Mult	λ=(My/Mcr)^0.5	χ	MultAba	λ=(My/McrAbaqus)^0.5	χ=Mult/My	Diff Mult
σ [mPa]	1633.31	0.18	1.21	1694.58	0.18	1.25	3.62%

. Table 4-17-Result Model-15

Model-15										Slenderness	
h_w *(mm)*	t_w (mm)	Ls (m)	b_f (mm)	t_f (mm)	Corrugation profile					Flat Web	Corrugated Web
					a	b	d	α		λ=(My/Mcr)^0.5	λ=(My/Mcr)^0.5
1500	16	2	600	16	70	54	58	65		0.23	0.17
										very low slender	very low slender

Flat web							
	Static analysis						
	Analytical	Abaqus	Difference (%)				
δ [mm]	0.0217	0.0235	-8.42%				
σ [mPa]	6.9732	6.966	-0.1%				
	Linear buckling						
	Analytical		Abaqus			Difference (%)	
δ [mm]	My	Mcr	Mref	Eigenvalue	McrAbaqus		
σ [mPa]	6179.66	118014.4	100	1191.2530	119125.3	-0.94%	
	Ultimate strength						
	Analytical Eurocode			Abaqus			
δ [mm]	Mult	λ=(My/Mcr)^0.5	χ	MultAba	λ=(My/McrAbaqus)^0.5	χ=Mult/My	Diff Mult
σ [mPa]	7154.74	0.23	1.16	7921.56	0.23	1.28	-10.72%

Corrugated web							
	Static analysis						
	Analytical	Abaqus	Difference (%)				
δ [mm]	0.0375	0.041	-9.46%				
σ [mPa]	12.0509	12.1564	0.1%				
	Linear buckling						
	Analytical		Abaqus			Difference (%)	
δ [mm]	My	Mcr	Mref	Eigenvalue	McrAbaqus		
σ [mPa]	3575.83	118193.12	100	1196.2345	119623.45	1.20%	
	Ultimate strength						
	Analytical Eurocode			Abaqus			
δ [mm]	Mult	λ=(My/Mcr)^0.5	χ	MultAba	λ=(My/McrAbaqus)^0.5	χ=Mult/My	Diff Mult
σ [mPa]	4343.1643	0.17	1.21	4765.2345	0.17	1.33	8.86%

Table 4-18: comparison Mcr Flat web vs corrugated web with very stocky

Model Number	Mcr-Flat [Mpa]	My-flat [Mpa]	Mcr-corrugated [Mpa]	My corrugated [Mpa]	Difference (Mcr) [Mpa]
Model 11	14531.7	2099.85	14548.928	1210.86	0.118%
Model 12	104185.41	2755.36	104245.61	1644.48	0.058%
Model 13	46241.52	2552.58	46412.45	1462.37	0.370%
Model 14	42156.54	2370.47	42315.44	1352.4	0.377%
Model 15	119125.3	6179.66	119623.45	3575.83	0.418%

The corrugation does not add any major ability for such non slender material due to the negligible value of second (2^{nd}) order effect for very stocky principal behavior. Thus, those types of have low contribution for corrugated web which gives compared with to a flat web.

4.5 Summary

My is dependent on cross section dimension, while M_cr is dependent on beam length and cross section constants. The corrugated shape increases M_cr significantly. Critical moment and slenderness are directly proportional and which leads to little role in increasing buckling strength. However, for conventional flat web I beam, not only the flanges can take tensile and compression forces from bending some of these forces will be resisted by the web as well. Rather, corrugated web there will be no tensile or compression forces from bending in the web which means that all axial forces will be taken in the flanges. Besides, flat web, web stiffeners are needed to prevent lateral torsional buckling. Meanwhile, corrugated webs (especially trapezoidal) because of geometrical high out of plane rigidity of corrugated web, stiffeners are not needed as it tested on the top,

So long unrestrained beams may have lower M_cr and shorter beam will have higher M_cr if other factors remain same, but for both beams (corrugated web and flat web) with the same flange dimensions and cross section height, M_y will be same. So stocky beams can utilize full plastic moment capacity while slender ones fail before reaching M_cr. Therefore, according to this research paper trapezoidal corrugated web would be able to provide lateral torsional resistance for both very slender and intermediate principal behaviors. However, the possible contribution of LTB resistance is higher for very slender type of beams while it compares with intermediate slenderness type of beams.

A comparative study of each model numerically studied in two methods, which are analytical and Abaqus FE-simulation. As mentioned in the result section, reduction factor and non-dimensional slenderness x-λ is calculating for each sample. Thus, for a better conclusion, the relation between reduction factor and non-dimensional slenderness x-λ are presented particularly for LTB curve of corrugated I beam as a reference of European buckling curve c and d which were experimented with by Eurocode 3-1-1, see Figure 4-17,4-18.

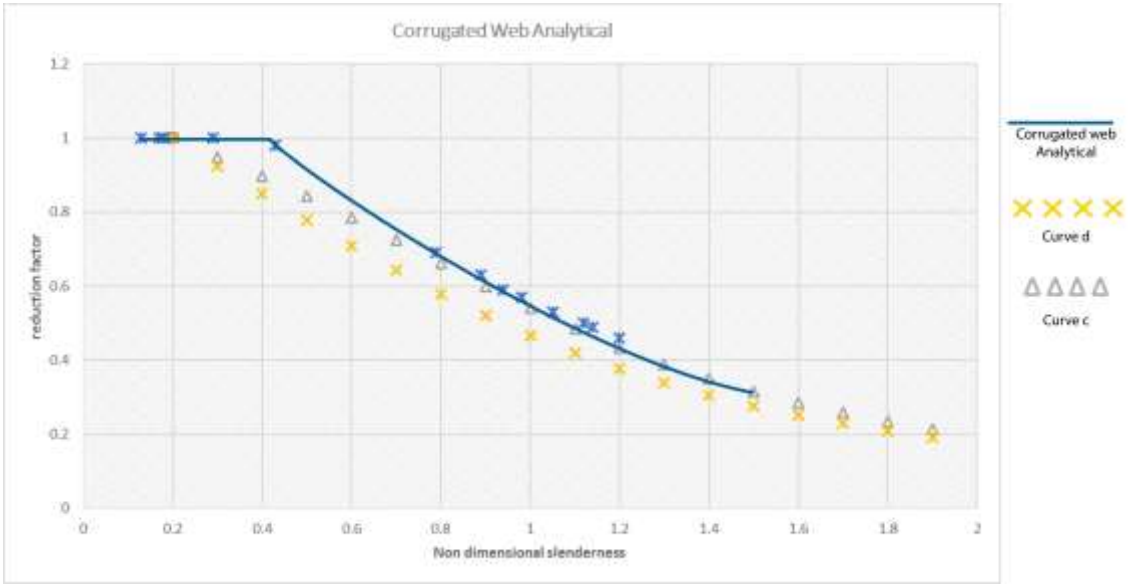

Figure 4-17: reduction factor vs non-dimensional slenderness -corrugated web analytic

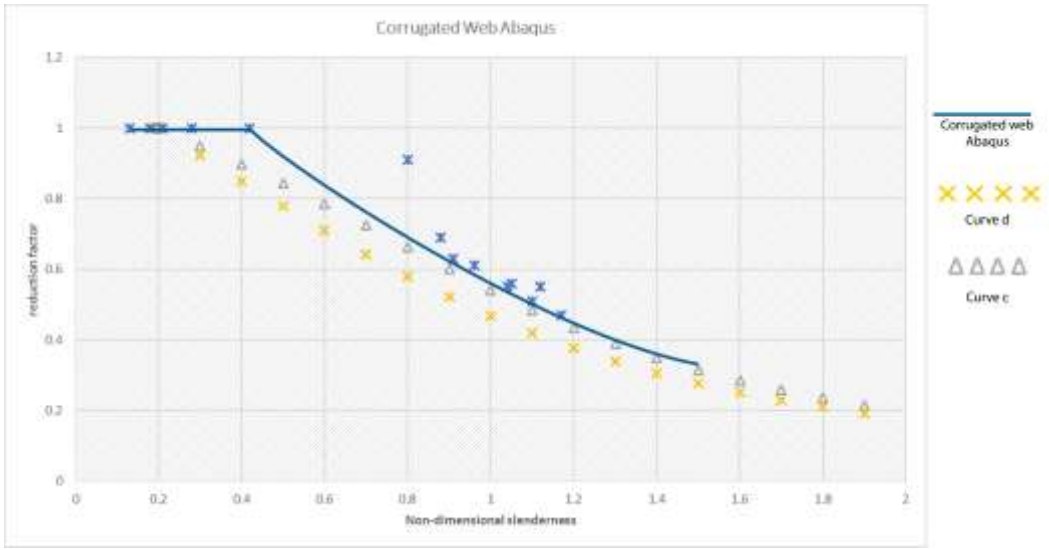

Figure 4-18 reduction factor vs non-dimensional slenderness -corrugated web Abaqus

CHAPTER 5 CONCLUSSION

5.1 Conclusion

To study the effect of the corrugated web on lateral-torsional buckling, thirty different samples have studied with conventional I beam and compare with steel beams with corrugated webs. The study was conducted under consideration of initial, geometrically, and materially imperfections focused on lateral-torsional buckling of beams in pure bending. The numerical study has revealed that the range of percentage has found the critical moment due to corrugated web. The calculations included both elastic-plasticity of the cross-section, residual stresses, elastic-perfectly plastic material behavior, and an initial bow imperfection presented in table 5:1 of EN-1993-1-1 (2005).

The effect of the corrugated web on the very stocky beam-columns is not much, the beam-column stays straight and reaches yield stress in its whole section. Unlike stocky beam-columns, slender beam-columns, it does not reach yield stress before it buckles elastically, thus the effect of the corrugated web to resist lateral-torsional buckling is high. Likewise, intermediate columns are sensitive to material imperfection (residual stress), geometrical and initial imperfection. This means, Yield in the cross-section limits its stiffness enough to cause buckling of its elastic part. However, still it has better performance even if there are many uncertainties since both initial imperfections and residual stresses play a major role in reducing the load capacity of beam-columns with intermediate slenderness.

Based on the results of the numerical analysis, the following conclusions have been drawn:

1. The finite elements and hand calculations showed that the corrugated web has an increased load capacity and stiffness by (32-67%), (12-31.3%) and (0.058%-0.418%) for Very slender, intermediate, and very stocky respectively than flat web beams.
2. Corrugated web beams are stiffer than flat web beams since they show higher strength and lower slenderness regarding lateral-torsional buckling. It is more appropriate to use corrugated web for more high slenderness ratio values.
3. Higher slenderness results in a greater tendency to fail within LTB which implies instability and it will lead to lower strength. However, the corrugated web is able

to introduce for increasing the bending resistance around a weak and strong axis which has a large contribution for LTB resistance when it compares to flat web.

4. The corrugated web would be able to provide additional restraint to the flange both torsional and lateral deflection for more slenderness behavior than very stocky beams. The main reason is due to corrugated webs a post-critical reserve strength which helps to enable redistribution as a strut-and-tie analogy (as it referred on Figure 2-4.)
5. Corrugated webs have the biggest impact on critical buckling load, critical momentum, cross-sectional area, slenderness ratio, and ultimate strength.

5.2 Significance of the Study

In bridge construction loads are larger than building or warehouse construction. As a result, the steel profiles used are larger. A more common solution is the use of a corrugated web instead of flat web due to its optimized web stiffness, economy and aesthetic look. Consequently, issues related to the behavior of beams with corrugated web still need further study. Therefore, this research tries to give deep insight regarding both flat and corrugated I beam for LTB. Besides, for local Structural Engineers will help to have confidence while using such Advance FE software's, Abaqus.

5.3 Future research question

A comparison study between flat web with web stiffeners and many types of corrugated web I beam is suggested as a topic for future research. In addition, it is also possible to compare the equivalent LTB resistance of corrugated I beam with in variable thickness of the Flat web-I beam.

REFERENCES

Al-Emrani, M., 2018. *Analysis of the load carring of beams with corrugated web with respect to lateral torstional buckling,* Götoberg,Sweden: Chalmers University of technology ,FEM-LAB.

Al-emrani, M. & Åkesson, B., 2013. Steel structures Literature. In: Göteborg,Sweden: Chalmers university of technology.

Ameer AL-Kanon, M. A. & suhiel, I. A., 2019. Flexural behavior of steel beam with corrguated web. *International journal of scientific and techonlogy research ,* 8(10), pp. 3004-3009.

Balzannikov, M. I., Kholopov, I. s., Alpatov, V. Y. & Lukin, A. A., 2015. Stress and strain state in beams with corrugated web and their use in hydraulic engineering Structures.. *Procedia Engineering,* Issue Elsevier ltd, pp. 72-81.

Elamary, A. S., Saddek, A. B. & Alwetaishi, M., 2017. Effect of corrugated web on flexural capacity of steel beams. *International Journal of applied Engineering Research,* 12(Research india publications), pp. 470-481.

EN-1993-1-1, (., 2005. EN-1993-1-1. (2005). In: *Eurocode 3:Design of steel structures - part 1-1: General rules and rules for buildings.*. s.l.:European Committee for Standardisation..

EN-1993-1-5, (., 2006. EN-1993-1-5. (2006).. In: *Eurocode 3: Design of steel structures - part 1-5: Plated structural elements.* s.l.:European Committee for Standardisation..

Gizejowski, M. A., Szezerba, B. R. & Gajewski, D. M., 2017. *LTB resistance of rolled I-Beams FEM verification of eurocode's buckling curve formulation.* Copenhagen,Denmark, Ernst &Sohn, pp. 13-15.

Gorecki, M., Pienko, M. & Lagoda, G., 2017. *Numerical Analysis of beam with sinusodially corrguated web.* s.l., AIP conference Proceeding .

k, K. k. & Mohanan, N., 2016. Lateral torsional buckling of castellated I beam with corrguated Web. *International research journal of engineering and technology(IRJET),* 03(www.irjet.net), pp. 717-720.

kumar, M. et al., 2018. A study on flexural capacity of steel Beams with corrguated Web.. *IJCIET,* 2018(ISSN), pp. 679-689.

P. A. G., P., P. M. M., V. R. & J.-M., F., 2000. *A simple model for lateral torsional buckling resistance of steel I beams under*. s.l., s.n.

Sarvestani, A. H., 2017. Behaviour of corrugated webbed beams in pos-tensioned semi rigid connections. *Advance in Structural Engineering ,* 20(3)(sagepub.com), pp. 394-410.

SN003a-EN-EU, August 2007. SN003a-EN-EU. In: *NCCI: Elastic critical moment for lateral torsional buckling.* Uk,France,Sweden,Germany and Spain: SCI, CTICM,SBI,RWTH,Labein and SCI Companies.

Sokolowski, D. & Kaminski, M., 2015. Reliability analysis of a corrugated I-beam girder with ribs. *Engineering and compuational Mechanics,* 168(ICE,Institution of civil Engineering), pp. 49-58.

Tohamy, S., Abu El Ela, O., Saddek, A. & Mohammed, A., 2013. Efficiency of plate girder with corrgauted web vs plate girder with flat web. *Minia Journal of engineering and Techonlogy,* Volume 32, pp. 62-77.

Vales, J. & Stan, T.-C., 2017. FEM modeling of Lateral Torsional Buckling using shell and solid Elements. *Procedia Engineering,* Issue Elsevier.ltd, pp. 464-471.

Wang, F. & Yang, J., 2016. *Finite element investigations of the the effect of residual stress in cold formed sigma Beams.* s.l., international speciality confernece on cold formed steel structure.

APPENDIX

Model 1-Appedix A

Model 2-Appendix B

Model 3-Appendix C

Model 4-Appendix D

Model 5-Appendix F

Model 6-Appendix G

Model 7-Appendix H

Model 8-Appendix I

Model 9-Appendix J

Model 10-Appendix K

Model 11-Appendix L

Model 12-Appendix M

Model 13-Appendix N

Model 14-Appendix O

Model 15-Appendix P

Model-1

Geometry	
h,web [mm]	150
t,web [mm]	3
L,span [m]	1.5
b,flange[mm]	75
t,flange [mm]	5
a [mm]	70
b [mm]	29
d [mm]	25
α	60

Material Property	
S355	Material
fy [Mpa]	355
E [Gpa]	210
fu [Mpa]	600
ε,p	0.1167
ε	0.813616513
G [Gpa]	80.77

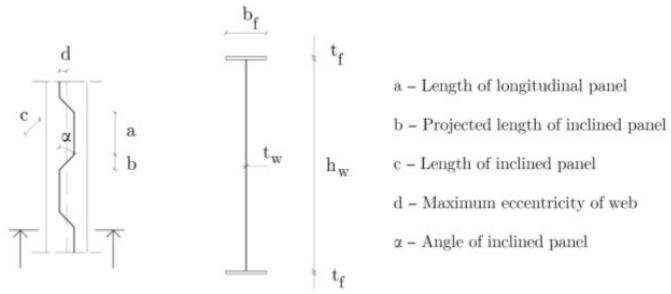

Notations for the geometry of the cross-section and corrugation profile.

Flat Web

Flange	c	36		
	t	5		
	c/t	7.2	7.3225486	Class I

web	c	150		
	t	3		
	c/t	50	58.580389	Class I

h/b	2.133333333	Buckling curve d	α,LT	0.76

I,z [mm^4]	3.52E+05	Moment of inertia around weak axis (xy plane)
I,t [mm^4]	7.60E+03	Torsion constant
I,w [mm^4]	2.11E+09	Warping constant
I,y [mm^4]	5.35E+06	Moment of inertia around strong axis (xz plane)

Table 6.3: Recommended values for imperfection factors for lateral torsional buckling curves

Buckling curve	a	b	c	d
Imperfection factor α_{LT}	0,21	0,34	0,49	0,76

Table 6.5: Recommendation for the selection of lateral torsional buckling curve for cross sections using equation (6.57)

Cross-section	Limits	Buckling curve
Rolled I-sections	h/b ≤ 2 h/b > 2	b c
Welded I-sections	h/b ≤ 2 h/b > 2	c d

$$I_w = \frac{I_z (h - t_f)^2}{4}$$

$$I_z = 2 \cdot \frac{t_f b_f^3}{12} = \frac{t_f b_f^3}{6}$$

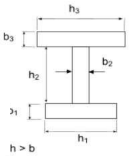

$$I_t = \frac{1}{3}\sum_{i=1}^{n} b_i^3 h_i$$

M,y=2* fy*(bf*tf*(hw+tf)/2+(hw*tw/2)*hw/4) [kN-m]			26.63		
M,cr [kN-m]			28.811613		

According to 1993-1-1:2005 section 6.3.2.3

λ_LT	0.961304611				
ϕ_LT	1.05983571				
χ_LT	0.582848893	<1	&	1/λ^2	1.082126
M,ult [kN-m]	15.51835178				

$$M_{cr} = \frac{\pi^2 E I_z}{L^2}\sqrt{\frac{I_w}{I_z} + \frac{L^2}{\pi^2 E I_z}(G I_t + c_w)}$$

Corrugated Web

I,z [mm^4]	351562.5			
I,y [mm^4]	4.51E+06	5.63E+04	19.996	

M,y= 2*fy*(bf*tf*(hw+tf)/2 [kN-m]			20.63

u,x	9.49452E-05				
C,w	748038774.2				
M,cr [kN-m]			32.73473		
λ_LT	0.793946574				
ϕ_LT	0.886081384				
χ_LT	0.692047166	<1	&	1/λ^2	1.586417

$$u_x = \frac{h_w}{2Gat_w} + \frac{h_w^2 (a+b)^3}{25a^2 E b_f t_f^3}$$

$$c_w = \frac{(2d)^2 h_w^2}{8u_x(a+b)}$$

Model -2

Geometry	
h,web [mm]	200
t,web [mm]	4
L,span [m]	1
b,flange[mm]	100
t,flange [mm]	7
a [mm]	70
b [mm]	31
d [mm]	33
α	65

Material Property	
S355	Material
fy [Mpa]	355
E [Gpa]	210
fu [Mpa]	600
ε,p	0.1167
ε	0.813616513
G [Gpa]	80.77

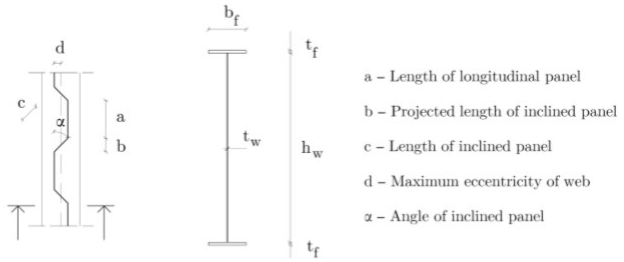

Notations for the geometry of the cross-section and corrugation profile.

Flat Web

Flange	c	48	
	t	7	
	c/t	6.857142857	7.3225486 Class I

web	c	200	
	t	4	
	c/t	50	58.580389 Class I

h/b	2.14	Buckling curve d	α,LT 0.76

Table 6.3: Recommended values for imperfection factors for lateral torsional buckling curves

Buckling curve	a	b	c	d
Imperfection factor α_{LT}	0,21	0,34	0,49	0,76

Table 6.5: Recommendation for the selection of lateral torsional buckling curve for cross sections using equation (6.57)

Cross-section	Limits	Buckling curve
Rolled I-sections	h/b ≤ 2 h/b > 2	b c
Welded I-sections	h/b ≤ 2 h/b > 2	c d

$$I_w = \frac{I_z (h - t_f)^2}{4}$$

$$I_z = 2 \cdot \frac{t_f b_f^3}{12} = \frac{t_f b_f^3}{6}$$

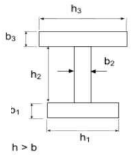

$$I_t = \frac{1}{3}\sum_{i=1}^{n} b_i^3 h_i$$

I,z [mm^4]	1.17E+06	Moment of inertia around weak axis (xy plane)
I,t [mm^4]	2.71E+04	Torsion constant
I,w [mm^4]	1.25E+10	Warping constant
I,y [mm^4]	1.77E+07	Moment of inertia around strong axis (xz plane)

M,y=2* fy*(bf*tf*(hw+tf)/2+(hw*tw/2)*hw/4) [kN-m]	65.64
M,cr [kN-m]	260.8698

According to 1993-1-1:2005 section 6.3.2.3

λ_LT	0.501615244				
ϕ_LT	0.632970488				
χ_LT	0.91463024	<1	&	1/λ^2	3.974281
M,ult [kN-m]	60.03587166				

$$M_{cr} = \frac{\pi^2 E I_z}{L^2}\sqrt{\frac{I_w}{I_z} + \frac{L^2}{\pi^2 E I_z}(G I_t + c_w)}$$

Corrugated Web

I,z [mm^4]	1166666.667
I,y [mm^4]	1.50E+07

M,y= 2*fy*(bf*tf*(hw+tf)/2 [kN-m]		51.44

u,x	5.11279E-05		
C,w	4217724929		
M,cr [kN-m]		279.62399	
λ_LT	0.428905048		
ϕ_LT	0.579968746		
χ_LT	0.975245099	<1 &	1/λ^2 5.435978

$$u_x = \frac{h_w}{2Gat_w} + \frac{h_w^2 (a+b)^3}{25a^2 E b_f t_f^3}$$

$$c_w = \frac{(2d)^2 h_w^2}{8u_x(a+b)}$$

Geometry	
h,web [mm]	250
t,web [mm]	5
L,span [m]	3.5
b,flange[mm]	125
t,flange [mm]	8
a [mm]	70
b [mm]	31
d [mm]	42
α	70

Model-3

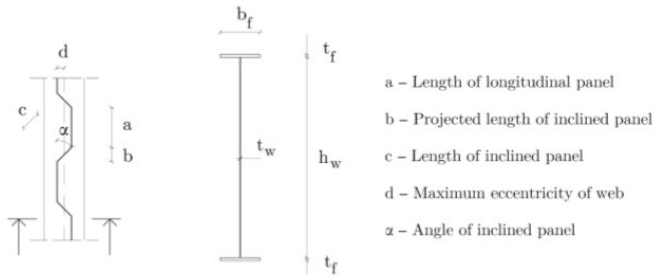

Notations for the geometry of the cross-section and corrugation profile.

Material Property	
S355	Material
fy [Mpa]	355
E [Gpa]	210
fu [Mpa]	600
ε,p	0.1167
ε	0.813616513
G [Gpa]	80.77

Flat Web

Table 6.3: Recommended values for imperfection factors for lateral torsional buckling curves

Buckling curve	a	b	c	d
Imperfection factor α_{LT}	0,21	0,34	0,49	0,76

Flange	c	60		
	t	8		
	c/t	7.5	7.3225486	Class II

web	c	250		
	t	5		
	c/t	50	58.580389	Class I

Table 6.5: Recommendation for the selection of lateral torsional buckling curve for cross sections using equation (6.57)

Cross-section	Limits	Buckling curve
Rolled I-sections	h/b ≤ 2 h/b > 2	b c
Welded I-sections	h/b ≤ 2 h/b > 2	c d

h/b	2.128	Buckling curve d		α,LT	0.76

I,z [mm^4]	2.61E+06	Moment of inertia around weak axis (xy plane)
I,t [mm^4]	5.31E+04	Torsion constant
I,w [mm^4]	4.34E+10	Warping constant
I,y [mm^4]	3.98E+07	Moment of inertia around strong axis (xz plane)

$$I_w = \frac{I_z (h - t_f)^2}{4}$$

$$I_z = 2 \cdot \frac{t_f b_f^3}{12} = \frac{t_f b_f^3}{6}$$

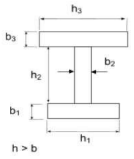

$$I_t = \frac{1}{3}\sum_{i=1}^{n} b_i^3 h_i$$

M,y=2* fy*(bf*tf*(hw+tf)/2+(hw*tw/2)*hw/4) [kN-m]			119.32		
M,cr [kN-m]			71.610566		

According to 1993-1-1:2005 section 6.3.2.3

λ_LT	1.290850748				
ϕ_LT	1.463384155				
χ_LT	0.415330572	<1	&	1/λ^2	0.600134
M,ult [kN-m]	49.55906089				

$$M_{cr} = \frac{\pi^2 E I_z}{L^2}\sqrt{\frac{I_w}{I_z} + \frac{L^2}{\pi^2 E I_z}(G I_t + c_w)}$$

Corrugated Web

I,z [mm^4]	2604166.667
I,y [mm^4]	3.33E+07

M,y= 2*fy*(bf*tf*(hw+tf)/2 [kN-m]			91.59

u,x	4.35336E-05				
C,w	12537256176				
M,cr [kN-m]			103.18409		
λ_LT	0.942144791				
ϕ_LT	1.038878823				
χ_LT	0.594547702	<1	&	1/λ^2	1.126587

$$u_x = \frac{h_w}{2Gat_w} + \frac{h_w^2 (a+b)^3}{25a^2 E b_f t_f^3}$$

$$c_w = \frac{(2d)^2 h_w^2}{8u_x(a+b)}$$

Model-4

Geometry	
h,web [mm]	300
t,web [mm]	6
L,span [m]	4.8
b,flange[mm]	150
t,flange [mm]	10
a [mm]	70
b [mm]	47
d [mm]	50
α	65

Material Property	
S355	Material
fy [Mpa]	355
E [Gpa]	210
fu [Mpa]	600
ε,p	0.1167
ε	0.813616513
G [Gpa]	80.77

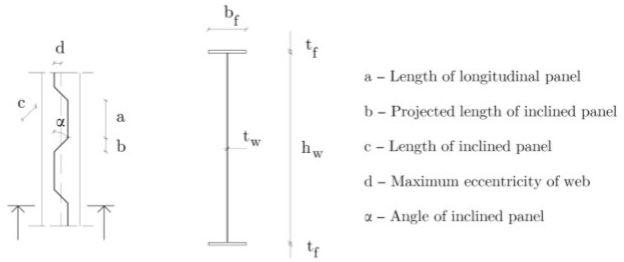

Notations for the geometry of the cross-section and corrugation profile.

Flat Web

Flange	c	72	
	t	10	
	c/t	7.2	7.3225486 Class I

web	c	300	
	t	6	
	c/t	50	58.580389 Class I

h/b	2.133333333	Buckling curve d	α,LT	0.76

I,z [mm^4]	5.63E+06	Moment of inertia around weak axis (xy plane)
I,t [mm^4]	1.22E+05	Torsion constant
I,w [mm^4]	1.35E+11	Warping constant
I,y [mm^4]	8.56E+07	Moment of inertia around strong axis (xz plane)

Table 6.3: Recommended values for imperfection factors for lateral torsional buckling curves

Buckling curve	a	b	c	d
Imperfection factor α_{LT}	0,21	0,34	0,49	0,76

Table 6.5: Recommendation for the selection of lateral torsional buckling curve for cross sections using equation (6.57)

Cross-section	Limits	Buckling curve
Rolled I-sections	h/b ≤ 2 h/b > 2	b c
Welded I-sections	h/b ≤ 2 h/b > 2	c d

$$I_w = \frac{I_z (h - t_f)^2}{4}$$

$$I_z = 2 \cdot \frac{t_f b_f^3}{12} = \frac{t_f b_f^3}{6}$$

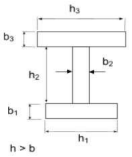

$$I_t = \frac{1}{3}\sum_{i=1}^{n} b_i^3 h_i$$

M,y=2* fy*(bf*tf*(hw+tf)/2+(hw*tw/2)*hw/4) [kN-m]	213.00	
M,cr [kN-m]	105.53644	

According to 1993-1-1:2005 section 6.3.2.3

λ_LT	1.420654886				
ϕ_LT	1.644696472				
χ_LT	0.36547334	<1	&	1/λ^2	0.495476
M,ult [kN-m]	77.84582142				

$$M_{cr} = \frac{\pi^2 E I_z}{L^2}\sqrt{\frac{I_w}{I_z} + \frac{L^2}{\pi^2 E I_z}(G I_t + c_w)}$$

Corrugated Web

I,z [mm^4]	5625000
I,y [mm^4]	7.21E+07

M,y= 2*fy*(bf*tf*(hw+tf)/2 [kN-m]		165.08

$$u_x = \frac{h_w}{2Gat_w} + \frac{h_w^2 (a+b)^3}{25a^2 E b_f t_f^3}$$

$$c_w = \frac{(2d)^2 h_w^2}{8u_x(a+b)}$$

u,x	4.17771E-05				
C,w	23015904135				
M,cr [kN-m]			150.90903		
λ_LT	1.045882852				
ϕ_LT	1.155637086				
χ_LT	0.533806645	<1	&	1/λ^2	0.914185

Model 5

Geometry	
h,web [mm]	350
t,web [mm]	7
L,span [m]	6.3
b,flange[mm]	175
t,flange [mm]	12
a [mm]	70
b [mm]	42
d [mm]	58
α	70

Material Property	
S355	Material
fy [Mpa]	355
E [Gpa]	210
fu [Mpa]	600
ε,p	0.1167
ε	0.813616513
G [Gpa]	80.77

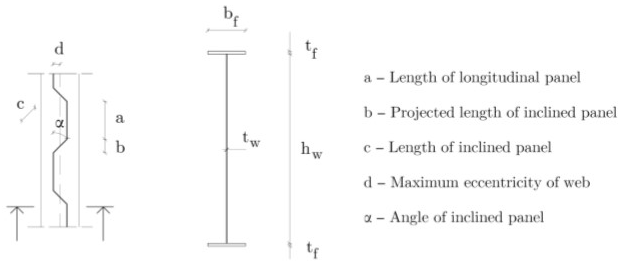

Notations for the geometry of the cross-section and corrugation profile.

Flat Web

Flange	c	84	
	t	12	
	c/t	7	7.3225486 Class I

web	c	350	
	t	7	
	c/t	50	58.580389 Class I

h/b	2.137142857	Buckling curve d	α,LT	0.76

I,z [mm^4]	1.07E+07	Moment of inertia around weak axis (xy plane)
I,t [mm^4]	2.42E+05	Torsion constant
I,w [mm^4]	3.51E+11	Warping constant
I,y [mm^4]	1.63E+08	Moment of inertia around strong axis (xz plane)

Table 6.3: Recommended values for imperfection factors for lateral torsional buckling curves

Buckling curve	a	b	c	d
Imperfection factor α_{LT}	0,21	0,34	0,49	0,76

Table 6.5: Recommendation for the selection of lateral torsional buckling curve for cross sections using equation (6.57)

Cross-section	Limits	Buckling curve
Rolled I-sections	h/b ≤ 2 h/b > 2	b c
Welded I-sections	h/b ≤ 2 h/b > 2	c d

$$I_w = \frac{I_z (h - t_f)^2}{4}$$

$$I_z = 2 \cdot \frac{t_f b_f^3}{12} = \frac{t_f b_f^3}{6}$$

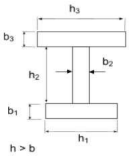

$$I_t = \frac{1}{3}\sum_{i=1}^{n} b_i^3 h_i$$

M,y=2* fy*(bf*tf*(hw+tf)/2+(hw*tw/2)*hw/4) [kN-m]	345.97	
M,cr [kN-m]	145.66024	

According to 1993-1-1:2005 section 6.3.2.3

λ_LT	1.541172683				
ϕ_LT	1.824350584				
χ_LT	0.3259375	<1	&	1/λ^2	0.421015
M,ult [kN-m]	112.7659412				

$$M_{cr} = \frac{\pi^2 E I_z}{L^2}\sqrt{\frac{I_w}{I_z} + \frac{L^2}{\pi^2 E I_z}(G I_t + c_w)}$$

Corrugated Web

I,z [mm^4]	10718750
I,y [mm^4]	1.38E+08

M,y= 2*fy*(bf*tf*(hw+tf)/2 [kN-m]		269.87

u,x	2.65452E-05				
C,w	69304004167				
M,cr [kN-m]			244.92645		
λ_LT	1.04968809				
ϕ_LT	1.160073381				
χ_LT	0.531700494	<1	&	1/λ^2	0.907569

$$u_x = \frac{h_w}{2Gat_w} + \frac{h_w^2 (a+b)^3}{25a^2 E b_f t_f^3}$$

$$c_w = \frac{(2d)^2 h_w^2}{8u_x(a+b)}$$

Model -6

Geometry	
h,web [mm]	450
t,web [mm]	8
L,span [m]	8
b,flange[mm]	225
t,flange [mm]	14
a [mm]	70
b [mm]	67
d [mm]	58
α	60

Material Property	
S355	Material
fy [Mpa]	355
E [Gpa]	210
fu [Mpa]	600
ε,p	0.1167
ε	0.813616513
G [Gpa]	80.77

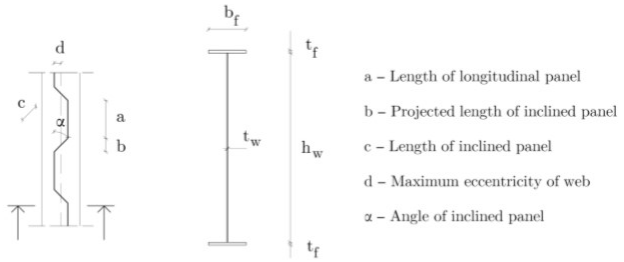

Notations for the geometry of the cross-section and corrugation profile.

Flat Web

Flange	c	108.5	
	t	14	
	c/t	7.75	7.3225486 Class II

web	c	450	
	t	8	
	c/t	56.25	58.580389 Class I

h/b	2.124444444	Buckling curve d	α,LT	0.76

Table 6.3: Recommended values for imperfection factors for lateral torsional buckling curves

Buckling curve	a	b	c	d
Imperfection factor α_{LT}	0,21	0,34	0,49	0,76

Table 6.5: Recommendation for the selection of lateral torsional buckling curve for cross sections using equation (6.57)

Cross-section	Limits	Buckling curve
Rolled I-sections	h/b ≤ 2 h/b > 2	b c
Welded I-sections	h/b ≤ 2 h/b > 2	c d

I,z [mm^4]	2.66E+07	Moment of inertia around weak axis (xy plane)
I,t [mm^4]	4.88E+05	Torsion constant
I,w [mm^4]	1.43E+12	Warping constant
I,y [mm^4]	4.00E+08	Moment of inertia around strong axis (xz plane)

$$I_w = \frac{I_z (h - t_f)^2}{4}$$

$$I_z = 2 \cdot \frac{t_f b_f^3}{12} = \frac{t_f b_f^3}{6}$$

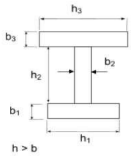

$$I_t = \frac{1}{3}\sum_{i=1}^{n} b_i^3 h_i$$

M,y=2* fy*(bf*tf*(hw+tf)/2+(hw*tw/2)*hw/4) [kN-m]			662.64		
M,cr [kN-m]			271.86616		
According to 1993-1-1:2005 section 6.3.2.3					
λ_LT	1.561213246				
ϕ_LT	1.855281083				
χ_LT	0.319925775	<1	&	1/λ^2	0.410275
M,ult [kN-m]	211.9965754				

$$M_{cr} = \frac{\pi^2 E I_z}{L^2}\sqrt{\frac{I_w}{I_z} + \frac{L^2}{\pi^2 E I_z}(G I_t + c_w)}$$

Corrugated Web

I,z [mm^4]	26578125
I,y [mm^4]	3.39E+08

M,y= 2*fy*(bf*tf*(hw+tf)/2 [kN-m]			518.87

u,x	3.77587E-05				
C,w	65843660627				
M,cr [kN-m]			361.29075		
λ_LT	1.198395086				
ϕ_LT	1.341946677				
χ_LT	0.456067716	<1	&	1/λ^2	0.696306

$$u_x = \frac{h_w}{2Gat_w} + \frac{h_w^2 (a+b)^3}{25a^2 E b_f t_f^3}$$

$$c_w = \frac{(2d)^2 h_w^2}{8u_x(a+b)}$$

Model-7

Geometry	
h,web [mm]	500
t,web [mm]	9
L,span [m]	8.8
b,flange[mm]	250
t,flange [mm]	16
a [mm]	70
b [mm]	54
d [mm]	58
α	65

Material Property	
S355	Material
fy [Mpa]	355
E [Gpa]	210
fu [Mpa]	600
ε,p	0.1167
ε	0.813616513
G [Gpa]	80.77

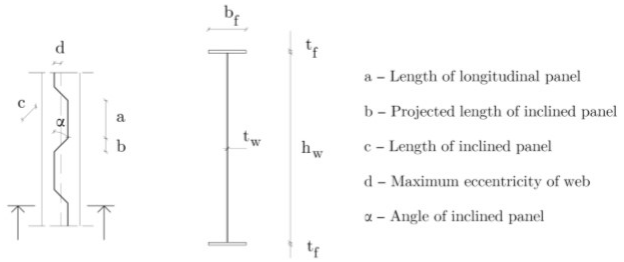

Notations for the geometry of the cross-section and corrugation profile.

Flat Web

Flange	c	120.5	
	t	16	
	c/t	7.53125	7.3225486 Class II

web	c	500	
	t	9	
	c/t	55.55555556	58.580389 Class I

h/b	2.128	Buckling curve d	α,LT 0.76

Table 6.3: Recommended values for imperfection factors for lateral torsional buckling curves

Buckling curve	a	b	c	d
Imperfection factor α_{LT}	0,21	0,34	0,49	0,76

Table 6.5: Recommendation for the selection of lateral torsional buckling curve for cross sections using equation (6.57)

Cross-section	Limits	Buckling curve
Rolled I-sections	h/b ≤ 2 h/b > 2	b c
Welded I-sections	h/b ≤ 2 h/b > 2	c d

$$I_w = \frac{I_z (h - t_f)^2}{4}$$

$$I_z = 2 \cdot \frac{t_f b_f^3}{12} = \frac{t_f b_f^3}{6}$$

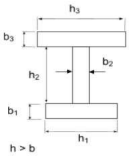

$$I_t = \frac{1}{3}\sum_{i=1}^{n} b_i^3 h_i$$

I,z [mm^4]	4.17E+07	Moment of inertia around weak axis (xy plane)
I,t [mm^4]	8.04E+05	Torsion constant
I,w [mm^4]	2.78E+12	Warping constant
I,y [mm^4]	6.26E+08	Moment of inertia around strong axis (xz plane)

M,y=2* fy*(bf*tf*(hw+tf)/2+(hw*tw/2)*hw/4) [kN-m]	932.41
M,cr [kN-m]	394.19118

According to 1993-1-1:2005 section 6.3.2.3

λ_LT	1.537975538				
ϕ_LT	1.819443987				
χ_LT	0.326910651	<1	&	1/λ^2	0.422767
M,ult [kN-m]	304.8139429				

$$M_{cr} = \frac{\pi^2 E I_z}{L^2}\sqrt{\frac{I_w}{I_z} + \frac{L^2}{\pi^2 E I_z}(G I_t + c_w)}$$

Corrugated Web

I,z [mm^4]	41666666.67
I,y [mm^4]	5.33E+08

M,y= 2*fy*(bf*tf*(hw+tf)/2 [kN-m]		732.72

u,x	2.30077E-05				
C,w	1.47391E+11				
M,cr [kN-m]			565.36747		
λ_LT	1.138422881				
ϕ_LT	1.266603191				
χ_LT	0.485021869	<1	&	1/λ^2	0.771601

$$u_x = \frac{h_w}{2Gat_w} + \frac{h_w^2 (a+b)^3}{25a^2 E b_f t_f^3}$$

$$c_w = \frac{(2d)^2 h_w^2}{8u_x(a+b)}$$

Model -8

Geometry	
h,web [mm]	550
t,web [mm]	10
L,span [m]	10.1
b,flange[mm]	275
t,flange [mm]	18
a [mm]	70
b [mm]	42
d [mm]	58
α	70

Material Property	
S355	Material
fy [Mpa]	355
E [Gpa]	210
fu [Mpa]	600
ε,p	0.1167
ε	0.813616513
G [Gpa]	80.77

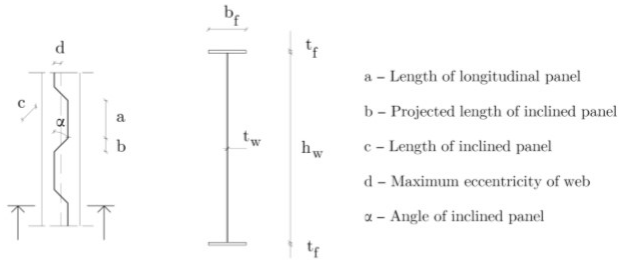

Notations for the geometry of the cross-section and corrugation profile.

Flat Web

Flange	c	132.5	
	t	18	
	c/t	7.361111111	7.3225486 Class II

web	c	550	
	t	10	
	c/t	55	58.580389 Class I

h/b	2.130909091	Buckling curve d	α,LT	0.76

I,z [mm^4]	6.24E+07	Moment of inertia around weak axis (xy plane)
I,t [mm^4]	1.25E+06	Torsion constant
I,w [mm^4]	5.04E+12	Warping constant
I,y [mm^4]	9.37E+08	Moment of inertia around strong axis (xz plane)

Table 6.3: Recommended values for imperfection factors for lateral torsional buckling curves

Buckling curve	a	b	c	d
Imperfection factor α_{LT}	0,21	0,34	0,49	0,76

Table 6.5: Recommendation for the selection of lateral torsional buckling curve for cross sections using equation (6.57)

Cross-section	Limits	Buckling curve
Rolled I-sections	h/b ≤ 2	b
	h/b > 2	c
Welded I-sections	h/b ≤ 2	c
	h/b > 2	d

$$I_w = \frac{I_z (h - t_f)^2}{4}$$

$$I_z = 2 \cdot \frac{t_f b_f^3}{12} = \frac{t_f b_f^3}{6}$$

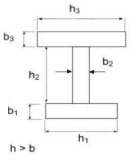

$$I_t = \frac{1}{3}\sum_{i=1}^{n} b_i^3 h_i$$

M,y=2* fy*(bf*tf*(hw+tf)/2+(hw*tw/2)*hw/4) [kN-m]	1266.59	
M,cr [kN-m]	508.06982	

According to 1993-1-1:2005 section 6.3.2.3

λ_LT	1.578904168				
ϕ_LT	1.882835473				
χ_LT	0.314743072	<1	&	1/λ^2	0.401133
M,ult [kN-m]	398.6494047				

$$M_{cr} = \frac{\pi^2 E I_z}{L^2}\sqrt{\frac{I_w}{I_z} + \frac{L^2}{\pi^2 E I_z}(G I_t + c_w)}$$

Corrugated Web

I,z [mm^4]	62390625
I,y [mm^4]	7.99E+08

M,y= 2*fy*(bf*tf*(hw+tf)/2 [kN-m]		998.12

u,x	1.51648E-05				
C,w	2.99569E+11				
M,cr [kN-m]			798.55585		
λ_LT	1.11799097				
ϕ_LT	1.241550497				
χ_LT	0.495359082	<1	&	1/λ^2	0.800062

$$u_x = \frac{h_w}{2Gat_w} + \frac{h_w^2 (a+b)^3}{25a^2 E b_f t_f^3}$$

$$c_w = \frac{(2d)^2 h_w^2}{8u_x(a+b)}$$

Model -9

Geometry	
h,web [mm]	650
t,web [mm]	12
L,span [m]	7
b,flange[mm]	260
t,flange [mm]	22
a [mm]	70
b [mm]	67
d [mm]	58
α	60

Material Property	
S355	Material
fy [Mpa]	355
E [Gpa]	210
fu [Mpa]	600
ε,p	0.1167
ε	0.813616513
G [Gpa]	80.77

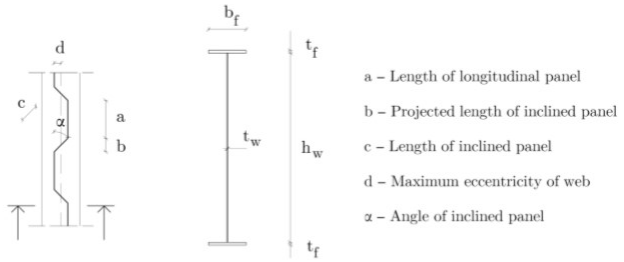

Notations for the geometry of the cross-section and corrugation profile.

Flat Web

Flange	c	124	
	t	22	
	c/t	5.636363636	7.3225486 Class I

web	c	650	
	t	12	
	c/t	54.16666667	58.580389 Class I

h/b	2.669230769	Buckling curve c	α,LT	0.76

Table 6.3: Recommended values for imperfection factors for lateral torsional buckling curves

Buckling curve	a	b	c	d
Imperfection factor α_{LT}	0,21	0,34	0,49	0,76

Table 6.5: Recommendation for the selection of lateral torsional buckling curve for cross sections using equation (6.57)

Cross-section	Limits	Buckling curve
Rolled I-sections	h/b ≤ 2 h/b > 2	b c
Welded I-sections	h/b ≤ 2 h/b > 2	c d

$$I_w = \frac{I_z (h - t_f)^2}{4}$$

$$I_z = 2 \cdot \frac{t_f b_f^3}{12} = \frac{t_f b_f^3}{6}$$

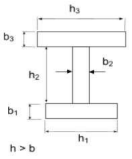

$$I_t = \frac{1}{3}\sum_{i=1}^{n} b_i^3 h_i$$

I,z [mm^4]	6.45E+07	Moment of inertia around weak axis (xy plane)
I,t [mm^4]	2.22E+06	Torsion constant
I,w [mm^4]	7.29E+12	Warping constant
I,y [mm^4]	1.57E+09	Moment of inertia around strong axis (xz plane)

M,y=2* fy*(bf*tf*(hw+tf)/2+(hw*tw/2)*hw/4) [kN-m]	1814.53	
M,cr [kN-m]	1153.6202	

According to 1993-1-1:2005 section 6.3.2.3

λ_LT	1.254151909				
ϕ_LT	1.414414105				
χ_LT	0.430951564	<1	&	1/λ^2	0.63577
M,ult [kN-m]	781.9726876				

$$M_{cr} = \frac{\pi^2 E I_z}{L^2}\sqrt{\frac{I_w}{I_z} + \frac{L^2}{\pi^2 E I_z}(G I_t + c_w)}$$

Corrugated Web

I,z [mm^4]	64445333.33
I,y [mm^4]	1.29E+09

M,y= 2*fy*(bf*tf*(hw+tf)/2 [kN-m]		1364.56

u,x	2.00445E-05				
C,w	2.58784E+11				
M,cr [kN-m]			1426.3015		
λ_LT	0.978117806				
ϕ_LT	1.078452682				
χ_LT	0.572761046	<1	&	1/λ^2	1.045244

$$u_x = \frac{h_w}{2Gat_w} + \frac{h_w^2 (a+b)^3}{25a^2 E b_f t_f^3}$$

$$c_w = \frac{(2d)^2 h_w^2}{8u_x(a+b)}$$

Model -10

Geometry	
h,web [mm]	750
t,web [mm]	12
L,span [m]	7
b,flange[mm]	300
t,flange [mm]	22
a [mm]	70
b [mm]	54
d [mm]	58
α	65

Material Property	
S355	Material
fy [Mpa]	355
E [Gpa]	210
fu [Mpa]	600
ε,p	0.1167
ε	0.813616513
G [Gpa]	80.77

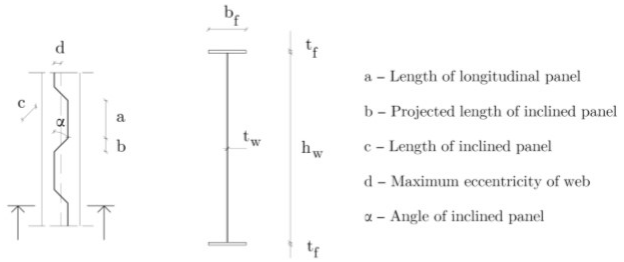

Notations for the geometry of the cross-section and corrugation profile.

Flat Web

Flange	c	144	
	t	22	
	c/t	6.545454545	7.3225486 Class I
web	c	750	
	t	12	
	c/t	62.5	58.580389 Class II

h/b	2.646666667	Buckling curve c	α,LT 0.76

Table 6.3: Recommended values for imperfection factors for lateral torsional buckling curves

Buckling curve	a	b	c	d
Imperfection factor α_{LT}	0,21	0,34	0,49	0,76

Table 6.5: Recommendation for the selection of lateral torsional buckling curve for cross sections using equation (6.57)

Cross-section	Limits	Buckling curve
Rolled I-sections	h/b ≤ 2 h/b > 2	b c
Welded I-sections	h/b ≤ 2 h/b > 2	c d

I,z [mm^4]	9.91E+07	Moment of inertia around weak axis (xy plane)
I,t [mm^4]	2.56E+06	Torsion constant
I,w [mm^4]	1.48E+13	Warping constant
I,y [mm^4]	2.39E+09	Moment of inertia around strong axis (xz plane)

$$I_w = \frac{I_z (h - t_f)^2}{4}$$

$$I_z = 2 \cdot \frac{t_f b_f^3}{12} = \frac{t_f b_f^3}{6}$$

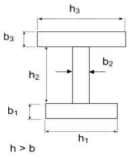

$$I_t = \frac{1}{3}\sum_{i=1}^{n} b_i^3 h_i$$

M,y=2* fy*(bf*tf*(hw+tf)/2+(hw*tw/2)*hw/4) [kN-m]	2407.86
M,cr [kN-m]	1867.0188

According to 1993-1-1:2005 section 6.3.2.3

λ_LT	1.135641187				
ϕ_LT	1.263173991				
χ_LT	0.486414931	<1	&	1/λ^2	0.775386
M,ult [kN-m]	1171.218325				

$$M_{cr} = \frac{\pi^2 E I_z}{L^2}\sqrt{\frac{I_w}{I_z} + \frac{L^2}{\pi^2 E I_z}(G I_t + c_w)}$$

Corrugated Web

I,z [mm^4]	99000000
I,y [mm^4]	1.97E+09

M,y= 2*fy*(bf*tf*(hw+tf)/2 [kN-m]		1808.80

u,x	1.85781E-05				
C,w	4.107E+11				
M,cr [kN-m]			2280.7412		
λ_LT	0.890546883				
ϕ_LT	0.983810473				
χ_LT	0.627112048	<1	&	1/λ^2	1.260917

$$u_x = \frac{h_w}{2Gat_w} + \frac{h_w^2 (a+b)^3}{25a^2 E b_f t_f^3}$$

$$c_w = \frac{(2d)^2 h_w^2}{8u_x(a+b)}$$

Model 11-(Class 4)

Geometry	
h,web [mm]	1000
t,web [mm]	14
L,span [m]	2.2
b,flange[mm]	400
t,flange [mm]	10
a [mm]	70
b [mm]	45
d [mm]	39
α	60

Material Property	
S355	Material
fy [Mpa]	355
E [Gpa]	210
fu [Mpa]	600
ε,p	0.1167
ε	0.813616513
G [Gpa]	80.77

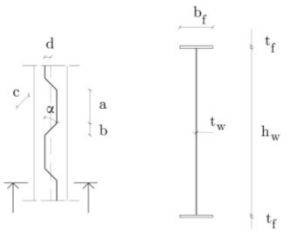

a – Length of longitudinal panel

b – Projected length of inclined panel

c – Length of inclined panel

d – Maximum eccentricity of web

α – Angle of inclined panel

Notations for the geometry of the cross-section and corrugation profile.

Flat Web

Flange	c	193		
	t	10		
	c/t	19.3	7.32254862	Class IV

web	c	1000		
	t	14		
	c/t	71.42857143	58.580389	Class III

h/b	2.55	Buckling curve c	α,LT	0.76

Table 6.3: Recommended values for imperfection factors for lateral torsional buckling curves

Buckling curve	a	b	c	d
Imperfection factor α_{LT}	0,21	0,34	0,49	0,76

Table 6.5: Recommendation for the selection of lateral torsional buckling curve for cross sections using equation (6.57)

Cross-section	Limits	Buckling curve
Rolled I-sections	h/b ≤ 2 h/b > 2	b c
Welded I-sections	h/b ≤ 2 h/b > 2	c d

Ψ	1.0	
Kσ	0.43	
w	5.00	mm
b_{bar}	185.93	
λ_p	1.23	
ρ	1.00	
	0.69	
ρ	0.60	
bf_c	111.56	mm
b1	251.26	mm

$$bbar := \frac{\left(b_f - t_w - 2w\sqrt{2}\right)}{2}$$

$$\lambda_p := \frac{\frac{b_{bar}}{t_f}}{28.4 \cdot \varepsilon \cdot \sqrt{\kappa_\sigma}}$$

- outstand compression elements:

$\rho = 1{,}0$ for $\bar{\lambda}_p \le 0{,}748$

$\rho = \frac{\bar{\lambda}_p - 0{,}188}{\bar{\lambda}_p^2} \le 1{,}0$ for $\bar{\lambda}_p > 0{,}748$

where $\bar{\lambda}_p = \sqrt{\frac{f_y}{\sigma_{cr}}} = \frac{\bar{b}/t}{28{,}4\,\varepsilon\sqrt{k_\sigma}}$

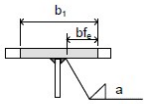

Calculation of the effective part of the web should be based on the gross section of the web and the effective width of the flange (4.4 (3) in 1993-1-5)

New position of the NA

∑A*Y_{bar}	9710257.07	
y_{bar}	20512.57	
ytp=yb	473.38	mm
yt	546.62	mm
b1x	237.26	mm
B1x	386.00	mm
ht	536.62	mm
hb	463.38	mm

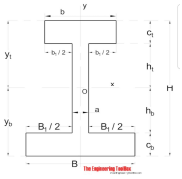

$$y_{tp} := \frac{\left(t_f \cdot b_f\right)\cdot\frac{t_f}{2} + h \cdot t_w\left(\frac{h}{2} + t_f\right) + b_1 \cdot t_f\left(h + \frac{3}{2}t_f\right)}{t_f \cdot b_f + t_f \cdot b_1 + t_w \cdot h}$$

I,z [mm^4]	6.68E+07	Moment of inertia around weak axis (xy plane)
I,t [mm^4]	1.13E+06	Torsion constant
I,w [mm^4]	1.70E+13	Warping constant
I,y [mm^4]	2.80E+09	Moment of inertia around strong axis (xz plane)
wy [mm^3]	5.92E+06	

$$I_w = \frac{I_z(h - t_f)^2}{4}$$

$$I_z = 2 \cdot \frac{t_f b_f^3}{12} = \frac{t_f b_f^3}{6}$$

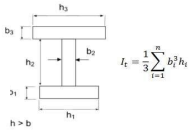

$$I_t = \frac{1}{3}\sum_{i=1}^{n} b_i^3 h_i$$

Iy= $(1/3)\,(B\,y_b^3 - B_1\,h_b^3 + b\,y_t^3 - b_1\,h_t^3)$

M,y= (fy*wy) [kN-m]					2099.85
M,cr [kN-m]		14531.74			

According to 1993-1-1:2005 section 6.3.2.3

λ_LT	0.380132839				
ϕ_LT	0.546638345				
χ_LT	1.017262867	<1	&	1/λ^2	6.9203685
M,ult [kN-m]	2136.10				

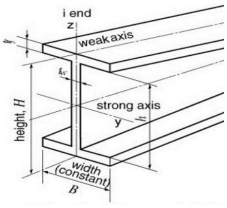

Corrugated Web

I,z [mm^4]	6.6552E+07	wy	
I,y [mm^4]	1.61464E+09	3.4109E+06	
M,y= fy*(wy) [kN-m]		1210.86	
u,x	0.000154118		
C,w	42908958117		
M,cr [kN-m]		1.4549E+04	
λ_LT	0.288490468		
ϕ_LT	0.488836409		
χ_LT	1.100104928	<1 &	1/λ^2 12.01536763
M,ult [kN-m]	1332.073008		

$$M_{cr} = \frac{\pi^2 E I_z}{L^2}\sqrt{\frac{I_w}{I_z} + \frac{L^2}{\pi^2 E I_z}(G I_t + c_w)}$$

$$u_x = \frac{h_w}{2Gat_w} + \frac{h_w^2(a+b)^3}{25a^2Eb_f t_f^3}$$

$$c_w = \frac{(2d)^2 h_w^2}{8u_x(a+b)}$$

Geometry	
h,web [mm]	1050
t,web [mm]	14
L,span [m]	1
b,flange[mm]	420
t,flange [mm]	14
a [mm]	70
b [mm]	47
d [mm]	50
α	60

Material Property	
S355	Material
fy [Mpa]	355
E [Gpa]	210
fu [Mpa]	600
ε,p	0.1167
ε	0.813616513
G [Gpa]	80.77

Model 12 (Class 4)

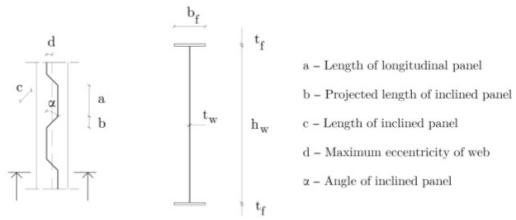

Notations for the geometry of the cross-section and corrugation profile.

Flat Web

Flange	c	203		
	t	14		
	c/t	14.5	7.32254862	Class IV

web	c	1050		
	t	14		
	c/t	75	58.580389	Class III

h/b	2.566666667	Buckling curve c		α,LT	0.76

Table 6.3: Recommended values for imperfection factors for lateral torsional buckling curves

Buckling curve	a	b	c	d
Imperfection factor α_{LT}	0,21	0,34	0,49	0,76

Table 6.5: Recommendation for the selection of lateral torsional buckling curve for cross sections using equation (6.57)

Cross-section	Limits	Buckling curve
Rolled I-sections	h/b ≤ 2 h/b > 2	b c
Welded I-sections	h/b ≤ 2 h/b > 2	c d

Ψ	1.0	
Kσ	0.43	
w	5.00	mm
b_{bar}	195.93	
λ_p	0.92	
ρ	1.00	
	0.86	
ρ	0.38	
bf_c	74.45	mm
b1	177.05	mm

$$bbar := \frac{\left(b_f - t_w - 2w\sqrt{2}\right)}{2}$$

$$\lambda_p := \frac{\frac{b_{bar}}{t_f}}{28.4 \cdot \varepsilon \cdot \sqrt{\kappa_\sigma}}$$

- outstand compression elements:

$\rho = 1{,}0$ for $\bar{\lambda}_p \le 0{,}748$

$\rho = \frac{\bar{\lambda}_p - 0{,}188}{\bar{\lambda}_p^2} \le 1{,}0$ for $\bar{\lambda}_p > 0{,}748$

where $\bar{\lambda}_p = \sqrt{\frac{f_y}{\sigma_{cr}}} = \frac{\bar{b}/t}{28{,}4\,\varepsilon\sqrt{k_\sigma}}$

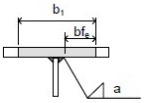

Calculation of the effective part of the web should be based on the gross section of the web and the effective width of the flange (4.4 (3) in 1993-1-5)

New position of the NA

∑A*Y_{bar}	10619119.57	
y_{bar}	23058.67	
ytp=yb	460.53	mm
yt	617.47	mm
b1x	163.05	mm
B1x	406.00	mm
ht	603.47	mm
hb	446.53	mm

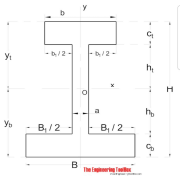

$$y_{tp} := \frac{\left(t_f \cdot b_f\right)\cdot\frac{t_f}{2} + h \cdot t_w\left(\frac{h}{2} + t_f\right) + b_1 \cdot t_f\left(h + \frac{3}{2}t_f\right)}{t_f \cdot b_f + t_f \cdot b_1 + t_w \cdot h}$$

I,z [mm^4]	9.32E+07	Moment of inertia around weak axis (xy plane)
I,t [mm^4]	1.51E+06	Torsion constant
I,w [mm^4]	2.64E+13	Warping constant
I,y [mm^4]	3.57E+09	Moment of inertia around strong axis (xz plane)
wy [mm^3]	7.76E+06	

Iy= $(1/3)\,(B\,y_b^3 - B_1\,h_b^3 + b\,y_t^3 - b_1\,h_t^3)$

$$I_w = \frac{I_z (h - t_f)^2}{4}$$

$$I_z = 2 \cdot \frac{t_f b_f^3}{12} = \frac{t_f b_f^3}{6}$$

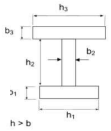

$$I_t = \frac{1}{3}\sum_{i=1}^{n} b_i^3 h_i$$

M,y= (fy*wy) [kN-m]					2755.36
M,cr [kN-m]		102825.39			
According to 1993-1-1:2005 section 6.3.2.3					
λ_LT	0.163696276				
ϕ_LT	0.420253261				
χ_LT	1.22568006	<1	&	1/λ^2	37.31834741
M,ult [kN-m]	3377.19				

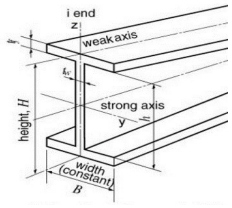

Corrugated Web

I,z [mm^4]	9.2911E+07	wy	
I,y [mm^4]	2.13332E+09	4.632E+06	
M,y= fy*(wy) [kN-m]		1644.48	
u,x	6.61916E-05		
C,w	1.77951E+11		
M,cr [kN-m]		1.0286E+05	
λ_LT	0.12644238		
ϕ_LT	0.402043483		
χ_LT	1.267608049	<1 &	1/λ^2 62.54817995
M,ult [kN-m]	2084.56142		

$$M_{cr} = \frac{\pi^2 E I_z}{L^2}\sqrt{\frac{I_w}{I_z} + \frac{L^2}{\pi^2 E I_z}(G I_t + c_w)}$$

$$u_x = \frac{h_w}{2Gat_w} + \frac{h_w^2 (a+b)^3}{25a^2 E b_f t_f^3}$$

$$c_w = \frac{(2d)^2 h_w^2}{8u_x(a+b)}$$

Geometry	
h,web [mm]	1100
t,web [mm]	12
L,span [m]	1.5
b,flange[mm]	440
t,flange [mm]	12
a [mm]	70
b [mm]	42
d [mm]	58
α	60

Material Property	
S355	Material
fy [Mpa]	355
E [Gpa]	210
fu [Mpa]	600
ε,p	0.1167
ε	0.813616513
G [Gpa]	80.77

Model 13-(Class 4)

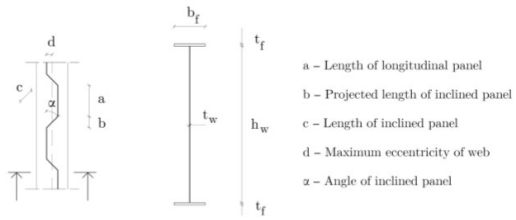

Notations for the geometry of the cross-section and corrugation profile.

Flat Web

Flange	c	214		
	t	12		
	c/t	17.83333333	7.32254862	Class IV

web	c	1100		
	t	12		
	c/t	91.66666667	58.580389	Class III

h/b	2.554545455	Buckling curve c	α,LT	0.76	

Table 6.3: Recommended values for imperfection factors for lateral torsional buckling curves

Buckling curve	a	b	c	d
Imperfection factor α_{LT}	0,21	0,34	0,49	0,76

Table 6.5: Recommendation for the selection of lateral torsional buckling curve for cross sections using equation (6.57)

Cross-section	Limits	Buckling curve
Rolled I-sections	h/b ≤ 2 h/b > 2	b c
Welded I-sections	h/b ≤ 2 h/b > 2	c d

Ψ	1.0	
Kσ	0.43	
w	5.00	mm
b_{bar}	206.93	
λ_p	1.14	
ρ	1.00	
	0.73	
ρ	0.32	
bf_e	66.22	mm
b1	158.58	mm

$$bbar := \frac{\left(b_f - t_w - 2w\sqrt{2}\right)}{2}$$

$$\lambda_p := \frac{\frac{b_{bar}}{t_f}}{28.4 \cdot \varepsilon \cdot \sqrt{\kappa_\sigma}}$$

- outstand compression elements:

$\rho = 1{,}0$ for $\bar{\lambda}_p \le 0{,}748$

$\rho = \frac{\bar{\lambda}_p - 0{,}188}{\bar{\lambda}_p^2} \le 1{,}0$ for $\bar{\lambda}_p > 0{,}748$

where $\bar{\lambda}_p = \sqrt{\frac{f_y}{\sigma_{cr}}} = \frac{\bar{b}/t}{28{,}4\,\varepsilon\sqrt{k_\sigma}}$

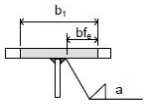

Calculation of the effective part of the web should be based on the gross section of the web and the effective width of the flange (4.4 (3) in 1993-1-5)

New position of the NA

∑A*Y_{bar}	9577544.37	
y_{bar}	20382.92	
ytp=yb	469.88	mm
yt	654.12	mm
b1x	146.58	mm
B1x	428.00	mm
ht	642.12	mm
hb	457.88	mm

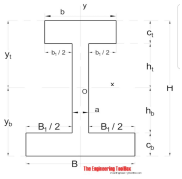

$$y_{tp} := \frac{\left(t_f \cdot b_f\right)\cdot\frac{t_f}{2} + h \cdot t_w\left(\frac{h}{2} + t_f\right) + b_1 \cdot t_f\left(h + \frac{3}{2}t_f\right)}{t_f \cdot b_f + t_f \cdot b_1 + t_w \cdot h}$$

I,z [mm^4]	8.93E+07	Moment of inertia around weak axis (xy plane)
I,t [mm^4]	9.78E+05	Torsion constant
I,w [mm^4]	2.76E+13	Warping constant
I,y [mm^4]	3.38E+09	Moment of inertia around strong axis (xz plane)
wy [mm^3]	7.19E+06	

$$I_w = \frac{I_z (h - t_f)^2}{4}$$

$$I_z = 2 \cdot \frac{t_f b_f^3}{12} = \frac{t_f b_f^3}{6}$$

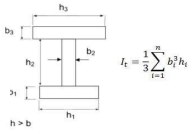

$$I_t = \frac{1}{3}\sum_{i=1}^{n} b_i^3 h_i$$

Iy= (1 / 3) (B y_b^3 - B_1 h_b^3 + b y_t^3 - b_1 h_t^3)

M,y= (fy*wy) [kN-m]					2552.58
M,cr [kN-m]		45822.89			

According to 1993-1-1:2005 section 6.3.2.3

λ_LT	0.236019867				
ϕ_LT	0.458577066				
χ_LT	1.150640069	<1	&	1/λ^2	17.95158826
M,ult [kN-m]	2937.10				

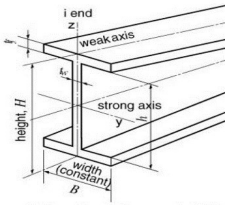

Corrugated Web

I,z [mm^4]	8.9172E+07	wy
I,y [mm^4]	1.93560E+09	4.119E+06

M,y= fy*(wy) [kN-m]			1462.37		
u,x	9.50201E-05				
C,w	1.9124E+11				
M,cr [kN-m]			4.5953E+04		
λ_LT	0.17838947				
ϕ_LT	0.42772155				
χ_LT	1.209821578	<1	&	1/λ^2	31.42400762
M,ult [kN-m]	1769.205067				

$$M_{cr} = \frac{\pi^2 E I_z}{L^2}\sqrt{\frac{I_w}{I_z} + \frac{L^2}{\pi^2 E I_z}(G I_t + c_w)}$$

$$u_x = \frac{h_w}{2Gat_w} + \frac{h_w^2 (a+b)^3}{25a^2 E b_f t_f^3}$$

$$c_w = \frac{(2d)^2 h_w^2}{8u_x(a+b)}$$

Geometry	
h,web [mm]	1200
t,web [mm]	10
L,span [m]	1.5
b,flange[mm]	480
t,flange [mm]	10
a [mm]	70
b [mm]	31
d [mm]	42
α	60

Material Property	
S355	Material
fy [Mpa]	355
E [Gpa]	210
fu [Mpa]	600
ε,p	0.1167
ε	0.813616513
G [Gpa]	80.77

Model 14-(Class 4)

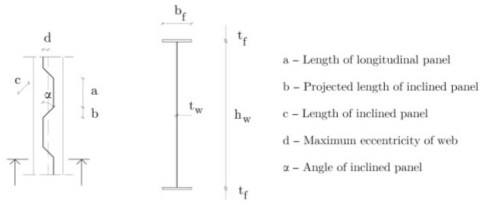

Notations for the geometry of the cross-section and corrugation profile.

Flat Web

Flange	c	235	
	t	10	
	c/t	23.5	7.322548621 Class IV

web	c	1200	
	t	10	
	c/t	120	58.58038897 Class IV

h/b	2.541666667	Buckling curve c	α,LT 0.76

Table 6.3: Recommended values for imperfection factors for lateral torsional buckling curves

Buckling curve	a	b	c	d
Imperfection factor α_{LT}	0,21	0,34	0,49	0,76

Table 6.5: Recommendation for the selection of lateral torsional buckling curve for cross sections using equation (6.57)

Cross-section	Limits	Buckling curve
Rolled I-sections	h/b ≤ 2	b
	h/b > 2	c
Welded I-sections	h/b ≤ 2	c
	h/b > 2	d

Flange-Class IV

Ψ	1.0	
Kσ	0.43	
w	0.00	mm
b_{bar}	235.00	
λ_p	1.55	
ρ	1.00	
	0.57	
ρ	0.24	
bf_e	56.40	mm
b1	122.80	mm

EC3 - table 4.2 gives for a uniform compressive stress

$$bbar := \frac{(b_f - t_w - 2w\sqrt{2})}{2}$$

$$\lambda_p := \frac{\frac{b_{bar}}{t_f}}{28.4 \cdot \varepsilon \cdot \sqrt{K_\sigma}}$$

- outstand compression elements:

$\rho = 1{,}0$ for $\bar{\lambda}_p \le 0{,}748$

$\rho = \frac{\bar{\lambda}_p - 0{,}188}{\bar{\lambda}_p^2} \le 1{,}0$ for $\bar{\lambda}_p > 0{,}748$

where $\bar{\lambda}_p = \sqrt{\frac{f_y}{\sigma_{cr}}} = \frac{\bar{b}/t}{28{,}4\,\varepsilon\sqrt{k_\sigma}}$

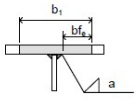

Calculation of the effective part of the web should be based on the gross section of the web and the effective width of the flange (4.4 (3) in 1993-1-5)

New position of the NA

∑A*Y_{bar}	8836020.00	
A	18028.00	
ytp=yb	490.13	mm
yt	729.87	mm
b1x	112.80	mm
B1x	470.00	mm
ht	719.87	mm
hb	480.13	mm

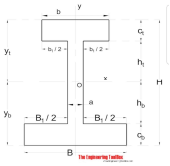

$$y_{tp} := \frac{\left(t_f \cdot b_f\right)\cdot\frac{t_f}{2} + h \cdot t_w \cdot \left(\frac{h}{2} + t_f\right) + b_1 \cdot t_f \cdot \left(h + \frac{3}{2}\cdot t_f\right)}{t_f \cdot b_f + t_f \cdot b_1 + t_w \cdot h}$$

Web-Class IV

Calculation of the effective part of the web should be based on the gross section of the web and the effective width of the flange (4.4 (3) in 1993-1-5)

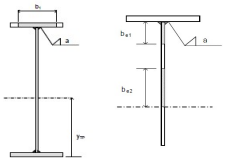

$$\psi := \frac{-y_{tp}}{h + 2\cdot t_f - y_{tp}}$$

Ψ	-0.671525003	
Kσ	16.44414248	
d	1200	
λ_p	1.280670884	
ρ	1	
	0.70	
ρ	0.64	
bwe	459.46	mm
be1	183.78	mm
be2	275.68	mm

Table 4.1: Internal compression elements

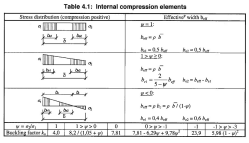

$$\frac{0 > \psi > -1}{7{,}81 - 6{,}29\psi + 9{,}78\psi^2}$$

$$K_\sigma := 7.81 - 6.29\cdot\psi + 9.78\cdot\psi^2$$

$$bw_e := \rho \cdot \frac{d}{1-\psi}$$

(2) The reduction factor ρ may be taken as follows:

- internal compression elements:

$\rho = 1{,}0$ for $\bar{\lambda}_p \le 0{,}673$

$\rho = \frac{\bar{\lambda}_p - 0{,}055(3+\psi)}{\bar{\lambda}_p^2} \le 1{,}0$ for $\bar{\lambda}_p > 0{,}673$, where $(3+\psi) \ge 0$

$$b_{e1} := 0.4\cdot bw_e + \sqrt{2}\cdot a$$

$$b_{e2} := 0.6\cdot bw_e$$

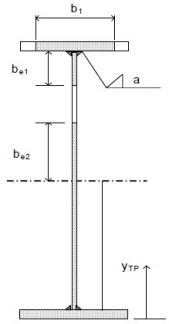

After reduction both web and flange,effective section

$$y_{TP} := \frac{\left(t_f \cdot b_f\right)\cdot\frac{t_f}{2} + \left(y_{tp} + b_{e2} - t_f\right)\cdot t_w \cdot \left(\frac{y_{tp} + b_{e2} - t_f}{2} + t_f\right) \ldots}{+\, b_{e1}\cdot t_w \cdot \left(h + t_f - \frac{b_{e1}}{2}\right) + b_1 \cdot t_f \cdot \left(h + \frac{3}{2}\cdot t_f\right)} \over t_f \cdot b_f + t_f \cdot b_1 + t_w \cdot \left(y_{tp} - t_f + b_{e1} + b_{e2}\right)$$

∑A*Y_{bar}	6502705.06	
A	15423.88	
yTP(New)	421.60	mm

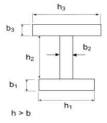

$$I_t = \frac{1}{3}\sum_{i=1}^{n} b_i^3 h_i$$

I,z [mm^4]	9.38E+07	Moment of inertia around weak axis (xy plane)
I,t [mm^4]	4.77E+05	Torsion constant
I,w [mm^4]	2.16E+13	Warping constant
I,y [mm^4]	2.815E+09	Moment of inertia around strong axis (xz plane)
wy [mm^3]	6.68E+06	

$$I_w = \frac{I_z\left(h - t_f\right)^2}{4}$$

$$I_z = 2\cdot\frac{t_f b_f^3}{12} = \frac{t_f b_f^3}{6}$$

M,y= (fy*wy) [kN-m]					2370.47
M,cr [kN-m]			41488.93		

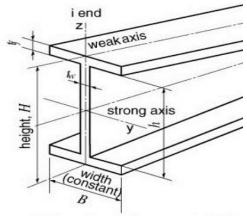

According to 1993-1-1:2005 section 6.3.2.3

λ_LT	0.239029067				
ϕ_LT	0.460256631				
χ_LT	1.147664905	<1	&	1/λ^2	17.50243876
M,ult [kN-m]	2720.50				

Corrugated Web

I,z [mm^4]	9.3703E+07	wy[mm^3]	
I,y [mm^4]	1.61E+09	3.81E+06	
M,y= fy*(wy) [kN-m]		1352.40	

u,x	0.000130764				
C,w	96166089969				
M,cr [kN-m]		41571.383496			
λ_LT	0.180366575				
ϕ_LT	0.428738837				
χ_LT	1.207714057	<1	&	1/λ^2	30.73886876
M,ult [kN-m]	1633.317888				

$$M_{cr} = \frac{\pi^2 E I_z}{L^2}\sqrt{\frac{I_w}{I_z} + \frac{L^2}{\pi^2 E I_z}(G I_t + c_w)}$$

$$u_x = \frac{h_w}{2Gat_w} + \frac{h_w^2(a+b)^3}{25a^2 E b_f t_f^3}$$

$$c_w = \frac{(2d)^2 h_w^2}{8u_x(a+b)}$$

Model 15(Class 4)

Geometry	
h,web [mm]	1500
t,web [mm]	15
L,span [m]	2
b,flange[mm]	600
t,flange [mm]	16
a [mm]	70
b [mm]	54
d [mm]	58
α	60

Material Property	
S355	Material
fy [Mpa]	355
E [Gpa]	210
fu [Mpa]	600
ε,p	0.1167
ε	0.813616513
G [Gpa]	80.77

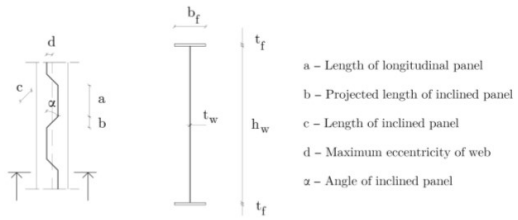

Notations for the geometry of the cross-section and corrugation profile.

Flat Web

Flange	c	292.5	
	t	16	
	c/t	18.28125	7.32254862 Class IV

web	c	1500	
	t	15	
	c/t	100	58.580389 Class III

h/b	2.553333333	Buckling curve c	α,LT	0.76

Table 6.3: Recommended values for imperfection factors for lateral torsional buckling curves

Buckling curve	a	b	c	d
Imperfection factor α_{LT}	0,21	0,34	0,49	0,76

Table 6.5: Recommendation for the selection of lateral torsional buckling curve for cross sections using equation (6.57)

Cross-section	Limits	Buckling curve
Rolled I-sections	h/b ≤ 2 h/b > 2	b c
Welded I-sections	h/b ≤ 2 h/b > 2	c d

Ψ	1.0		
Kσ	0.43		
w	5.00	mm	
b_{bar}	285.43		
λ_p	1.18		
ρ	1.00		
	0.71		
ρ	0.31		
bf_e	88.48	mm	
b1	206.11	mm	

$$bbar := \frac{\left(b_f - t_w - 2w\sqrt{2}\right)}{2}$$

$$\lambda_p := \frac{\frac{b_{bar}}{t_f}}{28.4 \cdot \varepsilon \cdot \sqrt{k_\sigma}}$$

- outstand compression elements:

$\rho = 1{,}0$ for $\bar{\lambda}_p \le 0{,}748$

$\rho = \frac{\bar{\lambda}_p - 0{,}188}{\bar{\lambda}_p^2} \le 1{,}0$ for $\bar{\lambda}_p > 0{,}748$

where $\bar{\lambda}_p = \sqrt{\frac{f_y}{\sigma_{cr}}} = \frac{\bar{b}/t}{28{,}4\,\varepsilon\sqrt{k_\sigma}}$

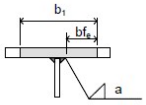

Calculation of the effective part of the web should be based on the gross section of the web and the effective width of the flange (4.4 (3) in 1993-1-5)

New position of the NA

∑A*Y_{bar}	22337539.27	
y_{bar}	35397.73	
ytp=yb	631.04	mm
yt	900.96	mm
b1x	191.11	mm
B1x	585.00	mm
ht	884.96	mm
hb	615.04	mm

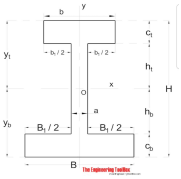

$$y_{tp} := \frac{\left(t_f \cdot b_f\right)\cdot\frac{t_f}{2} + h \cdot t_w \cdot \left(\frac{h}{2} + t_f\right) + b_1 \cdot t_f \cdot \left(h + \frac{3}{2} \cdot t_f\right)}{t_f \cdot b_f + t_f \cdot b_1 + t_w \cdot h}$$

I,z [mm^4]	3.00E+08	Moment of inertia around weak axis (xy plane)
I,t [mm^4]	2.79E+06	Torsion constant
I,w [mm^4]	1.72E+14	Warping constant
I,y [mm^4]	1.10E+10	Moment of inertia around strong axis (xz plane)
wy [mm^3]	1.74E+07	

$$I_w = \frac{I_z (h - t_f)^2}{4}$$

$$I_z = 2 \cdot \frac{t_f b_f^3}{12} = \frac{t_f b_f^3}{6}$$

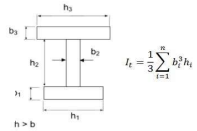

$$I_t = \frac{1}{3}\sum_{i=1}^{n} b_i^3 h_i$$

Iy= $(1/3)\,(B\,y_b^3 - B_1\,h_b^3 + b\,y_t^3 - b_1\,h_t^3)$

M,y= (fy*wy) [kN-m]					6179.66
M,cr [kN-m]		118014.42			
According to 1993-1-1:2005 section 6.3.2.3					
λ_LT	0.228830895				
ϕ_LT	0.454592082				
χ_LT	1.157789783	<1	&	1/λ^2	19.09724325
M,ult [kN-m]	7154.74				

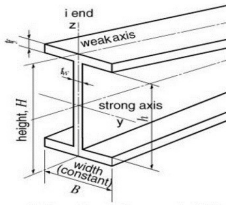

Corrugated Web

I,z [mm^4]	2.9967E+08	wy
I,y [mm^4]	6.35635E+09	1.007E+07

M,y= fy*(wy) [kN-m]			3575.83		
u,x	7.66983E-05				
C,w	3.97925E+11				
M,cr [kN-m]			1.1819E+05		
λ_LT	0.173937072				
ϕ_LT	0.425441377				
χ_LT	1.214590142	<1	&	1/λ^2	33.05336577
M,ult [kN-m]	4343.164315				

$$M_{cr} = \frac{\pi^2 E I_z}{L^2}\sqrt{\frac{I_w}{I_z} + \frac{L^2}{\pi^2 E I_z}(G I_t + c_w)}$$

$$u_x = \frac{h_w}{2Gat_w} + \frac{h_w^2 (a+b)^3}{25a^2 E b_f t_f^3}$$

$$c_w = \frac{(2d)^2 h_w^2}{8u_x(a+b)}$$